

LOAD-BEARING PROCESSES
IN
AGRICULTURAL WHEEL-SOIL SYSTEMS

ONTVANGEN

5 11 1980

ONKADDEX

CENTRALE LANDBOUWCATALOGUS



0000 0248 9975

BIBLIOTHEEK
LANDBOUWUNIVERSITEIT
WAGENINGEN

60951

Promotor: ir. H. Kuipers
hoogleraar in de grondbewerking en de gronddynamica

Co-promotor: Dr. ir. A.J. Koolen
universitair hoofddocent in de gronddynamica

F.G.J. Tijink

**LOAD-BEARING PROCESSES
IN
AGRICULTURAL WHEEL-SOIL SYSTEMS**

Proefschrift

ter verkrijging van de graad van
doctor in de landbouwwetenschappen,
op gezag van de rector magnificus,
Dr. C.C. Oosterlee,
in het openbaar te verdedigen
op woensdag 13 januari 1988
des namiddags te vier uur in de aula
van de Landbouwuniversiteit te Wageningen

ABSTRACT

Tijink, F.G.J. (1988). Load-Bearing Processes in Agricultural Wheel-Soil Systems. Doctoral thesis, Agricultural University Wageningen, The Netherlands, 173 p., 98 figs, 25 tables, 203 refs, English and Dutch summaries.

In soil dynamics we distinguish between loosening and load-bearing processes. Load-bearing processes which can occur under agricultural rollers, wheels, and tyres are dealt with in this dissertation.

We classify rollers, wheels, and tyres and treat some general aspects of these devices. Fundamentals of load-bearing processes, i.e. kinematic, dynamic, and soil physical aspects are discussed also.

Not only soil characteristics concerning load-bearing processes are dealt with but also the suitability of these characteristics for use in prediction methods. Special attention has been paid to predicting some process aspects of a towed tyre under different soil conditions and in different soil types. Under laboratory conditions the use of characterizing processes (cone, vane, and falling weight) and empirical prediction methods resulted in accurate predictions of rolling resistance, rut depth, and compaction caused by a towed tyre.

Additional keywords: load-bearing processes, soil dynamics, tyre performance, soil compaction, soil mechanical properties, soil characteristics, prediction methods.

ISBN 90-9001968-5

Printed by: Krips Repro, Meppel

Copyright F.G.J. Tijink, 1988.

No part of this book (with the exception of the abstract on this page) may be reproduced or published in any form and by any means without permission from the author.

STELLINGEN

1

Het nauwkeurig voorspellen van rolweerstand, insporing en verdichting bij het berijden van homogene grond is mogelijk met empirische voorspellingsmethoden.

Dit proefschrift

2

insporing is niet altijd een geschikte maat voor verdichting.

Dit proefschrift

3

Voor het weergeven van de karakteristieken van landbouwbanden dient een "standaard" ontwikkeld te worden.

Dit proefschrift

4

De benutting van het voor ploegwerk beschikbare trekkervermogen kan nog verbeterd worden.

Dit proefschrift

5

Indien het gewenst is bovenover te rijden bij de hoofdgrondbewerking dienen er grondbewerkingswerktuigen ter beschikking te komen die een kerende werking hebben en door de aftakas worden aangedreven.

6

De specifieke ploegweerstand neemt af bij een toename van de werkbreedte van een ploeg.

7

Voor ploegwerkzaamheden is een slijpregeling een goede aanvulling op de weerstandsregeling.

8

Het gebruik van een schijfkouter bij het voorste ploeglichaam vereist een langer ploegframe en een grotere hefkracht.

9

Een wentelploeg, gebouwd volgens het bouwdoosysteem, vereist een wentelsysteem dat het wentelen over 180 graden kan ondersteunen.

10

Bij onderzoek naar verdichting van bewerkte ondergrond behoort de invloed van de massa van de bouwvoor niet verwaarloosd te worden.

11

Het gebruik van gepilleerd zaai-zaad komt de zaadverdeling ten goede bij het zaaien van bleten.

12

Bij het ontwerpen van frames voor landbouwwerktuigen met een lange gebruiksduur, dient meer aandacht geschonken te worden aan het optreden van vermoeidheidsverschijnselen.

13

Het verminderen van de hoeveelheid spuitvloeistof in de gewasbescherming dient samen te gaan met een beter gebruik van persoonlijke beschermingsmiddelen.

14

Conus, shear vane en valgewicht zijn bruikbare hulpmiddelen bij het karakteriseren van mechanische eigenschappen van grond.

Dit proefschrift

15

Bij het ontwikkelen van een bewerkbaarheidstest verdient het aanbeveling het onderzoek te concentreren op methoden, die gebaseerd zijn op verkrumming.

Dit proefschrift

16

De invloed van de gelaagde opbouw van grond (toplaag, bouwvoor, ploegzool, ondergrond) op afsteunende processen is nog onvoldoende onderzocht.

Dit proefschrift

F.G.J. Tijink

Load-bearing processes in agricultural wheel-soil systems
Wageningen, 13 januari 1988

voor Agnes

VOORWOORD

Dit kleine stukje gebruik ik graag om iedereen te bedanken die een bijdrage heeft geleverd aan dit proefschrift.

Hiervoor ben ik allereerst dank verschuldigd aan mijn promotor prof. ir. H. Kuipers, die dit onderzoek mogelijk heeft gemaakt en die mij enthousiast heeft gemaakt voor dit vakgebied. Zijn warme belangstelling heeft mij erg geholpen bij het voltooien van dit proefschrift.

Mijn co-promotor Dr. ir. A.J. Koolen wil ik vooral danken voor de begeleiding van het onderzoek en de ondersteuning bij enkele met deze dissertatie samenhangende publicaties.

De heren B.W. Peelen en A. Boers dank ik voor hun hulp bij het verrichten van metingen.

De volgende studenten ben ik erkentelijk voor hun medewerking aan het promotie-onderzoek: Wim den Haan, Simon Hofstra, Harry Swinkels, Gertjan van Dijk, Jan Broekhuizen en Pieter Vaandrager.

Voor het tot stand komen van het manuscript wil ik graag danken: de heer B.W. Peelen voor het met zorg uitvoeren van al het tekenwerk en Mevr. drs. A.S.R. Riepma voor het met grote inzet corrigeren van de Engelse tekst.

De Stichting "Fonds Landbouw Export Bureau 1916/1918" en de Landbouwuniversiteit wil ik dank zeggen voor het beschikbaar stellen van subsidies ter bijdrage in de kosten verbonden aan dit proefschrift.

Dordrecht, 6 juli 1987

CONTENTS

CHAPTER 1	INTRODUCTION	13
CHAPTER 2	AGRICULTURAL ROLLERS, WHEELS, AND TYRES . . .	15
2.1.	ROLLERS	15
2.1.1.	Roller-packers	15
2.1.1.1.	Single roller-packers	15
2.1.1.2.	Composed roller-packers	16
2.1.2.	Roller-harrows	17
2.2.	WHEELS	17
2.3.	TYRES	18
2.3.1.	Highlights in tyre development	18
2.3.2.	Tyre construction	18
2.3.3.	Tyre size specification	20
2.3.4.	Tyres used in agriculture	22
2.3.4.1.	Tyres for driven wheels	23
2.3.4.2.	Tyres for undriven steered wheels	24
2.3.4.3.	Tyres for garden tractors	24
2.3.4.4.	Implement tyres	24
2.3.4.5.	Farm utility tyres	25
2.3.4.6.	Semi-tyres	25
2.3.4.7.	Other tyres used in agriculture	25
CHAPTER 3	KINEMATIC ASPECTS OF LOAD-BEARING PROCESSES	27
3.1.	STATE OF MOVEMENT OF A ROLLER, WHEEL OR TYRE	27
3.1.1.	Slip	28
3.1.1.1.	Zero-slip conditions	28
3.1.1.2.	Measuring methods for slip	32
3.1.1.3.	Wheel slip during ploughing	36
3.1.2.	Movements of a point at the rim of a roller or wheel	38
3.1.2.1.	Trajectory of a point at the rim of a roller or wheel	38
3.1.2.2.	Velocity of a point at the rim of a roller or wheel	39
3.2.	MOVEMENTS IN THE CONTACT AREA	39
3.2.1.	Tyre deformations	39
3.2.1.1.	Radial tyre deformation and sidewall bulging	39
3.2.1.2.	Tangential carcass and lug deformations	44
3.2.1.3.	Influence of tyre deformations on slip	46

3.2.2.	Movements of a point at the circumference of a roller, wheel, or tyre during motion in the mutual contact area	46
3.2.3.	Trajectories of soil particles in the contact area between the soil and a roller, a wheel, or a tyre	47
3.3.	SUBSURFACE MOVEMENTS	51
3.3.1.	Soil movements under rollers	51
3.3.1.1.	Distribution of soil velocities relative to the centre of a roller	51
3.3.1.2.	Flow zones under rollers	52
3.3.2.	Soil movements under wheels	52
3.3.3.	Soil movements under a tyre	53

CHAPTER 4 DYNAMIC ASPECTS OF LOAD-BEARING PROCESSES 55

4.1.	FORCES, MOMENTS, AND STRESSES ON ROLLERS, WHEELS, AND TYRES	55
4.1.1.	Mechanical equilibrium of rollers, wheels, and tyres	55
4.1.2.	Tractive performance	57
4.1.2.1.	Analysis	57
4.1.2.2.	Towed tyres	58
4.1.2.3.	Driven tyres	60
4.1.2.4.	Tractor tractive performance	64
4.1.2.5.	Ploughing capacity	68
4.2.	STRESSES IN THE CONTACT AREA	70
4.2.1.	Stresses in the contact area between soil and rigid wheel or roller	70
4.2.1.1.	Radial stress distribution	71
4.2.1.2.	Tangential stress distribution	71
4.2.2.	Stresses in the tyre contact area	71
4.2.2.1.	Average contact pressure	72
4.2.2.2.	Radial stress distribution	73
4.2.2.3.	Shear stress distribution	73
4.3.	STRESSES IN THE SOIL	75
4.3.1.	Stress distribution in the soil under tyres, wheels, and rollers	75
4.3.2.	Parameters that affect the stress distributions under agricultural driving equipment	77
4.3.2.1.	Soil parameters	77
4.3.2.2.	Trailer tyre concept	78
4.3.2.3.	Tractor type	79

CHAPTER 5	SOIL CHARACTERISTICS CONCERNING LOAD-BEARING PROCESSES	81
5.1.	RELATIONSHIPS BETWEEN "TREATMENT" AND "BEHAVIOUR" OF SOIL	81
5.2.	CHARACTERIZING PROPERTIES USED IN SOIL SCIENCE	84
5.3.	MECHANICAL PROPERTIES	87
5.3.1.	Compactibility	87
5.3.1.1.	Measures for compaction	87
5.3.1.2.	Measuring compactibility	88
5.3.1.3.	The influence of repeated loading, loading speed, and vibrations on compactibility	92
5.3.2.	Deformability	94
5.3.3.	Resistance against shear	95
5.4	CHARACTERIZATION PROCESSES	97
5.4.1.	Comparison of different cones	99
5.4.2.	Comparison of cone penetrometer, micro-penetrometer, vane, and torvane	101
5.4.3.	Relationships between cone-penetrometer, shear vane, and falling weight	103
CHAPTER 6	RELATIONSHIPS BETWEEN SOIL CHARACTERISTICS AND PROCESS ASPECTS AND THEIR SUITABILITY TO PREDICT PROCESS ASPECTS	105
6.1.	COMPARATIVE METHODS	105
6.2.	EMPIRICAL METHODS	106
6.2.1.	Empirical graphs	106
6.2.2.	Empirical methods using relationships between soil characteristics and process aspects	107
6.2.2.1.	Relationships between soil characteristics and tyre rolling resistance	109
6.2.2.2.	Relationships between soil characteristics and soil compaction due to wheel action	113
6.2.2.3.	Relationships between soil characteristics and rut depth	117
6.2.3.	Empirical formulas based on dimensional analysis	117
6.2.3.1.	Predicting off the road tyre rolling resistance	117
6.2.3.2.	Predicting tyre rolling resistance on a hard surface	126
6.3.	APPROXIMATE METHODS	128
6.4.	EXACT METHODS	131
6.4.1.	Slip line methods	131
6.4.2.	Finite element methods	131
6.5.	CLOSING REMARKS ON PREDICTION METHODS	131

CHAPTER 7	SOIL PHYSICAL ASPECTS OF LOAD-BEARING PROCESSES	133
7.1.	THE INFLUENCE OF PHYSICAL PROPERTIES ON MECHANICAL PROPERTIES	133
7.1.1.	The influence of aggregate diameter on uniaxial compressibility	134
7.1.2.	The influence of soil air on rebound	139
7.2.	THE INFLUENCE OF MECHANICAL TREATMENT ON PHYSICAL PROPERTIES	146
7.2.1.	The influence of mechanical treatment on micro-factors and soil qualities	146
7.2.2.	Tillability	147
7.2.2.1.	Tillability test	147
7.2.2.2.	Tillability tests based on processes other than crumbling	148
7.2.2.3.	Tillability tests based on crumbling processes	150
CHAPTER 8	SUMMARY	161
CHAPTER 9	SAMENVATTING	162
	REFERENCES	163

CHAPTER 1

INTRODUCTION

Research in agricultural soil mechanics focused first on soil loosening processes. Scientific papers on load-bearing processes have been published in fair amounts since the early 1950s. Generally these papers only deal with one single aspect of a particular load-bearing process.

Load-bearing processes can be induced by rollers, wheels, tyres, penetrating bodies, sliding and shearing bodies, or tracks. Agricultural traction and transport devices generally have rolling machine parts that touch the soil directly. Therefore, this dissertation concentrates on systems with rollers, wheels, or tyres.

The aim of this study is to cover fundamental, characterizing, and predicting aspects of load-bearing processes in agricultural wheel-soil systems.

A classification of agricultural rollers, wheels, and tyres is presented in chapter 2.

Process fundamentals are kinematic, dynamic, and soil physical aspects. The kinematic and dynamic aspects are discussed as follows:

- the kinematics of the roller, wheel, or tyre (3.1.)
- the movements in the contact area (3.2.)
- the subsurface movements (3.3.)
- the dynamics of a roller, wheel, or tyre (4.1.)
- the stresses in the contact area (4.2.)
- the stresses in the soil (4.3.)

The kinematics of the "wheel" concentrates on wheel slip, measuring methods for slip, and wheel slip during ploughing. Several parameters that affect the kinematic and dynamic aspects are discussed also.

Soil characteristics concerning load-bearing processes are discussed in chapter 5. Special attention is paid to characterizing processes (5.4.). We have made comparisons of different characterizing processes in order to choose those tests with which maximum information about the soil can be obtained with a minimum of tests.

Prediction methods have been divided into:

- comparative methods (6.1.)
- empirical methods (6.2.)
- approximate methods (6.3.)
- exact methods (6.4.)

The relationships between soil characteristics and process aspects have been tested for their suitability to predict process aspects. Predictions concentrate on predicting rolling resistance, rut depth, and soil compaction due to the passing of a towed tyre.

Chapter 7 deals with the soil physical aspects of load-bearing processes. Both the influence of soil physical properties on mechanical properties and the influence of soil mechanical properties on physical properties are discussed. The former concentrates on the influence of soil aggregate diameter and soil air, while the latter pays special attention to tillability.

CHAPTER 2

AGRICULTURAL ROLLERS, WHEELS, AND TYRES

A distinction needs to be made between rollers and wheels. Therefore, it is necessary to give some definitions before a classification can be made. Rollers have as most important functions: pressing and firming of the surface soil. The most important characteristic of wheels is their transport function. So a rolling device, with a narrow width relative to the diameter, is called roller when it is used for firming a strip of soil. The same device is called wheel if it has a transport function.

2.1. ROLLERS

Rollers can be divided into two groups: roller-packers and roller-harrows. Roller-packers have as most important functions: pressing and firming of soil. Roller-harrows are the intermediates between roller-packers and harrows. Rollers are often components of seed-bed preparing combinations.

2.1.1. ROLLER-PACKERS

Rollers can have one or more sections. A section consists of an operating part that has been mounted on a rectangular frame. An operating part can have one or more elements. Main parameters of agricultural roller-packers have been given by Schilling (1962), Bernacki et al. (1972), and Estier et al. (1984).

2.1.1.1. SINGLE ROLLER-PACKERS

These have operating parts with only one element. Plane rollers have smooth cylindrical elements. The light plane rollers are used for firming and smoothing of arable land. Clods are crushed to some extent and pressed into the soil. Narrow plane rollers, often fitted with semi-tyres, are used in drills to firm the seed-bed. The heavy plane rollers are used on grassland for recompaction after frost damage. Driven plane rollers are used as

part of disinfection equipment for soil. Rollers fitted with prickers can be used for maintenance of sports fields. A sheep-foot roller can be used for the puddling of wet rice fields. Sometimes a mudroller is used for this (Scheltema, 1974).

2.1.1.2. COMPOSED ROLLER-PACKERS

The sections of these rollers are composed of a number of elements which are either rings or discs. The elements can move independently of each other.

Smooth ring rollers. This type of roller leaves a rougher soil surface than a plane roller. As a result there is less danger of erosion.

Serrated rollers. Serrated rings have better ground contact than smooth rings. These rollers are often used in grass seeders.

Toothed rollers have crust-breaking qualities.

Cambridge rollers consist of smooth rings and flat-toothed discs of greater diameter set alternately. The toothed disc can rotate freely of the ring hub. Slight differences in number of revolutions of rings and discs, resulting from different diameters, cause the Cambridge rollers to be self-cleaning. Compared with smooth ring rollers Cambridge rollers crush soil clods more intensively and firm the soil more deeply, leaving shallow crevices on the surface and a slightly pulverized soil.

Croskill rollers consist of rings secured to the periphery with several lateral lugs. Croskill rollers provide aggressive breaking and crushing of clods and a somewhat shallower packing than Cambridge rollers. Similarly to the Cambridge roller the Croskill rings can be separated by toothed discs.

Furrow packers. The above-mentioned roller-packers can not accelerate the process of soil settlement. The use of very heavy packers for this purpose would cause better packing of soil sublayers, but the top soil would be packed too strongly. Furrow packers are used when there is not enough time for natural soil settlement between ploughing and seed-bed preparation. Working elements are narrow wedge rings, smooth or toothed, set on spokes. The ring penetrates easily into the soil to a depth of ten or more centimeters and firms the lower soil layers. The upper soil layer remains loose and can even be pulverized additionally by the ring spokes. Furrow packers are often used in combination with ploughs.

2.1.2. ROLLER-HARROWS

These rollers have no pronounced packing task, but are used for soil crushing.

Roller-crumblers or string-rollers form a thin well-pulverized surface on top of a slightly packed layer. Especially the roller-crumblers with small diameters have good crushing qualities. Roller-crumblers generally are components of combined tillage implements and are available in many designs and constructions.

Rotary harrows with spiked teeth or knives move like rollers, but according to their effects they should be classified as harrows.

2.2. WHEELS

The wheel, one of the greatest inventions of mankind, meant a big step forward in transportation. Archaeological evidence indicates that the essentially wheel-like form was invented in Sumer in ancient Mesopotamia around 3500 BC. The first wheels were solid-disc wheels of wood with a 0.50 - 1.00 m diameter and a width of 0.10 - 0.15 m. They were towed by oxen.

Even the earliest wheels were fitted with a kind of wearing surface (tyre). Copper was the first product used for this purpose (Freitag, 1979). The spoked wheel towed by horses appeared around 2000 BC.

The first-known concept of a powered vehicle is a drawing of a wind-powered vehicle, made by Valturo in 1472. In the 18th century the first attempts were made to create steam-powered vehicles.

The use of powered wheels in agriculture was much encouraged by the invention of the internal combustion engine. The first agricultural tractors had smooth steel wheels and therefore, had severe wheel-slip problems. The wheels were fitted with a few lugs to lower wheel slip. In the early 1900s wheels were available with different lug patterns.

After the introduction of tractor and implement tyres in the early 1930s, the rigid (steel) wheels almost completely disappeared from agricultural machines. In modern agriculture wheeled agricultural tractors are fitted with pneumatic tyres. Sometimes a remainder of the days before the agricultural pneumatic tyres is fitted to the tractor in addition to the driven wheel. One of the remainders is the strake: a device to improve traction under poor surface conditions on cohesive soils. Cage wheels can be used to reduce compaction of the seed-bed during seeding operations. A similar construction known as puddle wheels can be used in paddy field preparation because of their puddling effect. Sometimes steel wheels are used for depth control of tillage tools, but in general the steel wheel has only a supplementary task.

For transport purposes the rigid wheel has been almost completely replaced by wheels with pneumatic tyres.

2.3. TYRES

2.3.1. HIGHLIGHTS IN TYRE DEVELOPMENT

The first patent describing a pneumatic tyre was granted to R.W. Thompson in 1845 and the first practical tyred wheel was developed by J.B. Dunlop in 1888. His tyre was fitted on a bicycle wheel. Further development resulted in passenger car tyres at the turn of the century and availability of truck tyres in the early 1920s.

Because operating conditions in agriculture are considerably more rigorous than on the road it was not until the early 1930s that tyres with an adequate field performance were generally available. The first tractor rear tyres were introduced by Firestone and Continental, while Dunlop introduced the first implement tyre.

A further highlight in history of agricultural tyres was the introduction of the radial-ply tractor rear tyre by Pirelli about 1957.

Other important factors in the development of modern low pressure tyres are:

- the use of nylon as carcass material
- wide base rims
- tubeless tyres.

2.3.2. TYRE CONSTRUCTION

Fig. 2.1 shows the most important components of a pneumatic tyre.

The carcass consists of cord layers (plies) laid in specific directions. The flexible carcass carries the inflation stresses and gives strength to the tyre. Carcass strength depends on the properties of the cords used, the angle between the cord layers, and the number of plies in the carcass.

Originally the tensile strength of the carcass was specified by mentioning the number of plies of cotton. Later on other materials with a higher tensile strength than cotton were used in tyre construction, and therefore the strength is given in ply-rating (*PR*). This is an index of tyre strength to cotton strength and does not necessarily state the number of plies. *PR*-values do not give information about the allowed driving speed. In the near future *PR* will be replaced by a Load Index (*LI*) and a Speed Symbol. These new marks have been standardized in the E.E.C. for agricultural tyres, tyres for passenger cars, and truck tyres. The first tyres with these new marks are already on the market. More details about *LI* and Speed Symbols are given in section 2.3.3.

Detailed information about materials and their properties can be found in Clark (1971a).

Conventional tyres have a cross ply construction. Successive cord layers of this tyre type cross each other at an angle of about 60 to 80 degrees (Fig. 2.2). The cords of radial-ply tyres run

radially from bead to bead. A stiff belt for improved stability has been added to radial tyres. This construction makes for relatively flexible sidewalls together with a well-braced tread.

The *bead* must keep the inflated tyre on the rim seat and press the tyre against the rim flanges. Therefore, the bead usually has a coil of steel bead wires.

The *sidewall* protects the carcass. The rubber of the sidewall must have excellent resistance against fatigue and aging.

The *tread* is bonded to the carcass and the pattern is moulded in the tread. Tyre operating performance and driving qualities also depend on the type of tread pattern.

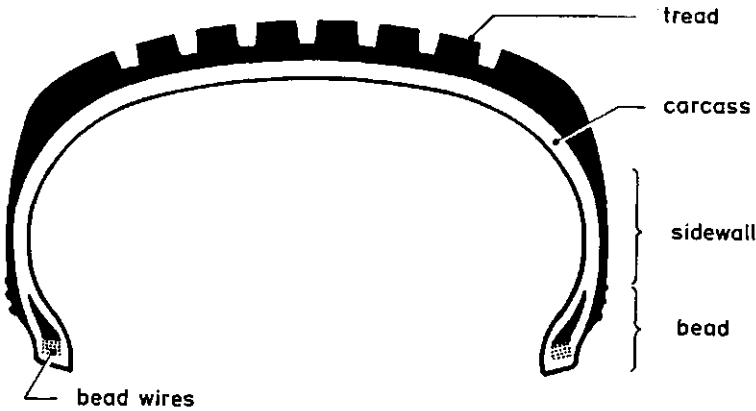


Fig. 2.1. Main components of a tyre.

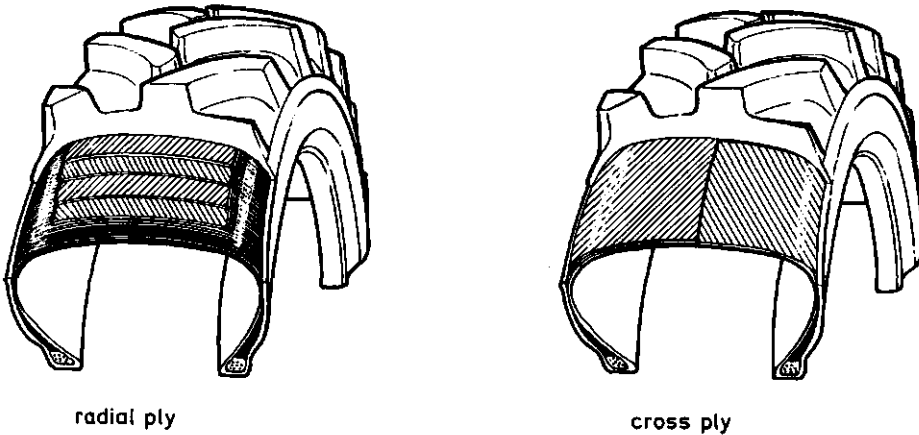


Fig. 2.2. Ply construction of tyres.

2.3.3. TYRE SIZE SPECIFICATION

The size of the early agricultural tyres was specified by quoting the section width b and the nominal rim diameter d , both specified in inches (Fig. 2.3). These tyres had an aspect ratio h/b of about 1.0. An 11-36 tyre had a section width of 11 inches and a rim diameter of 36 inches. This resulted in an approximate overall diameter D of $d + 2h = 58$ inches.

Introduction of the extra wide base rim in the middle of the 1950s resulted in a wider cross section b for the same section height h , and therefore the aspect ratio h/b decreased from about 1.0 to about 0.85. The new section width was added to the indication: 12.4/11-36.

Nowadays the old section width has disappeared from the size designation so that the tyre size 12.4/11-36 is now specified as 12.4-36.

The development of tyres with even lower aspect ratios resulted in the inclusion of the aspect ratio in the tyre designation: 9.0/75-18.

At present there are many tyre size specifications in agriculture. The reason is the continual introduction of new types of agricultural tyres and the use of tyres from other fields of application in agriculture.

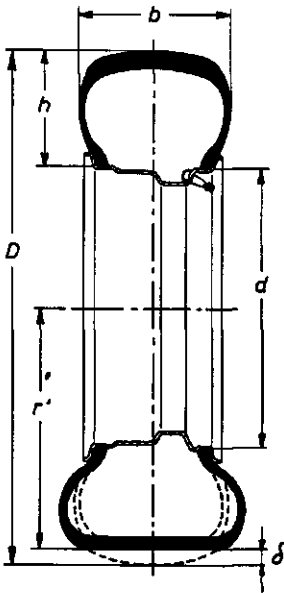


Fig. 2.3. Tyre and rim description.

b = tyre section width
 D = overall tyre diameter
 d = rim diameter

δ = tyre deflection
 h = tyre section height
 r' = static loaded radius

Recently standards for tyre size, Load Index (LI), and Speed Symbol have been accepted within the E.E.C. Load Index indicates the allowed tyre load W_A in a number code. Tyre catalogues generally contain tables with LI and W_A . LI can have values between 0 and 209; corresponding W_A values range from 450 N to 185,000 N. The relationship between W_A and LI can be expressed as:

$$W_A = 450.10^{(LI/80)}$$

Speed symbols up until 40 km/h are important for agricultural purposes. The speed symbol for this field of application is the letter A and a number between 1 and 8. This number multiplied by 5 shows the allowed driving speed. A6, for example, means an allowed driving speed of 30 km/h.

Although there was no agreement about a symbol for inflation pressure, some manufacturers nowadays mark their tyres with a symbol for this aspect as well. Inflation pressure is marked by one, two, or three stars. One star means that the allowed tyre load is based on an inflation pressure of 1.6 bar. At two or three stars allowed loads are based on inflation pressures of 2.4 bar and 3.2 bar respectively.

Fig. 2.4 shows an example of the marks that can be found on a modern West European tractor rear tyre:

18.4 R 38 146 A8 *

Where,

- 18.4 = tyre width of 18.4 inches (=46.7 cm)
- R = Radial tyre; Cross ply tyres do not have letter R
- 38 = rim diameter of 38 inches (=96.5 cm)
- 146 = Load Index: maximum allowed load of 30 kN
- A8 = maximum allowed driving speed of 40 km/h
- * = allowed load is based on an inflation pressure of 1.6 bar.

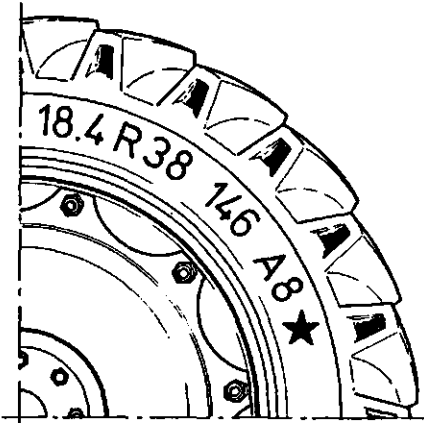


Fig. 2.4. Indications on a modern West European tractor tyre.

2.3.4. TYRES USED IN AGRICULTURE

A wide variety of tyre types and sizes is available. Each type has its own special fields of application. The tread pattern is based on the functional requirements of the tyre and is therefore a good visual guide to the expected use of the tyre.

Identification of the various types of agricultural tyres has been facilitated by the adoption of a uniform code-marking system (Table 2.1). This code has been initiated in the USA by the Tyre and Rim Association and has been adopted by the American Society of Agricultural Engineers (ASAE) and the European Tyre and Rim Technical Organization (ETRTO). The intention was to stamp the code on each tyre, but in practice the manufacturers marked their tyres with trade names. Sometimes the code marking is given in manufacturers' catalogues beneath the trade identifications.

A more simple identification code is used in West Germany. Tractor rear tyres have the code AS (Ackerschlepper). The codes AW (Ackerwagen) and AM (Ackermachine) are used for implement tyres. Tractor front tyres have the code AS-Front.

Table 2.1. International tyre code.

	tyre type	code marking
Rear Tractor:	Regular Agriculture	R ₁
	Rice and Cane	R ₂
	Industrial and Sand	R ₃
	Industrial-Lug Type	R ₄
Front Tractor:	Single Rib	F ₁
	Regular Agriculture	F ₂
	Industrial Rib	F ₃
Garden Tractor:	Regular Garden	G ₁
	Intermediate Tread	G ₂
	Rib Tread	G ₃
Implement:	Rib Tread	I ₁
	Utility	I ₂
	Traction Implement	I ₃
	Plough	I ₄
	Plough	I ₅
	Smooth Tread	I ₆

2.3.4.1. TYRES FOR DRIVEN WHEELS (Tractor Rear)

Tyres for driven wheels generally have a V-shaped tread pattern. The normal direction of rotation of these tyres is such that in the "footprint" the top of the V points in opposite travelling direction. Sometimes the rotation direction for driven front tyres is reversed to prevent excessive wear in road traffic. Tread patterns can be classified into groups with almost equal characteristics. These tread pattern groups are discussed below.

Conventional field tread pattern (R₁)

This is a general purpose open centre tread for maximum self-cleaning. Tread density is about 30 %. One manufacturer supplies a variant with a lug angle of 67 degrees instead of the normally used angle of 40 to 45 degrees.

Conventional field-road tread pattern (R₁)

Tyres with an increased tread density (of about 50 %) are useful when the tractor is often driven on the road. The lugs are wider in the middle than on the sides of the tread. These tyres are intended for use on grassland farms and on non-cohesive soils.

Half-high tread pattern (R₁)

Tyres with lugs which are about 30 % higher than those of tyres with a conventional field tread have been designed for use on cohesive soils. Modern tyres of this type often have a radial-ply construction and are also useful when much time needs to be spent on the road.

High-speed road-field tread pattern (R₁)

A tread with many low lugs characterizes tyres which can be used when the tractor is driven at a speed which is higher than the normal maximum of 40 km/h for agricultural tyres. Also, these tyres are useful on non-cohesive soils when relatively low pulls are needed.

High-lugged tread pattern (R₂)

Tyres with extra high, often curved, lugs and a low tread density are intended for use on very wet and cohesive soils. On the road they have uncomfortable driving qualities and excessive wear. Harvesters are often fitted with these tyres.

Sports Fields tread pattern (R₃)

Tyres with a continuous low tread pattern cause little turf disturbance in recreational grassfields. The self-cleaning ability and the power output of tyres with this tread are relatively low.

Industrial-lugged tread pattern (R₄)

Tyres with a high tread density (of about 70 %) are mainly intended for road work, but perform well off the road when high pulls are not required. Besides, these tyres can be used to advantage for earth-moving and in mining operations.

2.3.4.2. TYRES FOR UNDRIVEN STEERED WHEELS (Tractor Front)

Tractor front tyres generally have high circumferential ribs to provide easy steering and resistance to side slipping. Sometimes tractor front wheels are fitted with tyres having a sports field tread pattern.

Single Rib (F₁)

Marked by a smooth tread and having one circumferential rib, this tyre has been especially designed for use in extreme mud conditions found in wet rice and cane fields.

In the Netherlands some potato planters have been fitted with these tyres.

Regular Rib (F₂)

These tyres have one to three longitudinal ribs. Sometimes there are "climbing lugs" on the shoulders to make it easier to get out of a furrow.

Industrial Rib (F₃)

Front tyres with five longitudinal ribs and a wider tread than the previously mentioned two types of patterns, characterize this tyre.

2.3.4.3. TYRES FOR GARDEN TRACTORS

Regular Garden (G₁)

This is generally a small-sized tyre with conventional field or field-road tread. There are sometimes narrow connections between the lugs to prevent grass from winding around the tyres.

Intermediate Garden (G₂)

This is a tyre with a tread pattern similar to the sports field tread (R₃).

Garden Rib (G₃)

This tyre has a ribbed tread pattern for use on front wheels. Compared with a normal front tyre (F₁, F₂, F₃) this tyre has a wider tread for better flotation on soft wet lawns or on loose soils.

2.3.4.4. IMPLEMENT TYRES

Usually the tread of an implement tyre is rather wide because of the following requirements:

- low inflation pressure for good field performance
- small diameter for low trailer platform height
- high load-carrying capacity.

Implement Rib (I₁)

A general purpose implement tread has several longitudinal ribs

for good direction stability and limited side slip. A variant is the tyre with serrated grooves for use on non-cohesive soils and when much road traffic is necessary.

Implement Utility (12)

This tread is similar to the sports field tread (R₃).

Traction Implement (13)

Tyres of ground-driven implements usually have a conventional field or a conventional field-road tread pattern. The direction of rotation is opposite to the one of driven tractor rear tyres.

Plough (14, 15)

Here we deal with a tyre for the rear or tail wheel of ploughs. The tread has two (14) or three (15) heavy ribs. This tyre runs in the plough furrow at an angle of about 15 to 30 degrees. One shoulder takes the vertical stress due to load and the other one takes the side stress from ploughs on the vertical side of the furrow.

2.3.4.5. FARM UTILITY TYRES

This group contains tyres for small agricultural equipment such as hay tedders, elevators, and wheel-barrows. These tyres are available in many different tread patterns.

2.3.4.6. SEMI-TYRES

These special tyres are used without effective pressure and, as a consequence, are highly flexible and self-cleaning. The tread has ribs or very small lugs. Semi-tyres are used on narrow rollers of seed drills and on wheels of inter-row cultivation implements.

2.3.4.7. OTHER TYRES USED IN AGRICULTURE

Tyres, originally designed for other fields of application, are also used in agriculture. Farm waggons are sometimes fitted with second-hand tyres from passenger cars and trucks. Sometimes, when high load-carrying capacities are required earth-mover tyres, aircraft tyres or terra tyres are used.

Earth-mover tyres are flexible and have a high load-capacity at a relatively low inflation pressure. Earth-mover tyres used in agriculture are generally of the flotation-type (E₇): moulded with longitudinal ribs or with a sports field pattern.

Aircraft tyres usually have a wide tread, a high load-carrying capacity and are relatively cheap. They have a stiff carcass and a rather round cross section. Therefore, aircraft tyres generally

show lower field performance than tyres designed for agricultural purposes. Size specification deviates from normal agricultural specification. When aircraft tyres are remoulded with an agricultural tread pattern, they normally get an agricultural tyre size specification.

Terra tyres have been developed especially for applications where very high flotation properties are required. In comparison with conventional tyres they have a wider cross section, a larger air volume, a more flexible carcass, and they operate at lower inflation pressures. Because of the high flotation effect they have a rather good go-anywhere performance. The tread pattern of *terra* tyres is available in different designs: smooth, ribbed and lugged. They can be used, depending on tyre size and loading, at inflation pressures of 0.35 bar and higher. Tyre size specification is different from normal agricultural indications. In the Netherlands some heavy self-propelled slurry tanks, combine harvesters, and sugar beet harvesters are fitted with *terra* tyres.

CHAPTER 3

KINEMATIC ASPECTS OF LOAD-BEARING PROCESSES

3.1. STATE OF MOVEMENT OF A ROLLER, WHEEL, OR TYRE

A roller, wheel, or tyre can have two basic velocities: angular velocity ω and forward velocity v (Fig. 3.1). Moving traction and transport devices can be in five different situations:

- free rolling: the rolling circumference is equal to $2\pi r_0$
- slip: the rolling circumference $< 2\pi r_0$
- skid (negative slip): the rolling circumference $> 2\pi r_0$
- 100 % slip: when $\omega \neq 0$ and $v = 0$
- 100 % skid: when $\omega = 0$ and $v \neq 0$.

In normal road and field traffic a traction device always has travel reduction and a transport device skids. Free rolling is only possible when internal resistance and motion resistance are negligible. At 100 % skid the behaviour of a transport device will have properties of a bulldozing blade. A traction device at 100 % slip in the field digs itself more deeply into the ground.

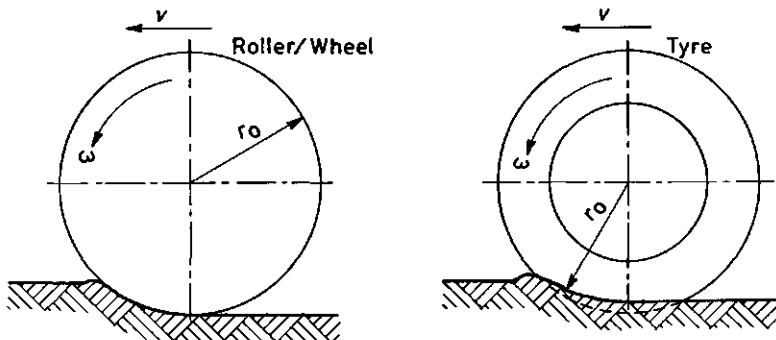


Fig. 3.1. Principal velocities of rollers, wheels, and tyres.

3.1.1. SLIP

Slip is the relative movement in the direction of travel at the mutual contact surface of the traction or transport device and the surface which supports it (ASAE Standard S296.2; Hahn et al., 1984). Travel reduction is defined as one minus the ratio of distance travelled per revolution of the traction device to the rolling circumference under the specified zero conditions. Slip and travel reduction are often used synonymously, and are frequently expressed in percentages.

Slip S (Bock, 1952; Söhne, 1952) is defined as:

$$S = \frac{s_0 - s_a}{s_0} = 1 - \frac{s_a}{s_0} \quad [3.1]$$

where, s_a = real travelled distance

s_0 = travelled distance at zero slip.

Slip can also be defined in velocities (Bailey et al., 1974):

$$S = \frac{\omega - v/r_0}{\omega} \quad [3.2]$$

where, ω = angular velocity of the traction device

v = linear velocity of the traction device

r_0 = rolling radius under specified zero condition.

Analyses of Söhne (1969) and Steiner (1979) show that wheel slip of a tyre on deformable soil is composed of three components:

- tangential carcass and lug deformation
- tangential soil deformation
- slipping in the contact area.

3.1.1.1. ZERO-SLIP CONDITIONS

For a flexible device such as a pneumatic tyre it is difficult to define zero slip and no one has been able to determine the exact position of the zero-slip point. The problem is that there is always relative movement in the mutual contact area when a vehicle system is in motion. Using the slip formulas has the following problems: r_0 can not be measured directly and s_0 can not be measured at zero slip. According to Gill and Van den Berg (1967) the problem of measuring wheel slip is a problem of defining and measuring zero slip.

Fig. 3.2 shows the principle path of gross traction T/r_0 , with T = torque, and pull P to slip after Schüring (1968). Slip is equal to zero somewhere between $T/r_0 = 0$ and $P = 0$. The exact place of the zero-slip point is unknown, but according to Söhne it is somewhat closer to the towed position ($T/r_0 = 0$) than to the self-propelled position ($P = 0$) because of the flow of soil particles in the run-in zone of the tyre.

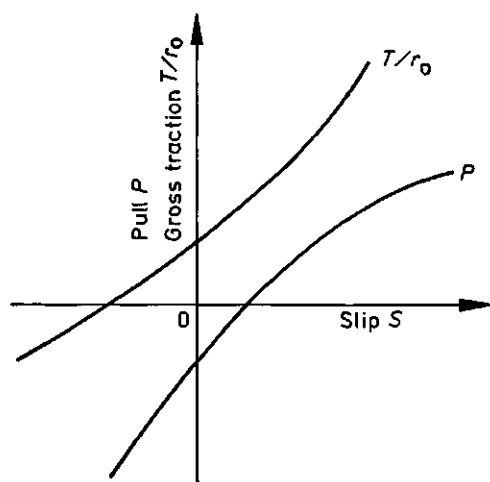


Fig. 3.2. Principal path of gross traction and pull to slip (Schüring, 1968).

The zero condition generally is a performance condition or is calculated from performance conditions. Conditions used to define zero slip are: the self-propelled position, the towed position, and the point halfway between the self-propelled position and the towed position. Other zero conditions may be used, but no other practical solutions have been found in literature. The specific zero conditions chosen should always be mentioned.

Self-propelled position (SPP)

The SPP on a hard surface was used by Wismer and Luth (1973), Melzer (1976), and others. Terpstra and van Maanen (1972) used the SPP on a grass-field as zero condition. Bailey et al. (1974), Dwyer et al. (1974), Gee-Clough et al. (1977), and many others used the SPP on the test surface.

The distance between SPP and towed point (TP) on the slip axis will be longer when the field conditions get worse. The definition slip is zero in the SPP will then be undesirable. A single wheel operating in the SPP on a field, where the performance conditions change gradually from good to bad, only has to overcome an increasing rolling resistance. If even in the worst conditions slip is supposed to be zero as long as $P = 0$ the wheel can not get stuck. However, a spinning wheel has 100 % slip and still $P = 0$.

On sandy loam with a moisture content of 23.5 % Holm (1969) measured with a 12.4/11-28 buffed tyre that pull was zero at 15 % slip (r_0 calculated from tyre deflection measurements). At a moisture content of 16.5 % and a somewhat lower wheel load he found zero pull at zero slip.

Steinkampf (1971) shows the influence of the way of determining rolling radius r_0 on the pull and rolling resistance curves. In Fig. 3.3 curve P_2 , which can be compared with Holm's curve (1969), has a value of $P = 0$ at $S = 15\%$ (rolling radius

$r_{02} = 0.78$ calculated from tyre deflection measurements). Calculating the rolling radius from the rolling circumference in the SPP, gives a value of $r_{01} = 0.67$ m and the path of pull and rolling resistance versus slip would be like P_1 and R_1 .

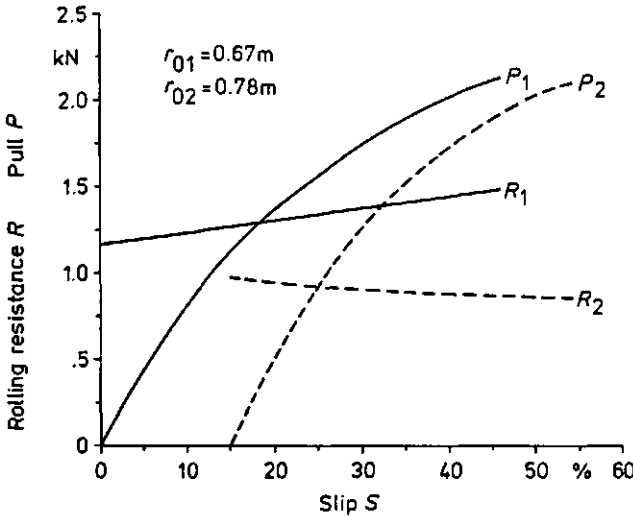


Fig. 3.3. Influence of rolling radius on pull and rolling resistance curves (Steinkampf, 1971).

Gee-Clough et al. (1978) found nearly 10 percent higher no-slip speeds on the road than in the field. These differences must be due mainly to slip when the tractor is in the self-propelling position in the field.

We drove an unballasted tractor under different good driving conditions on grassland (Wageningen sand), on a maize stubble field (Wageningen sand), and on concrete. The distance of 20 tyre revolutions was measured while we were driving at 2000 rpm in 6 different gears.

At an inflation pressure $p_1 = 0.8$ bar the ratio travelled distance grass/concrete had values ranging from 0.981 to 0.998. On the stubble field the ratio travelled distance stubble/concrete varied from 0.963 to 0.999. At $p_1 = 1.5$ bar this ratio had values ranging from 0.975 to 0.990. On concrete the ratio distance travelled of $p_1 = 0.8$ bar to $p_1 = 1.5$ bar varied from 0.978 to 0.981. The average travelled distances in the field were shorter than on concrete: 1.2 % and 1.5 % on grassland and stubblefields respectively.

The preceding results show clearly that the SPP as zero condition is only useful under good traction conditions. The use of the SPP as zero condition under less ideal traction conditions may give misleading and even useless results. The best SPP as zero condition is the one measured on a hard surface.

Towed position (TP)

Analogous to the self-propelled position the use of the towed point as zero slip condition is realistic under good traction conditions. The use of the TP as zero condition under less ideal traction conditions is undesirable. The most useful TP as zero condition is the one measured on a hard surface.

The point halfway between SPP and TP

Bock (1952) measured pull versus slip of a tractor in the field. As travelled distance he used s_0 in n revolutions at zero slip, the mean of the self-propelled distance s_1 and the distance travelled s_2 when towed by another tractor. Thus $s_0 = (s_1 + s_2)/2$.

At the Technical University of Munich (Steiner, 1978 and 1979) and the FAL of Braunschweig-Völkenrode (Steinkampf, 1971), the rolling radius r_0 of a tyre was found by iteration to that value for which the linear regression lines through measuring points of gross traction and pull intersect the slip-axis at equal distances from zero (Fig. 3.4).

The advantage of choosing the zero-slip condition at the point halfway between the SPP and the TP, above the zero conditions measured at SPP and TP, is that this point is nearest to the theoretical zero condition.

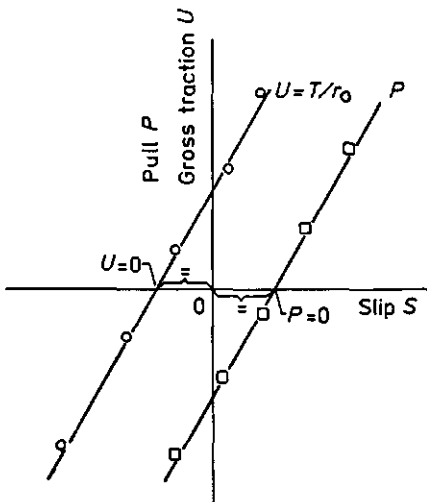


Fig. 3.4. Position of the zero-slip point (Steiner, 1978).

The way of determining the zero-slip condition used in Munich and Braunschweig-Völkenrode is, in theory, better than Bock's method because of the absence of front tyres using a single-wheel tester, but has as a disadvantage the need of very advanced test equipment. The presence of front tyres in the method of Bock can be the reason that there is still a force in the horizontal

direction at s_0 . Under good traction conditions this force can be neglected. Under worse conditions this force can cause small deviations from the theoretical zero-slip point. The advantage of the method of Bock is its simplicity of making measurements and calculations.

3.1.1.2. MEASURING METHODS FOR SLIP

There are many known slip-measuring methods. Two groups can be distinguished: methods measuring instantaneous slip and methods measuring mean slip over a travelled distance.

Measuring instantaneous slip

To measure instantaneous slip advanced measuring equipment is needed. In wheel testers as used by IMAG in Wageningen (Werkhoven, 1975) and NTML in Auburn (Bailey et al., 1974) electronic pulses for forward velocity and angular velocity, processed by a computer, can give instantaneous values of slip. Thansandote et al. (1977) used a microwave Doppler radar to measure the true ground velocity of the tractor and the circumferential velocity of the driven wheel. They concluded that the Doppler radar slip monitor seems to be feasible as a practical device for use on agricultural tractors. Since the late 1970s Doppler radar sensors are being installed in automatic sprayer control systems. In such a system the radar sensor, mounted on the tractor, is used for measuring the true driving speed. If the forward speed changes, the control system automatically alters the sprayer settings to maintain the target application rate. Since the early 1980s many makes of tractors can be equipped, standard or as an optional, with a tractor monitor. Such an instrument can display the true driving speed or the slip percentage of the driven wheels.

A new generation Doppler radar sensors was introduced in 1985. According to Kellermann (1985) these sensors can achieve an accuracy of $\pm 1\%$. Boll and Isensee (1987) found a much lower accuracy in farm fields.

A radar sensor must be mounted on the tractor so that it is pointing to the ground at a correct angle. This angle is crucial concerning the accuracy of the instrument: a change in this angle results in a deviation of about 1 % per degree (Schmitt, 1986).

A tractor linkage-control system with slip control was introduced at the 1985 agricultural machinery show "Agritechnica" in Frankfurt. In this system (Fig. 3.5), the electronics calculate slip by measuring the true speed of the tractor with a Doppler sensor and the theoretical (no slip) speed by measuring a shaft rotation in the final drive. During ploughing operations the electronic draft control system operates up until the pre-set slip ceiling (of 15 % slip). If slip exceeds this limit ploughing depth is controlled by the slip control which gives a signal to raise the plough in order to reduce wheel slip. The number of centimeters the plough is raised is less than 10 percent of ploughing depth. According to Hesse (1986) this system saves fuel and time at ploughing.

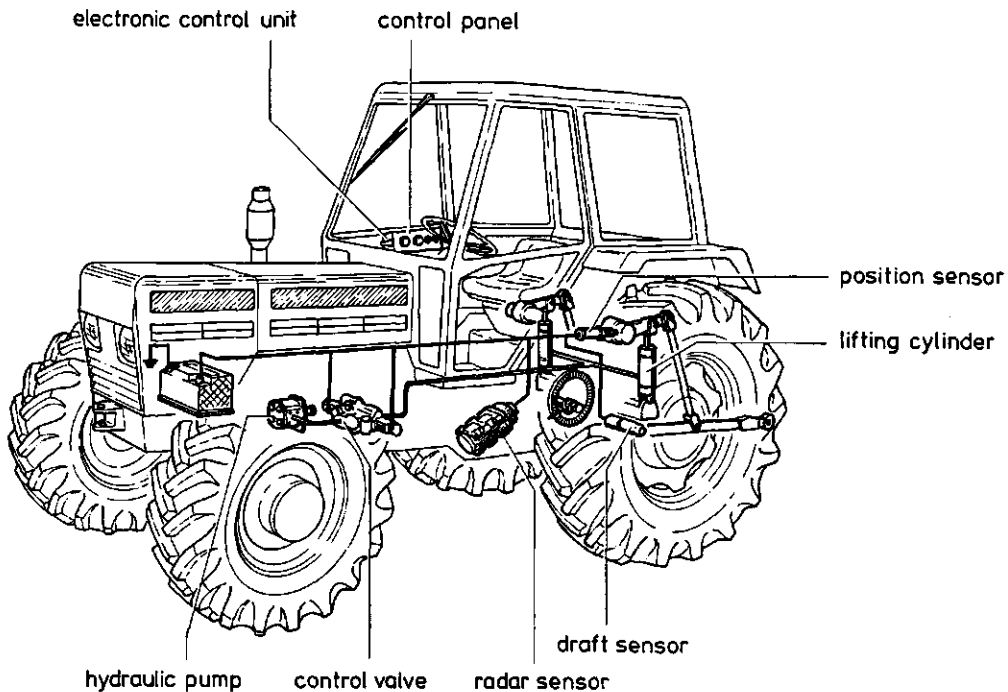


Fig. 3.5. Electronic linkage-control system with additional slip control (Bosch).

Mean slip over a travelled distance

The most popular method of measuring slip is the one that measures the travelled distance s_a in n revolutions and compares this with the travelled distance s_0 under the zero condition. A variation on this is counting the revolutions within a certain distance. Sometimes electronic equipment is used for counting the number of tyre revolutions.

For our investigation of slip during ploughing on farms, we needed a slip measuring method with the following qualities:

- easy to use and transport
- easy to fit up
- non-time-consuming for the farmer.

Except providing the self-propelled position, none of the methods from literature meet the first two requirements. Because measurements under bad field conditions were also envisaged, the SPP as zero condition was not useful. It would also have cost the farmer too much time. So we had to find a new method for our measurements.

Tyre manufacturers provide tables with tyre dimensions. From tables given by Continental, Dunlop, Fulda, B.F. Goodrich, Good Year, Kléber, Michelin, Trelleborg, Velth, and Vredestein, tyre diameter D and the rolling circumference RC_0 under the zero condition on a hard testsurface were used. For 298 tractor rear

tyres the ratio RC_0/D was calculated. This resulted in a mean value of 3.000 with a standard deviation of 0.032. So slip can also be defined as:

$$S = 1 - \frac{s_a}{3D} = 1 - \frac{s_a}{6r} \quad [3.3]$$

where, s_a = the actual travelled distance per revolution
 D = the tyre diameter
 r = the tyre radius.

The calculated rolling circumference values (using $RC_0=3D$) fitted the manufacturers values ($r=0.997$) very well. The largest deviations were $\pm 2.5\%$. These maximum deviations declined linearly with increasing slip from $\pm 2.5\%$ at $S = 0\%$ to 0% at $S = 100\%$. To calculate slip with formula 3.3 the tyre diameter D or radius r and the travelled distance per revolution have to be known. In practice this means measuring the radius of the tyre and the travelled distance in n revolutions.

The rolling circumferences RC_0 , given in manufacturers' tables, are determined when the wheel is self-propelling on a hard surface with a load equal to half of the maximum load and an appropriate inflation pressure. At a maximum load the rolling circumference can deviate 1 to 2%, depending on tyre construction. Our measurements with a 13.6-38 cross ply tyre at different inflation pressures on concrete and sand show little difference between calculated slip with formula 3.3 ($S = 1 - s_a/6r$) and calculated slip with $S = 1 - s_a/s_0$ (see Table 3.1). For practical purposes there is no need to correct formula 3.3 because of the use of a lower or higher inflation pressure than the inflation pressure used in the manufacturers' RC_0 -determinations. In general it is clear that measuring slip while using formula 3.3 is a simple and rather accurate method.

Table 3.1. Slip values calculated under different conditions with two different slip calculating formulas.

Slip A in %	Slip B in %			
	concrete $p_1=0.8$ bar	concrete $p_1=1.5$ bar	sand $p_1=0.8$ bar	sand $p_1=1.5$ bar
10.00	9.18	11.05	8.68	10.15
30.00	29.36	30.82	28.98	30.12

A: calculated with $S = 1 - s_a/6r$

B: calculated with $S = 1 - s_a/s_0$

It is also possible to measure slip with a stationary cine-camera. The cine-camera is installed in the field as follows: the camera-lens must be at axle-height of the wheel and the viewing direction perpendicular to the travelling direction. Because only relative values of sizes and distances are needed an appropriate size of projection can be chosen for illustration of the results. On the film screen tyre radius r , travelled distance

of the axle, and the rotated angle of the wheel can be measured. From the travelled distance and the angle of rotation the travelled distance s_a per revolution is calculated. Substitution of s_a and r in 3.3 gives the slip percentage.

We drove a tractor at different slip-levels on Wageningen sand. Slip was measured by a 16 mm cine-camera; the travelled distance in ten wheel revolutions was measured simultaneously. Table 3.2. shows the results of the two methods used. The conclusion is that slip can be measured with a cine-camera, provided the camera has been installed correctly.

Table 3.2. Comparison of three slip-measuring methods used on Wageningen sand.

Track	Slip A	Slip B	Slip C
1	8.4 %	7.6 %	8.1 %
2	15.7 %	15.0 %	15.3 %
3	24.8 %	24.2 %	23.8 %

A: s_a and r measured in the field; S calculated with

$$S = (1 - s_a/6r).100 \%$$

B: s_a and s_o measured in the field; S calculated with

$$S = (1 - s_a/s_o).100 \%$$

C: s_a and r measured on film-screen; S calculated with

$$S = (1 - s_a/6r).100 \%$$

In principle two frames suffice when the cine-camera method is used. So we tried slip measuring with 35 mm color-slides. At a concrete test surface the color-slide method was tested for different camera-lenses (50 mm, 85 mm, 105 mm and 135 mm focal distance) and viewing positions. The best measuring procedure was the following:

- a camera with a 50mm lens was mounted at axle height (on a tripod)
- a distance of 8 meters was kept between the camera and the track
- the camera viewing direction was perpendicular to the direction of travelling
- the first slide was taken at the moment that the wheel came completely in the picture
- the second slide was taken just before the wheel disappeared from the picture.

We measured r and s_a at the screen (color-slide method) and at the test surface and compared them afterwards. The color-slide method showed maximum absolute deviations in slip percentages of $\pm 2.5 \%$ slip. The mean values for slip measured at the screen and at the test surface were equal. So for practical purposes the color-slide method is accurate enough.

3.1.1.3. WHEEL SLIP DURING PLOUGHING

There is much discussion about wheel slip but information on slip in normal field work seems to be lacking completely. There is some literature about slip measurements taken during ploughing demonstrations in West Germany (Traulsen and Spingles, 1978) and Great Britain (N.N., 1980 and 1981a). Some results of these demonstrations can be found in Table 3.3 and 3.4.

Table 3.3. Slip during ploughing demonstration with 11 four-wheel drive tractors in West Germany (Traulsen and Spingles, 1978).

tractor	lowest slip %	highest slip %	mean slip %
front wheel	14	39	24
rear wheel	13	31	22

Table 3.4. Some results from Tractor at Work Events (N.N., 1980 and 1981a).

tractor	year	lowest slip %	highest slip %	mean slip %	number of entrants
two-wheel drive	1980	13.4	28.0	17.1	9
two-wheel drive	1981	11.8	19.4	16.3	3
four-wheel drive	1980	8.0	18.4	12.2	25
four-wheel drive	1981	6.9	16.9	13.2	24

These ploughing demonstrations give little information about slip during regular farm work, because all tools are working under the same field conditions and because the participants are well-prepared manufacturers or importers of tractors.

To collect more information about slip on the farm, we measured wheel slip during ploughing operations in 189 different places all over the Netherlands. For this slip measuring it was necessary to develop a new measuring method. The first idea was to measure slip "at a distance", because we did not want the ploughing behaviour of the farmer to be influenced by our presence. Thus the cine-camera method was born. Because the cine-camera method is rather expensive and its use time-consuming, we decided to use the color-slide method.

During spring 1980 we drove around in the Dutch regions with light soils until we saw a ploughing farmer. With his permission, slip was measured with the color-slide method. Driving speed, ploughing depth, ploughing width, driving conditions, and type of tractor, plough and tyres were also recorded.

It soon became clear that the ploughing behaviour of the farmer was not notably influenced by the presence of the measuring team. Therefore, and also because the color-slide method was time-consuming, the measurements of tyre radius and distance travelled

on the heavy soils were carried out on the spot. Slip measurements on heavy soils were taken in autumn 1980. At that time the measuring programme was extended with tyre inflation pressures. Detailed information about ploughing depth, ploughing speed, and tyre inflation pressures is given in Tijink and Den Haan (1981). On light soils, ploughed in spring, 100 slip measurements were taken. In autumn slip was measured on heavy soils in 89 places. The observed values for wheel slip have been plotted and are shown as a cumulative curve in Fig. 3.6. The median slip value is 14.6 % on light soils and 17.0 % on heavy soils. The highest measured slip on light and heavy soils is 54 % and 37 % respectively. In spring as well as in autumn more than 60 % of the participating farmers plough with slip values between 10 % and 20 %. On the light soils 23 % of the farmers plough with more than 20 % slip and even 33 % do this on heavy soils.

The wheel-slip measurements have also been analysed with respect to tyre construction. Some results of this analysis are shown in Table 3.5.

Tractors equipped with radial tyres had lower slip values on both types of soil. These differences between slip values of tractors with radial and those with cross ply tyres are not only due to tyre type. Among the group of tractors with radial tyres were many new and heavy tractors with a well-adjusted tractor-plough combination. So it is a combination of factors that leads to the lower slip values of tractors fitted with radial tyres.

The investigation of Tijink and den Haan (1981) concluded that a lot of farmers can plough with lower slip values provided they pay attention to the causes of wheel slip.

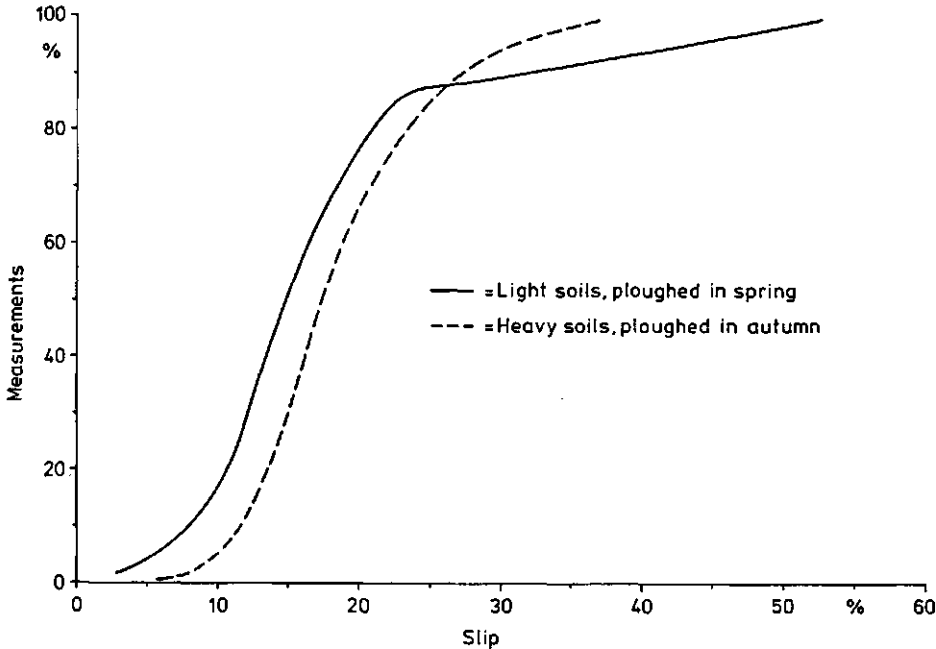


Fig. 3.6. Wheel slip during ploughing on farms.

Table 3.5. Wheel slip during ploughing in relation to tyre construction.

soil type	percentage radial tyres	mean slip radial tyres %	mean slip cross ply tyres %
light	26	13.7	22.8
heavy	37	16.1	20.1

3.1.2. MOVEMENTS OF A POINT AT THE RIM OF A ROLLER OR WHEEL

3.1.2.1. TRAJECTORY OF A POINT AT THE RIM OF A ROLLER OR WHEEL

Söhne (1952) has given a description of the trajectory of a point at the rim of a rigid wheel. Such a point of a free-rolling wheel on a rigid surface has the following motion parameters (Fig. 3.7):

$$\begin{aligned} x &= r_0 (\omega t - \sin \omega t) \\ y &= r_0 (1 - \cos \omega t) \end{aligned} \quad [3.4]$$

where, r_0 = radius of the wheel ω = angular velocity
 $r_0 \omega t$ = forward travelled distance t = time

The rigid wheel on the rigid surface can also have a slip S . The parameters for a slipping wheel are:

$$\begin{aligned} x &= r_0 [(1 - S)\omega t - \sin \omega t] \\ y &= r_0 (1 - \cos \omega t) \end{aligned} \quad [3.5]$$

The forward-travelled distance of the axle is now:

$$r_0(1 - S)\omega t = (1 - S)vt.$$

Fig. 3.7 shows remarkable changes in the trajectory because of slip and skid.

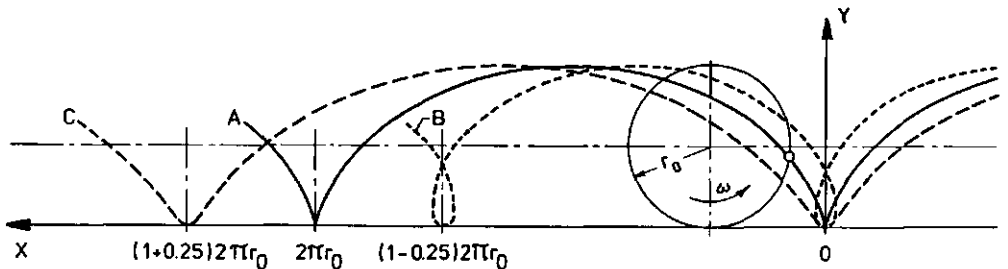


Fig. 3.7. Trajectory of a point at the rim of a rigid wheel on a hard surface. A=free rolling, B=slipping wheel ($S=25\%$), C=skidding wheel ($S=-25\%$).

3.1.2.2. VELOCITY OF A POINT AT THE RIM OF A ROLLER OR WHEEL

A moving wheel with a radius r_o and n revolutions per second, has a theoretical forward velocity $v_{th} = 2\pi r_o n$ and an actual forward velocity $v_a = (1 - S)2\pi r_o n$. The effective radius r_e is the actual displaced distance s_a per circumference divided by 2π (ASAE Standard 296.2; Hahn et al., 1984). In a formula:

$$r_e = \frac{s_a}{2\pi} = \frac{(1 - S)2\pi r_o}{2\pi} = (1 - S)r_o \quad [3.6]$$

This means that $r_e < r_o$ for a slipping wheel and $r_e > r_o$ for a skidding wheel. A wheel with a radius r_e moves without slip, with the same n , on an imaginary plane. The point where this plane touches the equivalent wheel is the instantaneous centre of rotation I. All the points of this wheel rotate around this instantaneous centre I.

It is possible by means of this instantaneous centre of rotation I and by using instantaneous kinematics to give the direction and the length of the absolute velocity vectors of points at the rim of a wheel. This is shown in Fig. 3.8. Note the influence of slip and skid on the velocity vectors.

All the points at the rim of a skidding wheel have a forward velocity above zero. A slipping wheel has two zones. The upper one with forward velocities above zero, while in the lower zone it is the opposite.

3.2. MOVEMENTS IN THE CONTACT AREA

3.2.1. TYRE DEFORMATIONS

A tyre under a static load shows radial deformation and sidewall bulging, while a moving tyre can show tangential carcass and lug deformations.

3.2.1.1. RADIAL TYRE DEFORMATION AND SIDEWALL BULGING

In general radial tyre deformation is accompanied by sidewall bulging. Measurements of Knight and Green (1962) show deflection and sidewall bulging of a moving tyre on surfaces ranging from firm to soft (Fig. 3.9).

In addition to inward carcass deformation (deflection) there can be outward deformation. Fig. 3.10 shows radial carcass deformation versus rotation angle of a radial and cross ply tyre. The radial tyre has an outward deformation in a rotation angle range from about 220 to 140 degrees. This outward deformation can be explained as follows. The cross ply tyre shows only inward defor-

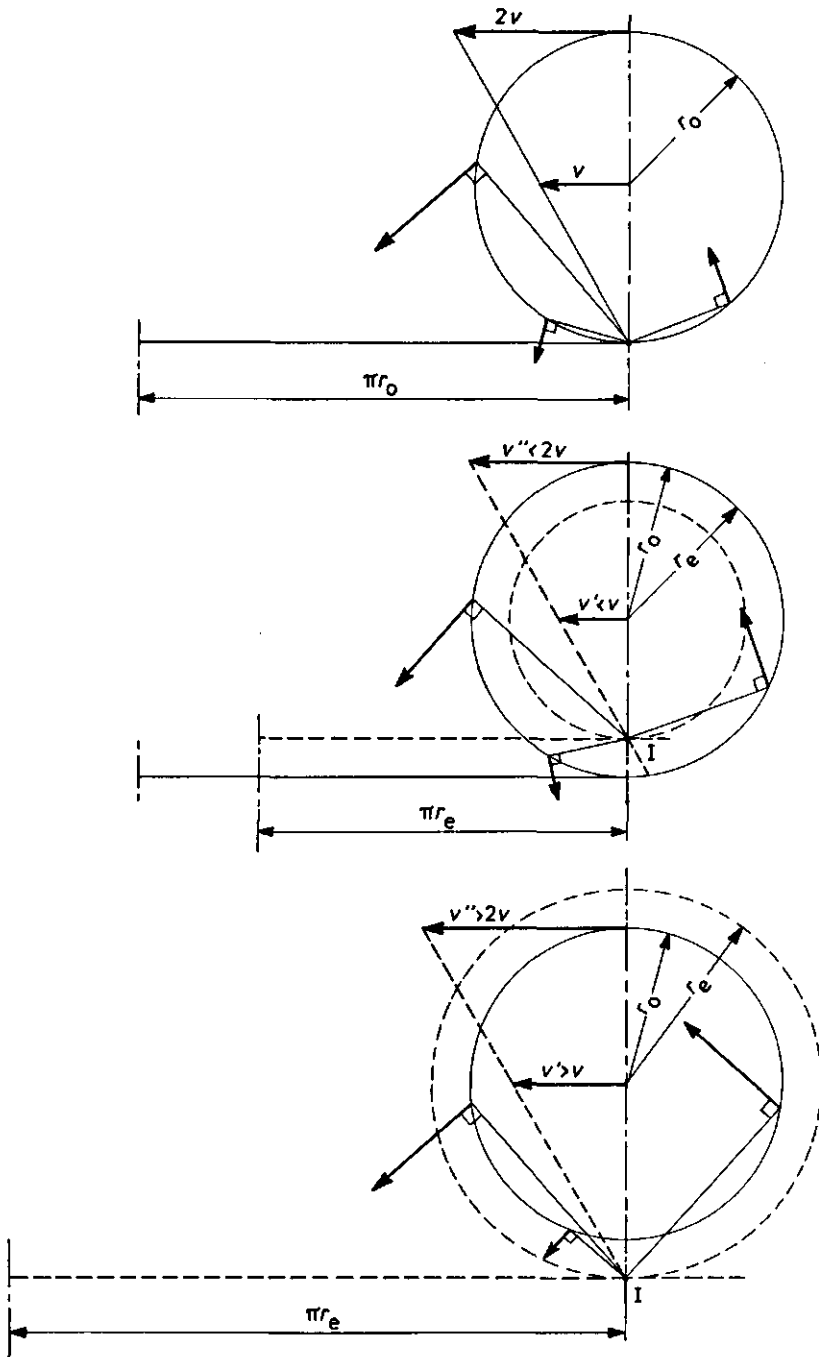


Fig. 3.8. Length and direction of velocity vectors of points at the rim of a wheel.

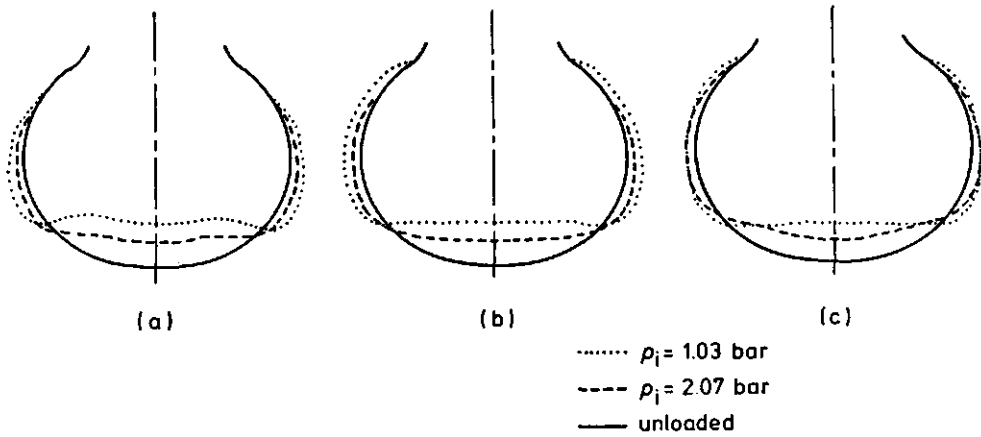


Fig. 3.9. Tyre deflection and sidewall bulging at different inflation pressures on (a) asphalt-paved concrete, (b) sand, and (c) silt (Knight and Green, 1962).

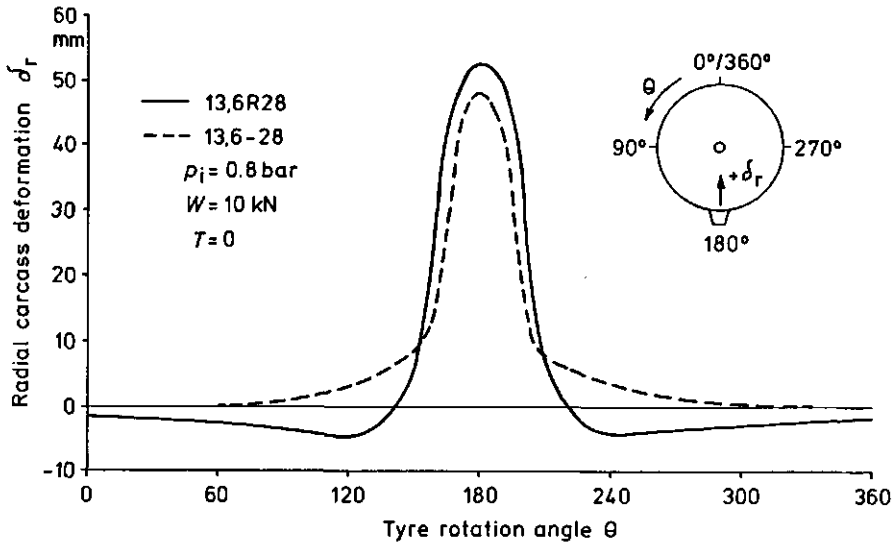


Fig. 3.10. Radial carcass deformations of a cross ply and a radial tyre (Steiner, 1979).

mation. Therefore, its carcass will be shortened. The radial tyre has a stiff belt in the tangential direction. This belt distributes the deformations over the whole circumference and is because of its stiffness the cause of the outward carcass deformation.

Mostly radial deformation is measured in a static situation and is called deflection δ . Tyre deflection has been measured by Hofferberth and Reinhold (1969), Sitkel (1969), Sonnen (1970),

and others. Static tyre deflection depends on inflation pressure, load, tyre construction, and on the character of the supporting surface. Sonnen measured remarkable differences in the deflection curves for loading and unloading. Sitkel (1969) measured tyre deflection and sinkage. Tyre deflection decreases with increasing sinkage (Fig. 3.11).

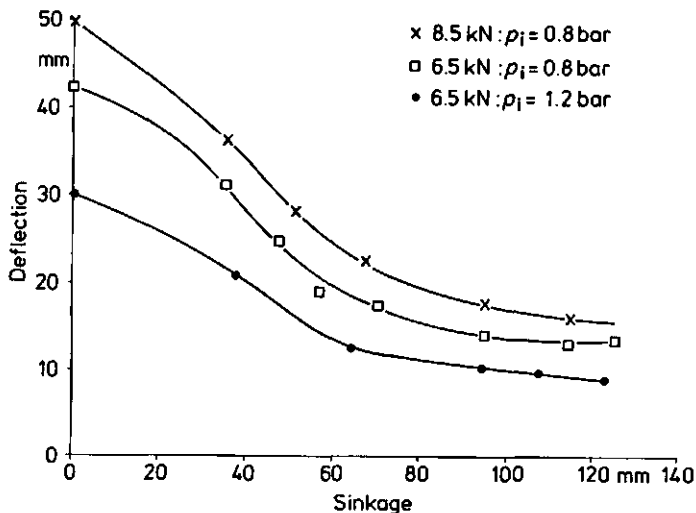


Fig. 3.11. Influence of sinkage on tyre deflection (Sitkel, 1969).

Maximum allowed tyre deflection

The maximum allowed tyre deflection $(\delta/h)_{max}$ can be calculated from manufacturers' tables.

Sitkel (1969) found $\delta/h = 0.15$ at maximum load for cross ply tractor rear tyres. From technical information from Continental, Krick (1969) calculated that $(\delta/h)_{max}$ lies between 0.13 and 0.17. Terpstra (1978) based his calculations of $(\delta/h)_{max}$ on information from European and American tyre manufacturers. He found values between 0.14 and 0.20. According to Inns and Kilgour (1978) maximum deflection of agricultural tractor and implement tyres is limited to about 18 % to 20 % of the section height h in order to prevent carcass damage.

Deflection models and geometry of the contact area

Bekker (1956) has provided a mathematical tyre deflection model. Furthermore, he assumes that the contact area A may be determined as an area of a rectangle reduced by 15 %. In a formula:

$$A = 0.85l \cdot B \tag{3.7}$$

where, A = the area
 l = the length of the contact area
 B = the width of the contact area.

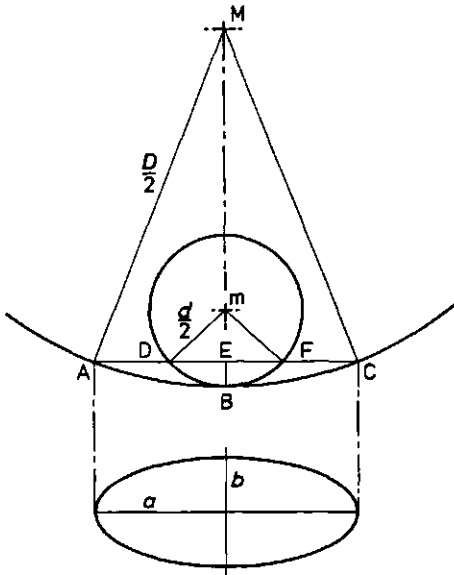


Fig. 3.12. Tyre deflection model of Krick.

Krick (1969) has provided a more simple model for deflection. He assumes that the shape of a tyre is a torus. This implies that the contact area is elliptical on a firm surface (Fig. 3.12). When deflection starts the arcs ABC and DBF , respectively in and perpendicular to the direction of travel, are compressed to the chords AEC and DEF or the chords AEC and DEF elongate sideways. The true lengths lie between the original chords and the arcs. The differences between the original chords and the arcs are relatively small because of the large diameters D and d . Thus the arcs ABC and DBF are equalized to the chords AEC and DEF respectively. The ellipse has the following half axes:

$$a = \sqrt{D\delta - \delta^2}$$

$$b = \sqrt{d\delta - \delta^2}$$

The contact area $A = \pi \sqrt{D\delta - \delta^2} \cdot \sqrt{d\delta - \delta^2}$

can, because of $\delta^2 \ll d\delta \ll D\delta$ be written as:

$$A = \pi \sqrt{Dd\delta^2} \quad [3.8]$$

This calculated relation between deflection and contact area correlates well with the measured relation. According to Painter (1981) the chords AEC and DEF can be approximated by the arcs ABC and DBF for small deflections. The ellipse now has half axes:

$$a = D/2 \arccos(1 - 2\delta/D)$$

$$b = d/2 \arccos(1 - 2\delta/d)$$

and an area :

$$A = (\pi/4).D.d.\arccos(1 - 2\delta/D).\arccos(1 - 2\delta/d) \quad [3.9]$$

Although the formulas 3.8 and 3.9 are both based on the same deflection model, formula 3.8 is easier to use.

3.2.1.2. TANGENTIAL CARCASS AND LUG DEFORMATIONS

Tangential carcass deformations are not only deformations in the sense of strains, but are relative displacements in relation to a fixed system of coordinates as well. Displacement depends on tyre construction, load, inflation pressure, and torque. Fig. 3.13 shows that tangential carcass deformation is almost symmetrical for a towed wheel ($T = 0$) and that the radial tyre shows displacement all over the circumference, while the cross ply tyre has half a circumference free from relative displacement. Calculations were made of the shortening of the carcass (see Table 3.6). The shortening of the cross ply carcass is about three times as much as the one of the radial tyre carcass. The carcass shortening of the radial tyre decreases when a torque is applied.

Table 3.6. Tangential strains of tyre carcass (Steiner, 1979).

tyre	inflation pressure (bar)	load (kN)	carcass shortening	
			at $T=0$ Nm	at $T= 3000$ Nm
13.6-28	0.8	10	32.3 mm	32.5 mm
13.6R28	0.8	10	10.1 mm	8.8 mm

True measurements of tangential lug deformations are unknown and difficult to make. Relative displacement of lugs in the mutual contact area consists of lug bending and carcass deformation. Measurements of lug movements in the mutual contact area were made by Cegnar and Faustl (1961), Wann and Reed (1962), and Steiner (1979). The most complicated method of determining lug movement is used by Steiner. He has drawn longitudinal tyre sections by using castings of the contact areas. He found a nearly linear relation between tangential lug displacement and the lug's longitudinal position in the contact area. Cegnar and Faustl used high-precision optical equipment, whereas Wann and Reed used scratch plates and a "bar table". Both the optical method and the bar table method showed a curved relation between tangential lug displacement and the lug's longitudinal position in the contact area (Fig. 3.14a). A comparison of the measured and the theoretical curves shows that the lugs, when entering the contact area, follow the carcass with a certain delay due to lug-to-surface friction. When the lugs leave the contact area, their relative displacement is greater due to their elastic reaction. This behaviour agrees with observations of the direction of lug movement made by Anslow and Warrilow (1962). The optical and the

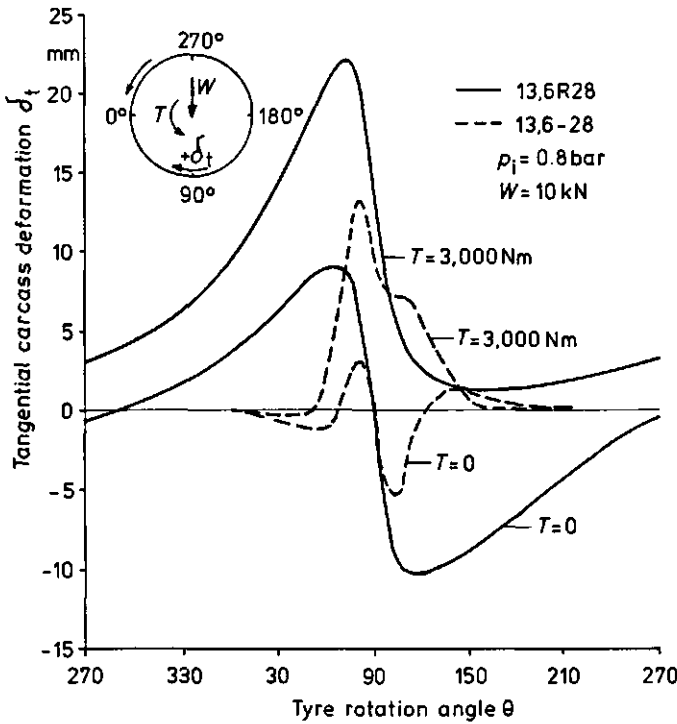


Fig. 3.13. Tangential carcass deformation of a cross ply and a radial tyre (Steiner, 1979).

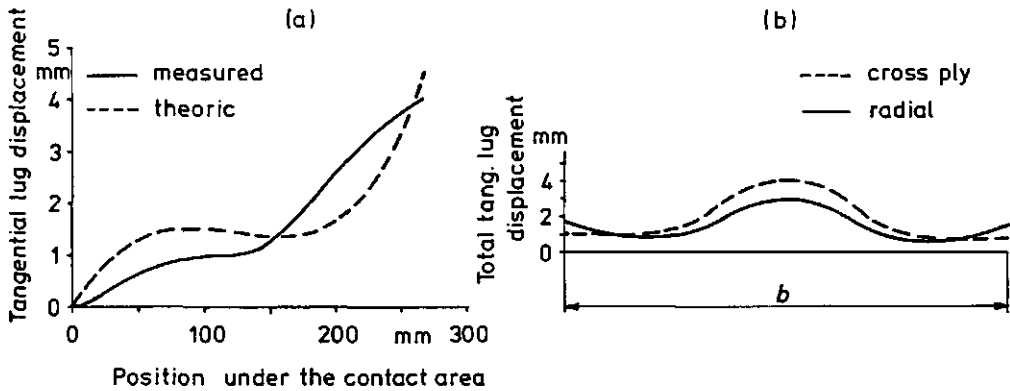


Fig. 3.14. Tangential lug displacement in the contact area of a point 10 mm from the centre plane of a cross ply tyre (a), and (b) total tangential lug displacement at different points of the cross section of a cross ply and a radial tyre.

bar table method also measure the tangential lug displacement at different points of the cross section. Fig. 3.14b shows the path of the total tangential lug displacement versus the width of the contact area. The total displacement is a measure for the energy lost in friction per wheel revolution, and is therefore a measure for wear. So Fig. 3.14b pictures tyre wear across the width. The area under the curve of the radial tyre was found to be 26 % smaller than the one of the cross ply tyre. Total lug displacement was higher at low inflation pressures than at high inflation pressures in the scratch plate tests. These results agree with the practical experience that radial tyres wear less than cross ply tyres and that wear is higher at low inflation pressures.

3.2.1.3. INFLUENCE OF TYRE DEFORMATIONS ON SLIP

Only tyre deformations in the mutual contact area can influence slip. On a firm surface, slip is influenced by carcass and lug deformation. Using his drawings of longitudinal tyre sections Steiner measured slip values due to tyre deformations of 7.54 % and 5.15 % of a cross ply and a radial tyre respectively (see Table 3.7). Slip is influenced more by lug deformations than by carcass deformations. Estimates of slip components on a deformable soil were also made. These show that the influence of tyre deformations on slip should not be neglected and that radial tyres have lower slip percentages due to fewer tyre deformations.

Table 3.7. Measured slip components on a firm surface and estimated slip components on a deformable soil (Steiner, 1979).

Tyre	Slip caused by				total
	carcass deformation	lug deformation	soil deformation	slipping in the contact area	
13.6-28	1.86 %	5.79 %	-----	-----	7.54 %
13.6R28	0.55 %	4.35 %	-----	-----	5.15 %
13.6-28	1.2 %	4.3 %	8.0 %	7.5 %	21.0 %
13.6R28	0.4 %	2.6 %	7.5 %	7.5 %	18.0 %

3.2.2. MOVEMENTS OF A POINT AT THE CIRCUMFERENCE OF A ROLLER, WHEEL, OR TYRE DURING MOTION IN THE MUTUAL CONTACT AREA

The trajectory of a point at the rim of a roller or wheel during motion in the contact area on a rigid surface can be described by formula 3.5. A rigid wheel with a radius r_0 and moving with n revolutions per second on a rigid surface, has a theoretical travelled distance $s_{th} = 2\pi r_0 n$. Söhne (1952) neglects tangential

tyre deformations and therefore assumes that tyres only deform in the radial direction. The trajectory of a point at the circumference of a tyre on a deformable surface can now be written as:

$$\begin{aligned} x &= r_0 \cdot (1 - S_t) \cdot \omega t - r \cdot \sin \omega t \\ y &= r_0 - r \cdot \cos \omega t \end{aligned} \quad [3.10]$$

where, $r = r_0 - \delta_r$
 δ_r = radial tyre deformation
 $S_t = (s_{th} - s) / s_{th}$

When we take tangential deformation δ_t into account, the formulas change into:

$$\begin{aligned} x &= r_0 \cdot (1 - S_t) \cdot \omega t - r \cdot \sin \omega t + \delta_t \cdot \cos \omega t \\ y &= r_0 - r \cdot \cos \omega t - \delta_t \cdot \sin \omega t \end{aligned} \quad [3.11]$$

The formulas for a point at the inside of the tyre carcass are:

$$\begin{aligned} x &= r_0 \cdot (1 - S_t) \cdot \omega t - (r + h) \cdot \sin \omega t + \delta_t \cdot \cos \omega t \\ y &= r_0 - (r + h) \cdot \cos \omega t - \delta_t \cdot \sin \omega t \end{aligned} \quad [3.12]$$

where, h = the distance between the inside of the carcass and the lug face.

Steiner (1979) calculates the parameters of a point at the lug face as follows: starting with a point (x_2, y_2) at the inside of the carcass, he assumes that the lug is perpendicular to the line through the nearest measuring points (x_1, y_1) and (x_3, y_3) at the inside of the carcass. There are measuring points at each 2.5 degrees. The direction of the lug is:

$$\tan \alpha_L = (y_3 - y_1) / (x_1 - x_3)$$

So the parameters of a point at the lug face are:

$$\begin{aligned} x_L &= x_2 - h \cdot \sin \alpha_L \\ y_L &= y_2 - h \cdot \cos \alpha_L \end{aligned} \quad [3.13]$$

These calculations do not take the bending of the lugs into account.

3.2.3. TRAJECTORIES OF SOIL PARTICLES IN THE CONTACT AREA BETWEEN THE SOIL AND A ROLLER, A WHEEL, OR A TYRE

Poletayev (1964) used the angle between the direction of the velocity vector and the radial at a point on a wheel rim to demarcate different zones in the wheel-soil interface.

Theoretical analyses of tangential displacement of a soil particle at the rim circumference were made by Janosi (1962), Onafeko and Reece (1967), and Wong and Reece (1967a, 1967b).

Wong (1967) determined the path of particles, on a clay soil, influenced by a roller (Fig. 3.15). The particles were first pushed forward and up in a straight line by the oncoming roller. They were then shifted backwards in a circle. After the roller

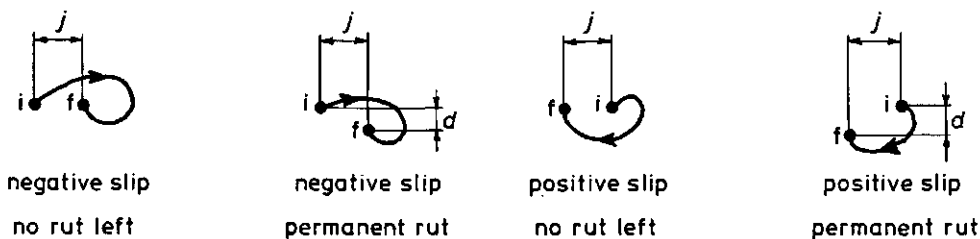


Fig. 3.15. Movement of a soil material point relative to the untouched soil, due to a roller passing from left to right.

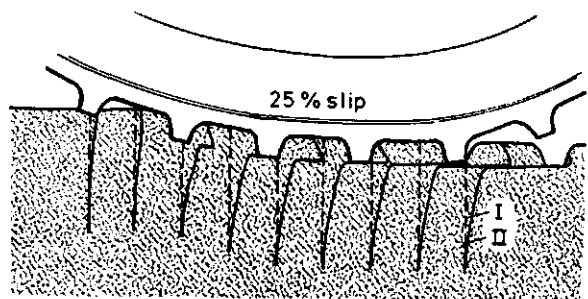
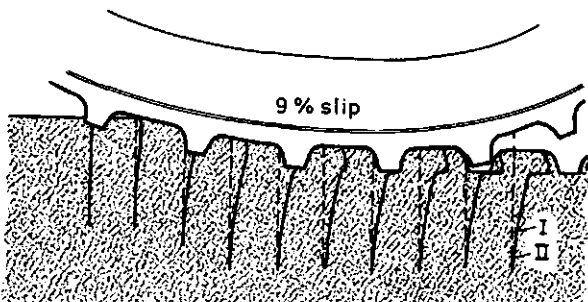
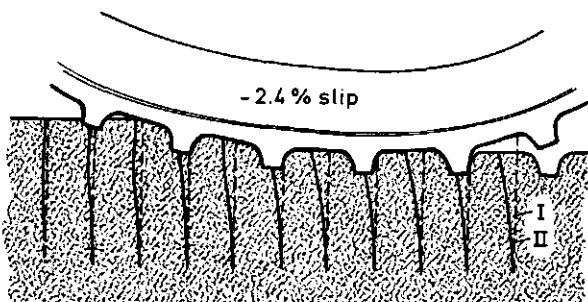


Fig. 3.16. Movements of soil under the action of towed and driven tyres (Söhne, 1952).

had passed by the particles were at the same vertical level as in their initial position because of the incompressibility of the soil used. The final positions of soil surface particles were ahead of their initial positions when a towed roller was used, while the final positions of the particles were behind their initial positions when a driven roller was used.

Söhne (1952) showed the trajectory of soil between the lugs of a tyre and of soil particles at the soil-lug interface (See Fig. 3.16).

We determined the trajectories of soil surface particles beneath a towed tyre from our measurements of three-dimensional soil deformation. Fig. 3.21 shows two such trajectories of soil surface particles in the central longitudinal section of the ruts formed by a towed tyre in Schinnen silt loam and in Wageningen silty clay loam. These trajectories differ from the ones found by Wong because we used deformable soils and a deflecting tyre.

Besides a vertical displacement j_v there is a resulting horizontal displacement j_h in deformable soils. We placed small dots at the soil surface in our soil bin investigations. The dots were placed in such places that after passing of the tyre, the dots were in the central longitudinal section of the rut. The positions of the dots were measured, in horizontal and vertical direction, before and after the first and second passing of a towed tyre. In the test five different soils were used at different moisture contents and bulk densities.

In Fig. 3.17 the resulting horizontal displacement j_h has been plotted versus the vertical displacement j_v of soil surface particles in the central longitudinal section of the formed rut. The vertical displacements are equal to the sinkage in the centre of the rut. The 48 measuring points fit a power function rather well ($r=0.98$). It is remarkable that the ratio j_h/j_v increases with increasing rut depth. This must be due to the presence of a rigid bottom at 15 cm depth. The soil under the tyre can move less easily downwards at an increase of rut depth and therefore will move more in a forward direction. Finally it is clear that horizontal displacement can not be neglected, especially when deep ruts are formed.

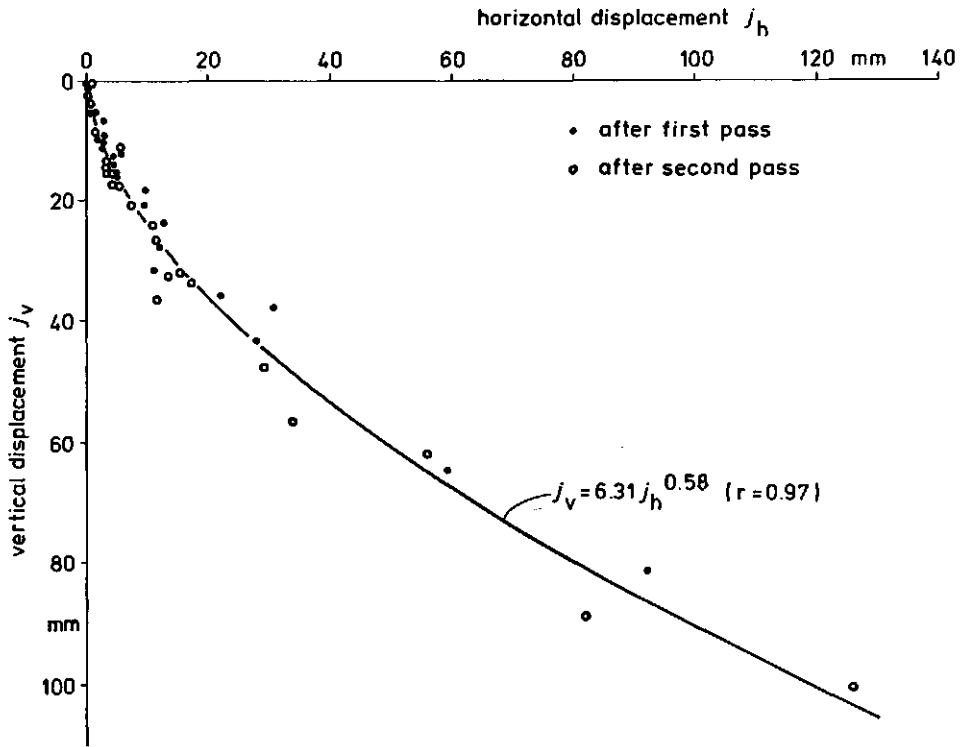


Fig. 3.17. Horizontal and vertical displacements of points at the soil surface in the wheel-centre plane.

3.3. SUBSURFACE MOVEMENTS

The most simple two-dimensional movement is the one under infinitely wide rollers because of the absence of a sideward movement. Soil under a wheel or a tyre can escape sideways. This sideward transport does not exist in the central longitudinal section of the formed rut. It is also possible to show the two-dimensional deformation in the cross section of the rut. This is already a projection of a three-dimensional deformation on a flat plane.

3.3.1. SOIL MOVEMENTS UNDER ROLLERS

When rollers are considered as infinitely wide rollers we have a true two-dimensional problem.

3.3.1.1. DISTRIBUTION OF SOIL VELOCITIES RELATIVE TO THE CENTRE OF A ROLLER

Wong (1967) used the principle of continuity of flow for rollers at incompressible soils. When a roller is moving and in equilibrium the soil surface, after passing of this roller, has to be at the same level as the undisturbed soil in front of the roller. Fig. 3.18a shows a horizontal distribution of soil velocities under the centre of a slipping roller. The relative velocity of the soil in front of the roller, where the soil is not influenced by the roller, is uniformly distributed down the depth of the soil and equal to the forward velocity v of the axle. The distribution of velocities beneath the axle requires sinkage of the roller. The higher the slip of the roller the higher the sinkage must be. Since the final level must be equal to the initial level in front of the roller, it is necessary that the slipping roller affects rut recovery.

The use of the principle of continuity of flow for a towed roller gives a velocity distribution as shown in Fig. 3.18b. Such a distribution requires no sinkage of the roller.

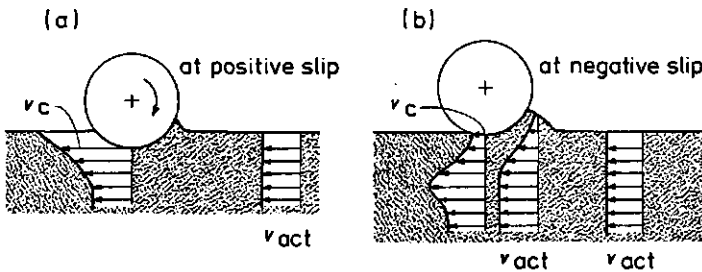


Fig. 3.18a,b. Velocity profiles deduced from continuity considerations.

3.3.1.2. FLOW ZONES UNDER ROLLERS

Flow patterns under rollers have been photographically determined by Wong and Reece (1966), and Wong (1967). Their observations on incompressible soils show that there are normally two flow zones beneath a towed or a driven roller: a forward zone *a* and a backward zone *b* (Fig. 3.19a+b). The zones degenerate into a single backward flow zone at 100 % slip (Fig. 3.19c). It is interesting that the locked roller is converted as a backward raked blade to a vertical blade made of soil (Fig. 3.19d). The boundaries of the flow zones are parts of logarithmic spirals in sand. In clay, those boundaries are sections of circles. Increasing the load of the towed roller leads to:

- Increased skid values
- growth of the flow zones *a* and *b*
- moving of the boundary between the two zones in the direction of travel

For a driven roller an increasing load at equal slip results in:

- more sinkage of the roller and, therefore, more rut recovery
- growth of the zones *a* and *b*
- moving of the boundary between these two zones in the direction of travel.

3.3.2. SOIL MOVEMENTS UNDER WHEELS

A difference between a conventional wheel and the infinitely wide roller is that it is possible for the soil to flow sideways under a wheel, but not under a roller.

Wong (1967) studied the flow patterns under narrow wheels in incompressible sand. These experiments show that even under a narrow wheel soil has two distinct flow zones in the longitudinal section. These two zones have boundaries with similar characteristics as those beneath rollers. Rut recovery under narrow wheels grows with increasing wheel width and slip. Longitudinal and sideward flows occur together. The relative extent of the two mechanisms depends on the degree of slip and on wheel width. Comparisons of the profiles of ruts and heaves left by a driven wheel and a narrow plate in an incompressible soil show that:

- the influence of the plate goes further sideways. The reason is that all the soil under a plate flows sideways, while the soil under a wheel also flows forwards and backwards.
- rut recovery is higher in the middle of the rut than on the sides.
- the heaves on the border of the wheel rut are higher.

So the soil under a wheel does not flow in the same way as under a plate.

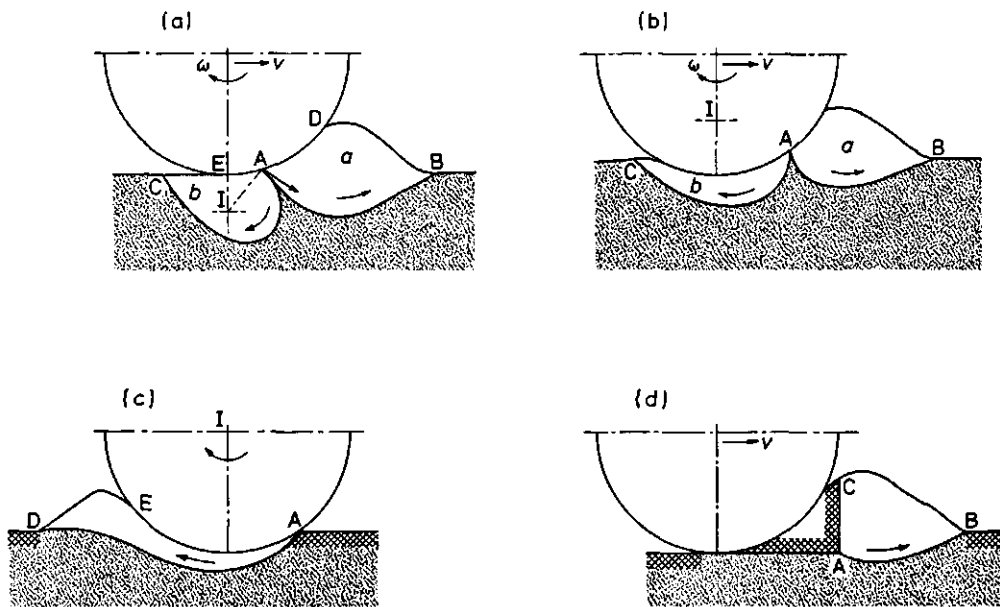


Fig. 3.19. Flow zones in sand under (a) a towed wheel, (b) a driven roller, (c) a driven roller at 100 % slip, and (d) a locked wheel with 100 % skid (Wong, 1967).

3.3.3. SOIL MOVEMENTS UNDER A TYRE

Measurements of soil deformation due to the passing of a towed tyre have been made by Tijink et al. (1988). From these measurements we took the central longitudinal sections (Fig. 3.20). These deformations agree with visualizations of the deformations under a tyre, given by Söhne (1956). Wageningen silty clay loam compacts strongly under the action of the towed tyre, while Schinnen silt loam shows more deformations and less compaction.

The measurements of Söhne (1952) indicate that the horizontal displacement under a tyre decreases with depth. Gliemeroth (1953) measured photographically the trajectories of soil particles under the action of a tractor in the field. He found that the horizontal movements decrease more with depth than the vertical movements.

The trajectories of soil particles at the surface and at 0.05 m and 0.10 m depth were determined from our longitudinal sections of the ruts formed by a towed tyre (Fig. 3.20). The resulting trajectories (Fig. 3.21) have a different shape for each of the two types of soils. It is also interesting that the shape of the trajectories changes with depth. The different shapes of the trajectories must be due to the different shapes and extents of the flow zones.

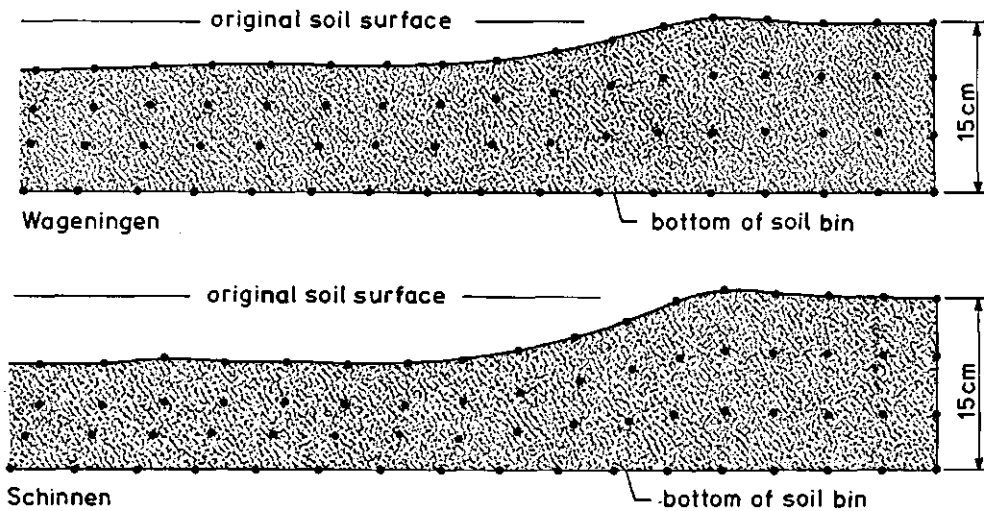


Fig. 3.20a,b. Deformation of soil under the tyre centre plane. The tyre moves from left to right.

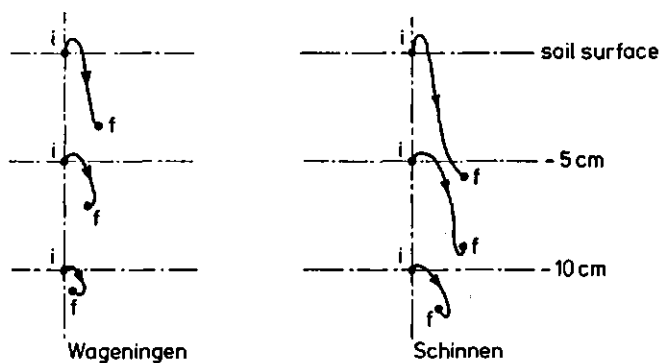


Fig. 3.21. Movements of soil particles at the soil surface and at 5 cm and 10 cm depth due to a towed tyre passing from left to right.

CHAPTER 4

DYNAMIC ASPECTS OF LOAD-BEARING PROCESSES

4.1. FORCES, MOMENTS, AND STRESSES ON ROLLERS, WHEELS, AND TYRES

There are three forces and three moments acting from the ground on a tyre.

F_x is the longitudinal, F_y is the cornering (=lateral), and F_z the normal component of the force from the ground to the tyre. The force F_y is important for steered wheels, but will not be discussed in this chapter.

The overturning moment T_x is the moment of force about the X-axis acting on the tyre from the road. The moment about the Y-axis is called rolling resistance moment T_y . Aligning torque T_z is the moment about the Z-axis acting on the tyre. A driving torque T about the rotation axis of the tyre produces a force that can accelerate or decelerate the vehicle.

4.1.1. MECHANICAL EQUILIBRIUM OF ROLLERS, WHEELS, AND TYRES

The forces, torques, and stresses acting on a roller, wheel, or tyre on a horizontal soil surface are illustrated in Fig. 4.1.

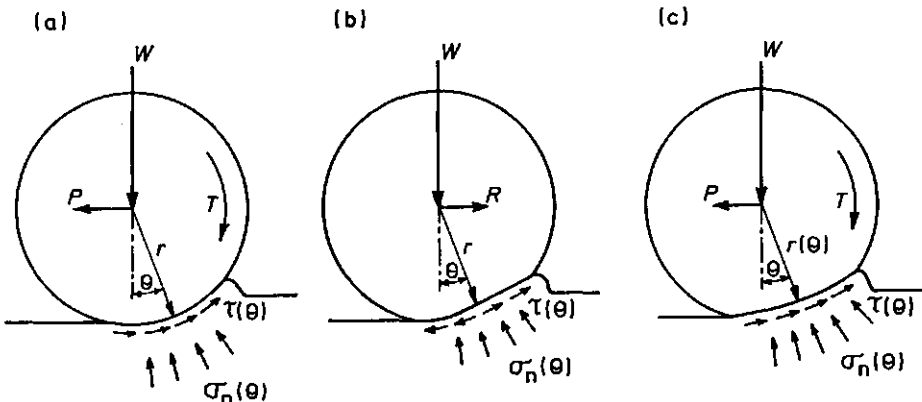


Fig. 4.1. Forces, torques, and stresses on (a) a driven roller, (b) a towed tyre, and (c) a driven tyre on deformable soil.

Roller and rigid wheel

The equilibrium of a stationary moving roller or rigid wheel on horizontal soil surface can be described by means of the following equations:

$$W = \sum \text{vertical components of } \sigma_{\theta} + \text{vertical components of } \tau_{\theta} \quad [4.1]$$

$$P = \sum \text{horizontal } \sigma_{\theta} + \text{horizontal } \tau_{\theta} \quad [4.2]$$

$$T = \sum r \cdot \tau_{\theta} \quad [4.3]$$

For a towed roller or wheel, input torque $T = 0$ and, therefore, shear stresses must occur in forward as well as backward direction. The rolling resistance of a towed roller or wheel can be equalized to the towing force (equation 4.2).

For a driven roller or wheel rolling resistance is more complex and can be illustrated by means of an energy balance:

$$\text{Input} = \text{Output} + \text{Loss.}$$

According to Corcoran (1979) energy components can be based on unit wheel travel and unit ground travel.

Based on unit wheel travel the components of the energy balance are:

$$\begin{aligned} \text{Input} &= T/(r_o \cdot W) \\ \text{output} &= P(1-S)/W \\ \text{loss} &= \text{rolling resistance energy} = (T-P \cdot r_e)/r_o \cdot W \end{aligned}$$

Based on unit ground travel the components are:

$$\begin{aligned} \text{Input} &= T/[r_o(1-S) \cdot W] \\ \text{output} &= P/W \\ \text{loss} &= \text{rolling resistance energy} = (T-P \cdot r_e)/r_e \cdot W \end{aligned}$$

Pneumatic tyres

The equations for P and W are the same as those for rollers and wheels. Because of the tyre deflection the equation for T changes. Because of this deflection the normal stresses σ contribute to the torque T and the equation for the torque now becomes:

$$T = \sum r \cdot (\text{components of } \sigma_{\theta} \text{ and } \tau_{\theta} \text{ that are perpendicular to } r).$$

Components of rolling resistance

Rolling resistance defines the total amount of energy lost and is composed of several components:

- rut forming in the soil
- friction between the rolling device and the travelling surface caused by sliding
- hysteresis in tyre materials due to deflections when the tyre is rolling
- resistance due to air circulating inside the tyre
- fan effect of the rotating wheel on the outside air
- friction of the wheel bearings.

The last three components are of secondary importance and can be

neglected for agricultural purposes. On the road 90 to 95 % of the energy losses are due to internal hysteresis of tyre materials.

4.1.2. TRACTIVE PERFORMANCE

Tractive performance of tractors and single wheels has been measured by many researchers. The presentation of the results in performance curves is sometimes confusing and, therefore, an analysis will be given of the most common tyre performance presentations.

4.1.2.1. ANALYSIS

The tractive performance of tractors have been measured by Bock (1953), Terpstra and van Maanen (1972), and others. Their results have been presented generally in pull-slip curves. Their presentations give information about the (drawbar) pull at different slip values, but no information about the efficiency of the operation. Because of weight transfer during the measurements it is difficult to transfer the characteristics into other tractors.

When tyres are tested with a single wheel tester it is generally possible to measure input torque, pull, and slip. The results of single wheel tests can be used for every tractor. Traction performance presentations (Fig. 4.2) of such tests can have the following coefficients:

- pull coefficient $\alpha = P/W$
- tractive efficiency: ratio between output and input
[$\eta = P.v/T.\omega$]
- gross traction ratio $\mu = U/W$; where $U = T/r_0$
- rolling resistance coefficient $\rho = R/W$

The pull coefficient versus slip combined with the tractive efficiency versus slip make it possible to choose a tyre that has a high efficiency at the pulls needed. Sometimes efficiency and slip are plotted versus pull.

The rolling resistance coefficient and the gross traction ratio are sometimes given in the presentations. This is rather confusing because it suggests that gross traction and rolling resistance of driven tyres can be measured. It also can give the impression that there are two horizontal forces in the tyre-soil contact area: gross traction (thrust) in a forward direction and a rolling resistance force in the opposite direction. According to Schuring (1968) these forces do not exist in the soil-tyre interface.

The most important aspects of tyre performance on farms are:

- for towed tyres: rolling resistance
- for driven tyres: pull, tractive efficiency, and slip.

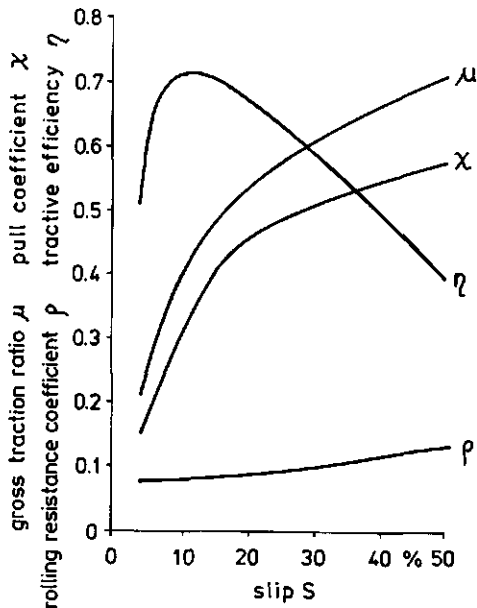


Fig. 4.2. Traction performance of a tractor tyre.

4.1.2.2. TOWED TYRES

The most important aspect of a towed tyre is the force needed to overcome motion resistance. This motion resistance can be equalized to the towed force. In this dissertation the terms "rolling resistance" and "motion resistance" are synonymous.

The rolling resistance depends on many parameters; the main ones are: tyre construction, tyre dimensions, inflation pressure, wheel load, surface conditions, and travelling speed.

Tyre construction has a significant influence on the rolling resistance. It is known of automobile tyres that radial tyres have lower rolling resistance than cross ply tyres (Clark, 1971a). Radial tractor rear tyres also have lower rolling resistance (Steiner and Söhne, 1979).

A larger number of carcass plies and thicker treads tends to increase the rolling resistance because of higher hysteresis losses. The type of rubber compound also affects rolling resistance.

Tyre width and diameter influence rolling resistance as well. Increasing the tyre width, at a constant tyre load and inflation pressure, results in a decrease of rolling resistance. On a rigid road the influence of the tyre diameter on rolling resistance is negligible. In field conditions the influence of the tyre diameter can be considerable (Inns and Kilgour, 1978).

Inflation pressure affects tyre flexibility. Based on measurements of Perdok (1978) fig. 4.3 was plotted. This figure shows that rolling resistance on a concrete surface decreases with increasing inflation pressure. On deformable soil high inflation pressure results in increased ground penetration work and therefore higher rolling resistance. Conversely, lower inflation pressure, while decreasing ground penetration, increases the deflection of the tyre and hence hysteresis losses. So there must be an optimum inflation pressure for a particular surface condition. Because of this interaction it is possible that lowly inflated and excessively overloaded tyres have higher rolling resistance on the road than in the field.

Wheel load affects tyre deflection and surface penetration. Increasing the wheel load results in an increase in rolling resistance (Fig. 4.3).

Surface conditions have influence on rolling resistance. On a hard, smooth, and dry surface rolling resistance is considerably lower than on a freshly ploughed field.

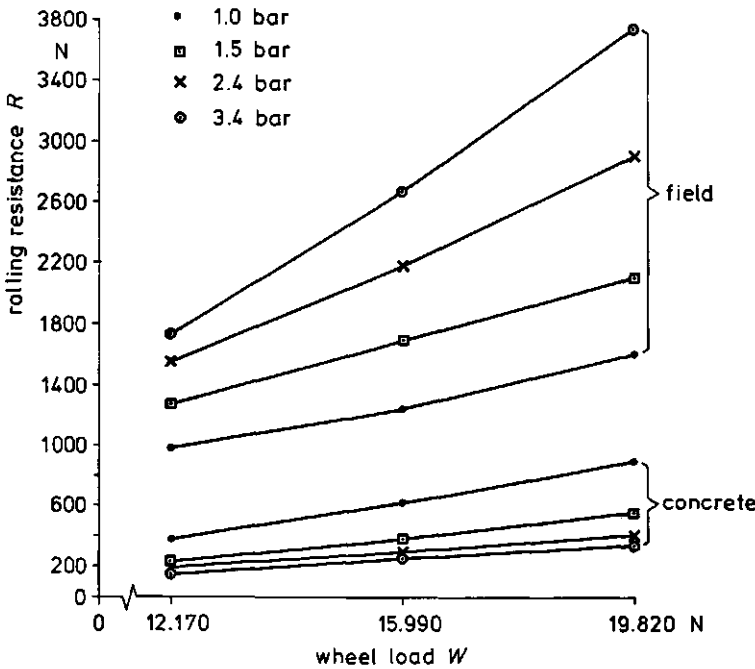


Fig. 4.3. Rolling resistance of a 13-16 agricultural implement tyre on the road and in the field at different inflation pressures and wheel loads.

Travelling speed can also affect rolling resistance. On a rigid road rolling resistance increases with increasing speed (Clark, 1971a). Steiner and Söhne (1979) found a nearly constant rolling resistance for a tractor rear tyre on the road at a speed ranging from 1 to 3 m/s. Measurements in the field by Steinkampf (1975) show increasing rolling resistance at increasing speed.

4.1.2.3. DRIVEN TYRES

Important aspects of the performance of driven tyres are pull coefficient and tractive efficiency. These aspects depend on parameters such as: slip, surface conditions, tyre load, inflation pressure, load ratio, tyre tread pattern, lug parameters, tyre construction, tyre dimensions, driving speed, and direction of rotation.

Pull coefficients and tractive efficiencies of driven tyres have been published by Taylor and Williams (1959), Forrest et al. (1962), Taylor (1973,1976), Dwyer et al. (1974), Steinkampf (1975,1981a+b), Steiner (1978,1979), Biller and Steinkampf (1978), and many others.

Slip

Slip has great influence on tractive performance. The pull coefficient generally increases with increasing slip. Tractive efficiency first increases with slip until a maximum is reached and then decreases with further increasing slip. The slip value at which maximum efficiency occurs depends strongly on surface conditions.

Surface condition

The soil is the most important factor affecting the pull coefficient (Domler and Williams, 1978).

Field conditions are classified in the Handbook of Agricultural Tyre Performance (Dwyer et al., 1974a) as follows: good, average, poor, and bad. Under these conditions the Cone Index has a value of 2000 kN/m², 400 kN/m², 250 kN/m², and 150 kN/m² respectively. Based on measurements of Dwyer et al. (1974), Steiner (1978,1979), and Steinkampf (1975,1981 a+b) we can give the following values for slip and pull coefficient at maximum tractive efficiency under different field conditions (Table 4.1).

Table 4.1. Slip and pull coefficient at maximum tractive efficiency and at 20 % slip.

field condition	max. efficiency (η_{max})	slip at η_{max}	χ at η_{max}	χ at 20% slip
good	0.82	0.08	0.28	0.51
average	0.68	0.10	0.28	0.41
bad	0.53	0.16	0.21	0.23

Tractive efficiency is highest on rigid surfaces and decreases with increasing deformability of the soil surface. The pull coefficient also decreases with worsening surface conditions.

Tyre load

Under good and average conditions increasing the wheel load generally results in better tractive performance. Under bad conditions there is no significant influence of wheel load on tractive performance.

Tyre Inflation pressure

Under good and average conditions decreasing the inflation pressure creates a larger contact area. This results in better tyre performance. At sinkage due to high slip and under bad conditions the influence of decreasing tyre inflation is less because the tyre becomes more rigid in relation to the soil.

Load ratio

The load ratio is the ratio of the wheel load to the maximum allowed wheel load. The load ratio can be increased by decreasing the tyre inflation pressure or by increasing the tyre load. Under good and average conditions increasing the load ratio results in better tyre performance. This effect is more influenced by tyre inflation than by wheel load (Fig. 4.4). Under worse conditions the influence of the load ratio is less clear.

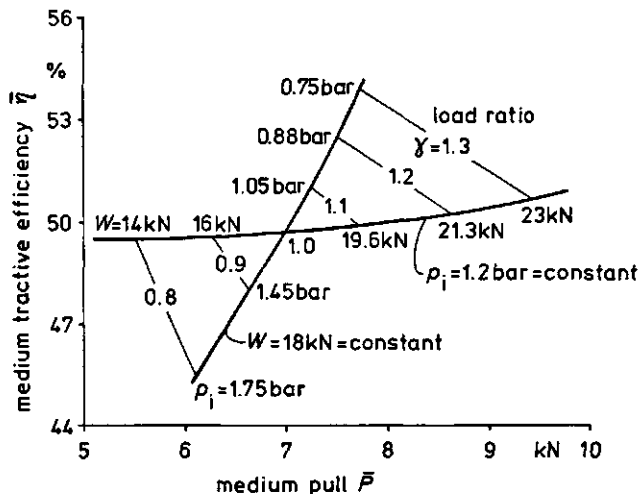


Fig. 4.4. Median tractive performance of a 16.9-30 tractor rear tyre at several tyre load ratios. Load ratio (γ) was changed by changing wheel load W ($p_i = \text{constant}$) or by changing inflation pressure p_i ($W = \text{constant}$) (Steiner, 1978).

Tread pattern

The main agricultural tread patterns are Regular Agricultural (R_1), High-Lugged (R_2), Sportsfield (R_3), and Industrial Lugged (R_4).

Measurements by Terpstra (1973), Taylor (1976), and Steinkampf (1981) lead to the following conclusions. Under good and average conditions the R_1 generally performs best, especially at high slip values. The R_2 is superior on wet, cohesive soils. Under good conditions R_2 performs less well than R_1 . The performance of the R_3 and R_4 types can nearly equal the one of R_1 , when operating under good conditions at low slip values. When high pulls are needed R_3 and R_4 are less useful. R_2 and R_1 have the highest tyre wear. R_3 is intended for use on grass fields, while R_4 is used when almost all traffic takes place on the road.

Lug parameters

Main lug parameters are lug height, lug angle, and lug spacing. Tractor rear tyres generally have a lug angle of about 45 degrees. One manufacturer supplies tyres with a lug angle of 67 degrees. This difference in lug angle is not likely to have a significant influence on tyre tractive performance (Taylor, 1973).

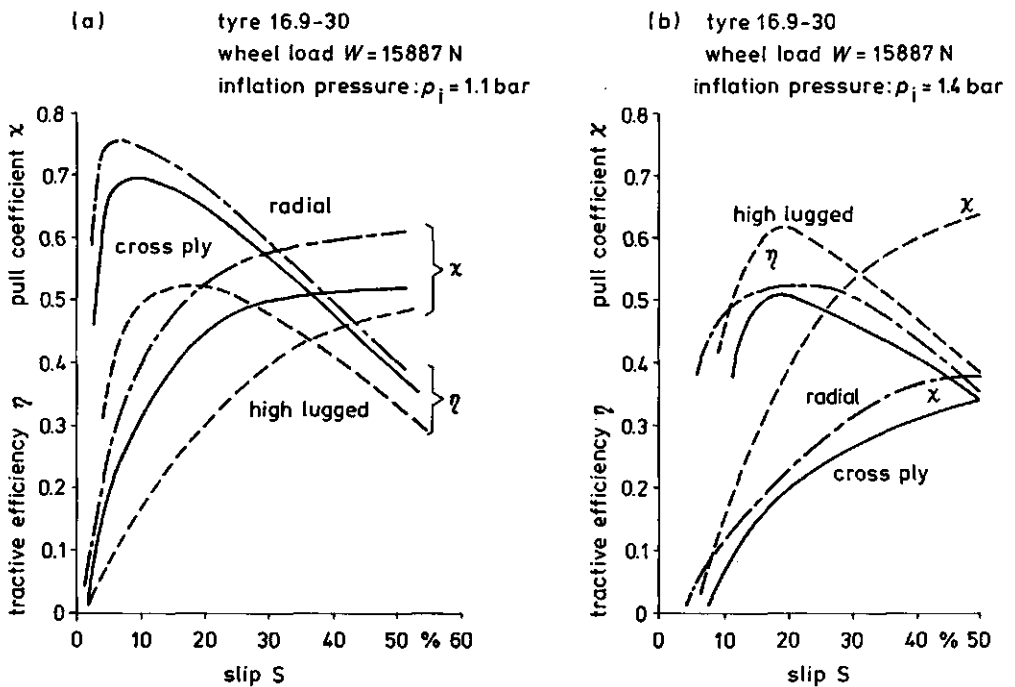


Fig. 4.5. Tractive performances of radial, cross ply, and high lugged tractor rear tyres under good (a) and poor (b) traction conditions (Steinkampf, 1974).

Under good conditions the number of lugs (lug spacing) has no significant influence on tyre performance either (Taylor, 1974). However, under bad conditions the self-cleaning ability of tyres with small lug spaces decreases, resulting in worse tractive performance.

According to Gee-Clough et al. (1977a) maximum tractive efficiency is independent of lug height. Furthermore, they found that the pull coefficient decreased when the lug height increased beyond 20 mm. Gill and van den Berg (1967) state that high lugs decrease efficiency, but that they may be required under poor traction conditions in order to increase maximum pull.

Terpstra (1973) and Steinkampf (1974, 1975, 1981) found that high-lugged tyres (R_2) result in better tractive performance than regular agricultural tyres, when operating on wet, cohesive soils (Fig 4.5).

Radial and cross ply construction

Radial tyres generally are characterized by better tractive performance than cross plies when the conditions are relatively good. Under bad conditions the differences in tractive efficiency are small, but the radial tyre still has a higher pull coefficient. Steinkampf (1981a+b) found great differences between tyres

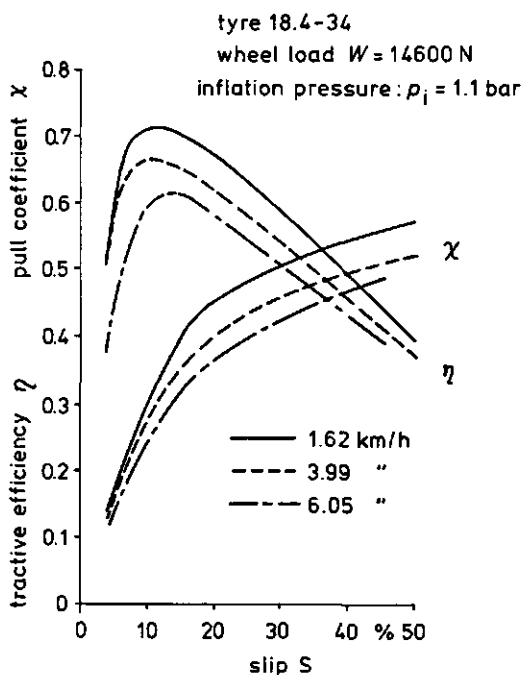


Fig. 4.6. Tractive performance of a 18.4-34 tractor rear tyre at different driving speeds.

in the groups of radials and cross plies as well. The tractive performance of a good radial tyre can be 25 % better than the one of a bad cross ply; on the other hand, the tractive performance of a good cross ply can be as much as 14 % better than the one of a bad radial one.

Tyre diameter and width

Increasing the diameter and increasing the width both result in a small improvement of tractive performance. The effect of width is more pronounced than the effect of diameter.

Driving speed

Under poor driving conditions Steinkampf (1975) measured the performance of a 18.4-34 tractor rear tyre at driving speeds of 1.62, 3.99 and 6.05 km/h. An increase in speed resulted in a decrease of pull coefficient and tractive efficiency (Fig. 4.6). These results only show a tendency and they need to be proved for tyres driven at higher speeds and under better field conditions.

Direction of rotation

Sometimes the direction of the rotation of front tyres of four-wheel drive tractors is reversed in order to decrease tyre wear. Reversed rotation direction results in a longer life of the front tyres when much road travel is done (Billier, 1983).

Billier and Steinkampf (1978) found that the direction of rotation hardly influenced tractive performance under good driving conditions. Under less ideal conditions the performance of the reversed tyres decreased.

The choice between low front tyre wear (reversed mounting) and best tractive performance under bad conditions (normal mounting) will depend on the use of the tractor.

Tyre wear

Tyre wear results in a decrease of lug height and an increase in the area of the lug faces. Therefore, on dry roads tyre performance increases with increasing tyre wear. In the field starting tyre wear has no pronounced influence on tractive performance. When driving conditions are poor tyre wear can result in a worse performance.

4.1.2.4. TRACTOR TRACTIVE PERFORMANCE

Tractive performance depends on the tractor type, the traction properties of the tyres, the weight, and the surface conditions.

Tractor type

The tractor type includes the number of driven axles and weight distribution. There are 4 tractor types available:

- TWD : a two-wheel drive tractor with driven rear tyres and towed front tyres
- FWDa : a four-wheel drive tractor with driven front tyres that are smaller in diameter and width compared to the driven rear tyres

- FWDb : a four-wheel drive tractor with driven front tyres that have equal width and a smaller diameter than the driven rear tyres
- FWdc : a four-wheel drive tractor with driven front tyres that are equal to the driven rear tyres

The rear tyres of a FWD perform better than the front tyres. Dwyer et al. (1977) found the pull for a 13.6-38 tyre to be approximately 7 % higher when the tractor was passing in the same track for the second time. This multi-pass behaviour also resulted in about 5 % higher maximum efficiency.

Dwyer and Pearson (1976) compared a TWD and a FWD in the field. The difference in performance between the two tractors was greater than was expected from the multi-pass effect. The reason must be the zero-slip condition used, and the fact that the FWD weighed more than the TWD. To make more realistic comparisons, we have made recalculations, using Dwyer and Pearson's results. The performances of the tractor types compared with respect to maximum drawbar power per unit tractor weight, show that the FWD with unequal wheels performs on the average 2.1 % better than the TWD, while the FWD with equal wheels performs on the average 8.7 % better than the TWD.

Weight distribution also affects tractor tractive performance. A TWD generally has a static weight distribution of about 35:65. This means that 35 % of the tractor weight acts on the front axle and 65 % on the rear axle. At a dynamic weight distribution of 15 : 85 a TWD performs somewhat better than at a distribution of 35 : 65 (Steinkampf, 1977).

Söhne and Bolling (1981) compared three FWD types at different dynamic weight distributions. They show weight distributions for optimum tractor tractive performance (Table 4.2). Type 2 performs better than type 1, and almost equally to type 3.

Table 4.2. Dynamic weight distribution for optimum tractor performance (Söhne and Bolling, 1981).

Tractor type	weight distribution
1: FWD a	32 : 68
2: FWD b	45 : 55
3: FWD c	50 : 50

Single and dual wheels

At a given slip and dynamic load, the pull of a single tyre is practically the same as the one of a dual system (Bailey and Burt, 1981). Because duals have greater load-carrying capacity than a single tyre they can develop greater pull if their greater load-carrying capacity is used. The tractive efficiency of a single tyre is slightly higher than the one of the dual system. On sand, pull coefficient and tractive efficiency of duals decrease with increasing spacing between duals (Melzer and Knight, 1973).

Weight

Many researchers give formulas for the optimum ratio of weight to available power (Table 4.3).

Table 4.3. Weight to power ratio for optimum tractor tractive performance.

tractor type	formula	references
TWD	$W/P_e = 1.17/v$	Reece (1970)
FWD	$W/P_e = 0.82/v$	Reece (1970)
FWD	$W_a/P = 1.50/v$	Brixius and Zoz (1976)
TWD and FWD	$W_a/P = 1.33/v$	Hofman (1977)
TWD and FWD	$W_a/P = 1.79/v$	Dwyer (1978)
TWD	$W/P_e = 1.2/v$	Melborg and Perdok (1979)

P = power available for a driven axle (kW)

P_e = engine power (kW)

v = driving speed (m/s)

W = tractor weight (kN)

W_a = weight on driven axle (kN)

We can see from these formulas that at the same weight to power ratio a TWD needs a higher velocity than a FWD for optimum performance. The drawback of all these formulas is that they are valid under one particular condition only. Neither do those formulas take into account the influence of slip and field conditions on the weight needed for optimum performance. The influence of slip on the weight to power ratio has been shown by Steinkampf (1975).

To calculate the optimum weight to power ratio for different field conditions, velocities, and tractor types it is necessary to use a more detailed formula:

$$P_e = P_t + P_f + P_r \quad [4.4]$$

where, P_e = effective engine power (kW)
 P_t = transmission power [$P_t = (1-\eta_t)P_e$]
 η_t = transmission efficiency
 P_f = front axle power (kW)
 P_r = rear axle power (kW)

For a TWD this formula changes into:

$$P_e = (1 - \eta_t)P_e + \rho \cdot W_f \cdot v + \frac{\chi \cdot W_r \cdot v}{\eta} \quad [4.5]$$

where, ρ = rolling resistance coefficient
 W_f = dynamic front axle load (kN)
 W_r = dynamic rear axle load (kN)
 v = velocity
 χ = pull coefficient
 η = tractive efficiency

For a FWD formula 4.4. changes into:

$$P_e = (1 - \eta_t)P_e + \frac{\chi_1 \cdot W_f \cdot v}{\eta_1} + \frac{\chi_2 \cdot W_r \cdot v}{\eta_2} \quad [4.6]$$

where, χ_1 = pull coefficient 1st pass
 χ_2 = pull coefficient 2nd pass
 η_1 = tractive efficiency 1st pass
 η_2 = tractive efficiency 2nd pass

Calculations of optimum tractor - tillage implement combinations have been presented by Jahns and Steinkampf (1982), and Schäfer(1983).

For optimum performance the ratio of weight on driving axle to engine power generally lies under 900 N/kW. Tractors available in the Netherlands generally have a tractor weight to engine power ratio between 500 and 700 N/kW. About two thirds of the weight of a TWD acts on the rear axle. At the often used ploughing velocities of 5 to 7 km/h the standard available weight to power ratio is not optimal. Therefore, the transfer as well as the adding of weight are important for optimum tractive performance during ploughing operations. The ratio W_a/P_e can also be enlarged by ballasting weights and filling the tyres with water.

When the tractor is driven in the furrow when the ploughing is done with a mouldboard plough, the largest allowed tyre width is 13.6, 16.9, or 18.4 inches depending on ploughing width. Therefore, the load-carrying capacity of the rear tyres determines up to which engine power TWD can be used and when FWD is needed for optimum performance. Table 4.4 shows the maximum TWD engine power that can be used for different tyre sizes and at certain weight to power ratios. The maximum power at a load to power ratio of $W_a/P_e = 900$ N/kW is also the heaviest TWD that can be loaded to 900 N/kW.

Table 4.4. Maximum allowed engine power (kW) of TWD at different levels of weight to power ratio for 3 tyre sizes. Inflation pressure 1.0 bar; load ratio 120 %.

Tyre Size	weight to power ratio W_a/P_e N/kW			
	600	700	800	900
13.6-38	51	44	38	34
16.9-30	66	56	49	44
16.9-38	74	63	55	49
18.4-30	80	69	60	53
18.4-38	90	77	68	60

4.1.2.5. PLOUGHING CAPACITY

One of the main traction aspects of a tractor is the steady pull needed for ploughing. To know more about ploughing capacity on farms we measured ploughing capacity during our slip measurements (see also 3.1.1.3).

Ploughing capacity was calculated with the following formula:

$$C = \frac{1000 \cdot v \cdot b \cdot d}{P_e}$$

where, C = ploughing capacity (m^3/kWh)
 v = ploughing velocity (km/h)
 b = ploughing width (m)
 d = ploughing depth (m)
 P_e = available effective engine power of the tractor (kW)

The results of our measurements have been plotted in Fig. 4.7. This figure shows that the ploughing capacity was generally higher on light soils than on heavy soils. It is amazing that the lowest and the highest capacity were equal on both soil types. The ploughing capacities varied from 11.4 to 64.6 m^3/kWh . The median value on light soils was 30.0 m^3/kWh . On heavy soils this was 24.0 m^3/kWh . The percentage measurements at a ploughing capacity below 18.0 m^3/kWh was 13 and 15 for light and heavy soils respectively. On the light soils the ploughing capacity of 35 % of the participating farmers was above 36.0 m^3/kWh . On heavy soils this was true for only 15 % of the farmers.

The median ploughing depth was 25 cm on both light and heavy soils. At a ploughing resistance of 25 kN/m^2 for light soils and 75 kN/m^2 for heavy soils, the energy needed for ploughing has been calculated. The median available tractor energy has been calculated from the median values of ploughing capacity and ploughing depth. A comparison of the needed and available energy (Table 4.5) shows that there is twice as much tractor energy available than is needed for ploughing.

The main reason for the sometimes low ploughing capacity is the inefficient use of the available tractor engine power. This is generally due to several of the following aspects: wheel slip, tractor load and weight transfer, traction conditions, tyre aspects, tractor-plough combination, ploughing width, ploughing depth, velocity, and adjustment of the plough.

A good tractor engine load at heavy ploughing includes an engine speed of 90 % of the rated engine speed and a torque of 90 % of torque at rated engine speed. This means that the tractor engine load (λ) equals 81 % of the power at rated engine speed. During ploughing on farms the values were generally lower due to non optimal settings of tractor, plough, and tractor-plough combination.

In West Germany a common figure for calculating is $\lambda = 83$ % (Renius, 1985). Rutherford (1973) found λ values between 44 % and 87 % when ploughing was done on farms.

We may conclude that there is a great potential for improvements of ploughing capacity.

Table 4.5. Energy during ploughing on farms.

	calculated median energy needed for ploughing (kWh/ha)	median available energy (kWh/ha)
light soils	17.4	83.3
heavy soils	52.1	104.2

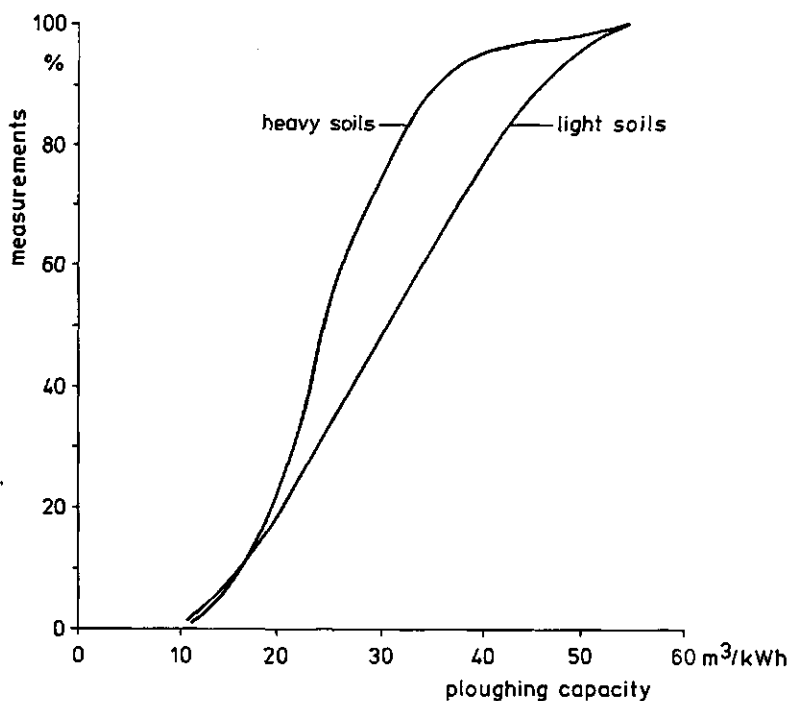


Fig. 4.7. Ploughing capacity on Dutch farms in 1980.

4.2. STRESSES IN THE CONTACT AREA

Radial (normal) stresses and tangential (shear) stresses generally occur in the contact area between the soil and a towed or driven device.

Stresses can be measured by making use of pressure transducers in the soil or by pressure cells embedded in the wheel periphery. The disadvantage of using pressure transducers in the soil is that they can move during the compacting process and, therefore, can provide erroneous information. All researchers referred to in section 4.2 have used pressure cells embedded in the wheel periphery.

4.2.1. STRESSES IN THE CONTACT AREA BETWEEN SOIL AND RIGID WHEEL OR ROLLER

Hegedus (1965) measured normal stress distribution in the soil-wheel interface and the influence of wheel load and slip on this distribution (Fig. 4.8). The distribution of both normal and shear stresses in the soil-wheel interface has been measured by Onafeko and Reece (1967) and Krick (1969). Wong and Reece (1967a, 1967b) and Wong (1967, 1978) relate stress distribution to flow zones beneath rollers and wheels.

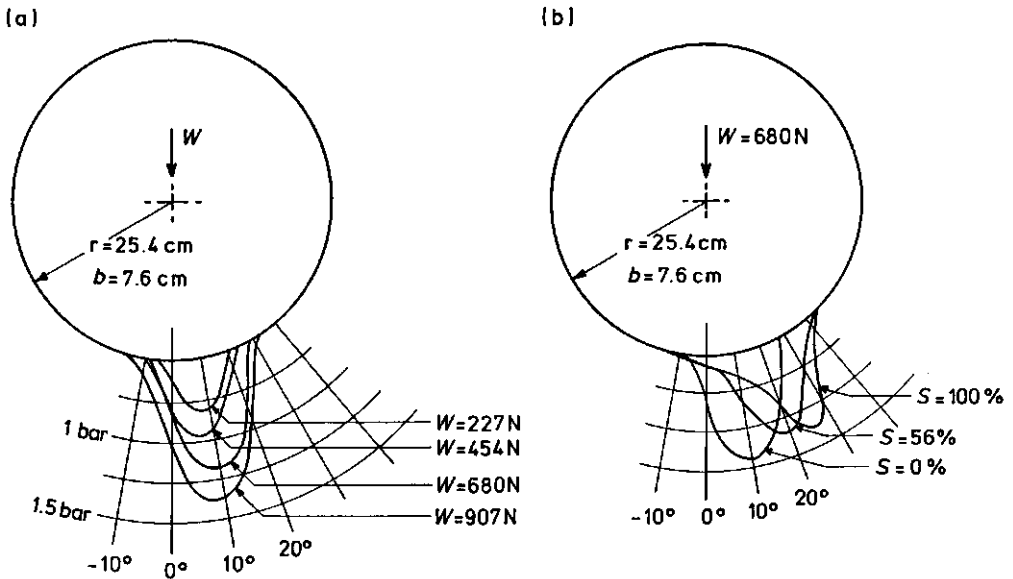


Fig. 4.8. Normal pressure distributions under a wheel on dry sand.

(a) non-slip with load as parameter

(b) constant load with slip as parameter.

4.2.1.1. RADIAL STRESS DISTRIBUTION

Maximum radial stress does not occur at the point beneath the axle as suggested by the plate sinkage analogy (Bekker, 1956). It actually occurs in front of the wheel axle and shifts forward at increasing slip. Maximum radial stress occurs at the point where the two soil failure zones beneath the wheel join each other. Increasing the wheel load results in an increase in maximum radial stress. At the edge of the wheel rim there is a concentration of stress which decreases at increasing slip (Table 4.6).

Table 4.6. Ratio of maximum radial stress σ_R at the edge of the wheel rim to maximum radial stress σ_M in the middle of the wheel rim (Krick, 1969).

	towed	slip=12 %	slip=25 %	slip=40 %
σ_R/σ_M	1.75	1.6	1.5	1.4

4.2.1.2. TANGENTIAL STRESS DISTRIBUTION

At the transition point (point A in Fig 3.19a) of a towed wheel shear stress changes its direction; having occurred in the direction opposite to wheel rotation (positive), it now occurs in the same direction in which the wheel rotates (negative).

In zone a (Fig. 3.19a+b) shear stress occurs in forward direction (positive). Beneath a towed wheel (Fig. 3.19a) the soil moves forward slowly between A and E while the wheel moves forward relatively fast. Therefore, shear stress occurs in the direction of wheel rotation (negative). Shear stress in the two zones occurs in opposite directions. These findings agree with the requirement that the sum of the moments equals zero.

Beneath a driven wheel both soil and wheel rim move backward in zone b (Fig. 3.19c). The wheel moves faster than the soil, and therefore, shear stress in zone b occurs in forward direction (positive).

4.2.2. STRESSES IN THE TYRE CONTACT AREA

The essential difference between a rigid wheel and a pneumatic tyre is the flexibility of the tyre. When the tyre moves on soft soil there generally will be an equilibrium between the tyre-deflecting forces and the rut-forming forces.

4.2.2.1. AVERAGE CONTACT PRESSURE

Average contact pressure is defined as: $p_m = W/A$ [4.7]

where, p_m = average contact pressure
 W = vertical wheel load
 A = area of the tyre-road interface

In terra mechanics this average contact pressure is often given as sum of tyre inflation pressure p_i and a pressure p_c for carcass stiffness:

$$p_m = p_i + p_c \quad [4.8]$$

Average contact pressure on a rigid surface

This pressure depends on inflation pressure, wheel load, and tyre parameters.

An increase in inflation pressure (at a constant wheel load) results in a decrease of carcass stiffness pressure p_c . An increase in wheel load (at a constant p_i) results in a small increase in p_c (Söhne, 1952).

The dynamic contact area of a tyre is larger than the static contact area (Van den Berg and Gill, 1962).

Tractor tyres with a closed centre tread have a higher average contact pressure than tyres with an open centre tread (Söhne, 1952).

Krick (1969) tested smooth tractor rear tyres, at nominal wheel load, over an inflation pressure range from 0.6 to 2.0 bar. He found a constant carcass stiffness pressure p_c of about 0.45 bar. Steiner and Söhne (1979) tested several lugged tractor rear tyres of different sizes and construction. They found the following empirical equations for the average contact pressure:

Cross ply tractor rear tyres:

$$p_m = 1.128 + 0.665p_i + 0.009W - 0.004D \quad [4.9]$$

Radial tractor rear tyres:

$$p_m = 2.677 + 0.575p_i + 0.011W - 0.016D \quad [4.10]$$

where, p_m = average contact pressure (bar)
 p_i = tyre inflation pressure (bar)
 W = wheel load (kN)
 D = tyre diameter (cm).

Average contact pressure on deformable soil

Contact pressure is generally smaller on deformable soil than on a rigid surface because the contact area is enlarged when ruts are formed.

When a tyre passes in a track for the second time wheel sinkage is generally lower than when it does so in the first pass. When the tyre passes for the second time the contact area is smaller and the average contact pressure is therefore higher than when the tyre passes for the first time.

Average contact pressure on deformable soil can be remarkably lower than inflation pressure (Baganz and Kunath, 1963; Söhne 1952 and 1963). Formula 4.8. is therefore not very useful for

field traffic.

4.2.2.2. RADIAL STRESS DISTRIBUTION

Smooth tyre on a rigid surface

Normal stress distributions in longitudinal and lateral directions have been given by Van den Berg and Gili (1962), Clarck (1971b), and Van Eldik Thieme and Pacejka (1971). Shear peaks occur at the edges (Fig. 4.9). Stress increases fast on the front side of the tyre, but decreases also fast at the end of the contact area.

Smooth tyre on deformable soil

On soft soil normal stress distribution is more uniform in both longitudinal and lateral directions (Fig. 4.9). At high slip values there are an initial and a terminal peak in the longitudinal stress distribution measured in the centre line of the tyre (Fig. 4.10)

Lugged tyre on deformable soil

Trabbic et al. (1959) and Liang and Yung (1966) measured normal pressure distribution across the lug face, on the undertread, and on the leading and trailing lug face. An increase in inflation pressure resulted in an increase in normal pressures in the middle of the tyre and a decrease in normal pressures at the edges of the tyre circumference. Normal pressure on the leading lug face and the undertread increased at higher pull, while normal pressure on the lug face and the trailing side decreased.

4.2.2.3. SHEAR STRESS DISTRIBUTION

Measurements of shear stress in the tyre contact area have been made by Liang and Yung (1966), Krick (1969), Van Eldik Thieme and Pacejka (1971), and Clarck (1971b).

Smooth tyre on a rigid surface

Shear stresses generally show peaks on the edges of the contact area. An increase in inflation pressure increases the maximum shear stress (Clark, 1971b).

Shear stress becomes positive by means of the action of a driving torque. Maximum shear stress moves backward with increasing driving torque. The stress peak becomes negative as a result of the action of a braking torque.

Smooth tyre on deformable soil

In longitudinal as well as lateral direction stress distribution for tyres is more uniform than for rigid wheels (Krick, 1969). There is still a stress increase towards the edge of the tyre at small slip values, but at high slip this disappears. Stress peaks have been observed in the middle of the tyre at high wheel slip (Fig. 4.10).

Lugged tyre on deformable soils

Shear stress on the lug face, the undertread, the leading lug side, and the trailing lug side have been measured by Liang and Yung (1968) for a 11 - 28 tractor rear tyre used on sand. Stresses were measured at two pulls. An increase in pull resulted in a decrease in shear stress on the lug face and the lug sides, while shear stress on the undertread increased.

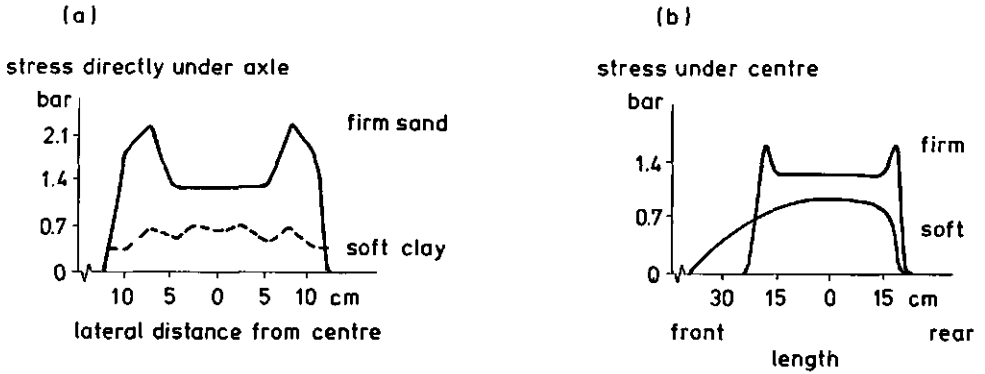


Fig. 4.9.a,b. Lateral and longitudinal stress distribution under a 11-38 towed smooth tyre at an inflation pressure of 1 bar (VandenBerg and Gill, 1962).

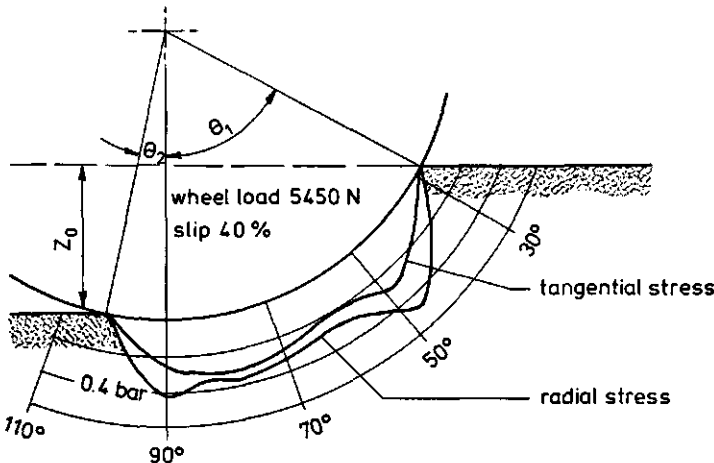


Fig. 4.10. Radial and tangential stress distribution under a smooth 11.5-15 tyre at 40 % slip (Krlick, 1969).

4.3. STRESSES IN THE SOIL

Soil compaction during agricultural field traffic is a result of stresses under tyres, wheels, and rollers.

To gain a better understanding of this problem, especially in order to predict soil compaction due to agricultural field traffic, it is important to know more about:

- stress distribution under the tyres
- the parameters that affect this stress distribution
- the resulting compaction of the soil and the parameters that affect this.

4.3.1. STRESS DISTRIBUTION IN THE SOIL UNDER TYRES, WHEELS, AND ROLLERS

Many theories about stress distribution under tyres are based on the equations of Boussinesq that describe stress distribution within isotropic and elastic materials such as steel. The principal stress (σ_r) in a volume element, induced by a point load (p) acting perpendicularly on the flat boundary of a semi-infinite mass, can be calculated with:

$$\sigma_r = \frac{3p}{2\pi r^2} \cos \theta \quad [4.11]$$

where, r = the distance between the volume element and the point load
 θ = the angle between the vertical line and the direction of the point load.

Civil engineers found that stress distribution in soil deviated from the one in a homogeneous isotropic mass. The more plastic the soil is, the larger these deviations will be.

Fröhlich (1934) introduced the concentration factor ν in formula 4.11 to account for the influence of soil plasticity on stress distribution:

$$\sigma_r = \frac{\nu p}{2\pi r^2} (\cos \theta)^{\nu-2} \quad [4.12]$$

For $\nu = 3$ the stress distribution is identical to Boussinesq's formula for an elastic isotropic mass. A concentration factor for $\nu = 4$ to $\nu = 6$ is common for soils.

During agricultural field traffic load transfer does not occur at one point, but in a finite contact area. Assuming that a tyre-soil system equals a uniformly loaded circle, Fröhlich (1934) calculated stresses σ_z :

$$\sigma_z = p_m (1 - \cos^{\nu} \alpha) \quad [4.13]$$

where, α = half top angle of a cone which has its top in the point in the soil in question and the area of the circle as its base.

p_m = mean pressure in the contact area.

Söhne (1953a) gives a numeric summation procedure. He divides the elliptical tyre-soil contact area into 25 elements of equal size. The load on each element is considered to be a vertical point load. The stress in a point A in the soil can be estimated as follows:

for all the elements the stress in point A is calculated with the point-load method. By summing all these contributions to the stress in A, an estimation of the principal stress in A is found.

In this way Söhne calculated many pressure distributions of agricultural tyres under different soil conditions. The results of these calculations can be shown in pressure bulbs (curves of equal principal stress). Fig. 4.11 shows calculated pressure bulbs under a tractor tyre for different soil conditions. Actually pressures measured by Reaves and Cooper (1960), and Grecenko (1967) are very similar to the computed distributions of Söhne.

tyre : 13.6 R28

inflation pressure : $p_i = 0.9$ bar

wheel load : $W = 10$ kN

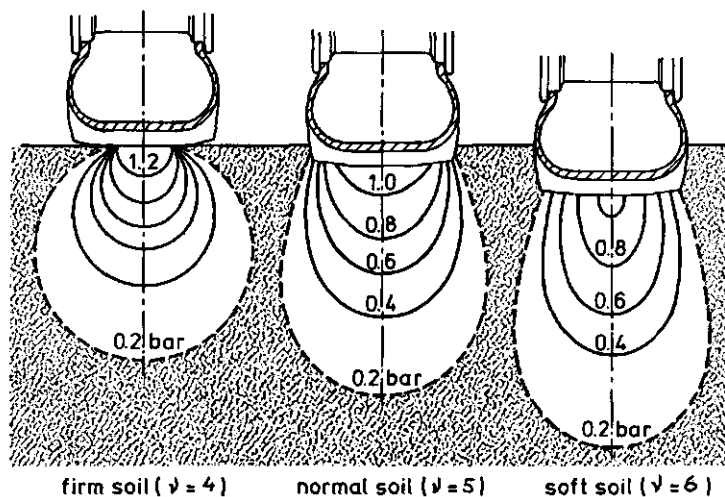


Fig. 4.11. Calculated curves of equal pressure σ_1 (pressure bulbs) under a tractor rear tyre for different soil conditions.

Bekker (1956) assumes that the tyre-soil system equals a strip load acting on a semi-infinite elastic medium. The width of the strip load is the tyre width. The stress V on the strip load is the mean normal stress in the tyre-soil interface.

The major principal stress follows:

$$\sigma_1 = \frac{v}{\pi} (\phi + \sin \phi)$$

where, ϕ = the angle (in radians) between the lines that connect the point considered with the sides of the strip load in a vertical plane.

From this equation Bekker assimilated the following rule of thumb: at a depth equal to the width of the loaded strip, the stress under the center of the strip load is about half of the stress on the strip load. Compared with the method of Söhne, the approach of Bekker results in values which are too high.

4.3.2. PARAMETERS THAT AFFECT THE STRESS DISTRIBUTION UNDER AGRICULTURAL DRIVING EQUIPMENT

Not only the soil but also the technical concept of the machinery affects stress distribution.

The concept of agricultural traction and transport devices with pneumatic tyres has changed drastically during the last 30 years. The mean engine power of the tractors increased by more than 300 %. The ratio tractor weight to engine power decreased with a factor of about 1.5. Therefore the driving speed of tractors at work increased. The mean weight of tractors more than doubled. By increasing tractor power the tractor type changed from two-wheel drive (TWD) to four-wheel drive (FWD). By increasing tractor power the load-carrying capacity of the transport devices increased.

Numerical data of these developments have been given by Danfors (1980), Söhne (1980), Söhne and Bolling (1981), Perdok and Terpstra (1983), and Renius (1986).

4.3.2.1. SOIL PARAMETERS

Soil properties influence stress distribution in the soil underneath the tyres. In the theories based on the Boussinesq equations, soil properties are characterized by the concentration factor ν . For agricultural soils ν has values between 4 and 6. This implies that soils are supposed to be isotropic.

In agricultural soils two or more layers can be distinguished: top soil, ploughing layer, plough sole, and subsoil. Most likely this layered structure of soil will influence the actual stress distribution.

4.3.2.2. TRAILER TYRE CONCEPT

Tyre parameters like inflation pressure (p_i), wheel load (W), tyre dimensions, and single/dual mounting influence pressure distribution.

Fig. 4.12 shows pressure bulbs under three contact areas according to Bolling and Söhne (1982). From this figure we can see that:

- the tyre with the lowest load has the smallest volume inside the pressure bulbs.
- Increasing the wheel load, at constant contact surface pressure, results in an increase in volume inside the pressure bulbs.
- equal wheel loads result in almost equal reach (in depth) of the pressure bulbs.

Figure 4.13 shows three tyre concepts at a constant wheel load W . A greater tyre width or double mounting results in less sinkage of the wheel and therefore less compaction near the surface. The pressure-bulbs of the three concepts reach nearly at equal depth into the subsoil.

Modern tyre agricultural transport devices have, despite their modern concept, pressure bulbs that reach deeply into the soil. The reason is that much heavier loads are applied.

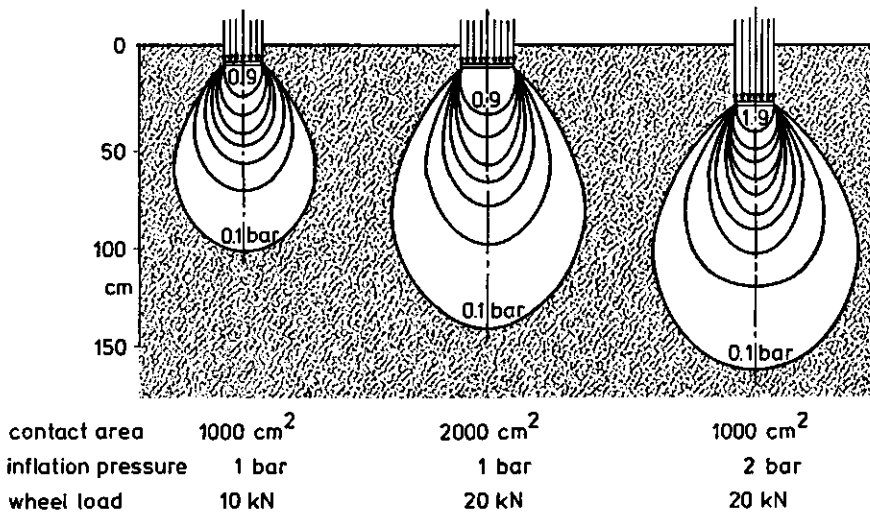


Fig. 4.12. Pressure bulbs under three contact areas.

4.3.2.3. TRACTOR TYPE

Increasing tractor power generally implies that tractor weight increases. To support this heavier weight, the tractor needs tyres with larger dimensions.

A limiting factor in increasing tractor tyre width is the width of the open furrow during in-furrow ploughing. Therefore at greater tractor power the front axle load increases. To prevent the front wheel rolling resistance from getting too high and to improve the weight-pull ratio, driven front wheels may be used. For these four-wheel drive tractors (FWD-tractors) different types are available. The pull-slip behaviour of these types has been discussed in section 4.1.2.4.

Bolling and Söhne (1982) present calculated pressure bulbs under one TWD and two FWD tractors (Fig. 4.14). We can see that, despite larger tyre dimensions, the pressure bulbs reach more deeply when tractor power is increased. This is mainly due to the increase of tractor weight at increasing tractor power. The backward bend in the pressure bulbs is caused by the pulling force. To calculate these distributions advanced computing programmes and extensive calculation facilities are needed.

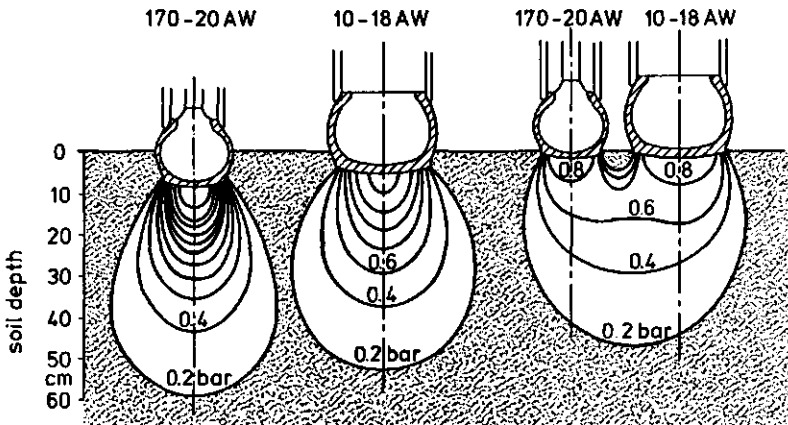


Fig. 4.13. Calculated pressure bulbs under tyres with 7.0 kN axle loads. From left to right: narrow tyres, wide tyres, and dual trailer tyres at inflation pressures of 3.0, 1.5 and 0.74 bar respectively (Söhne, 1953a).

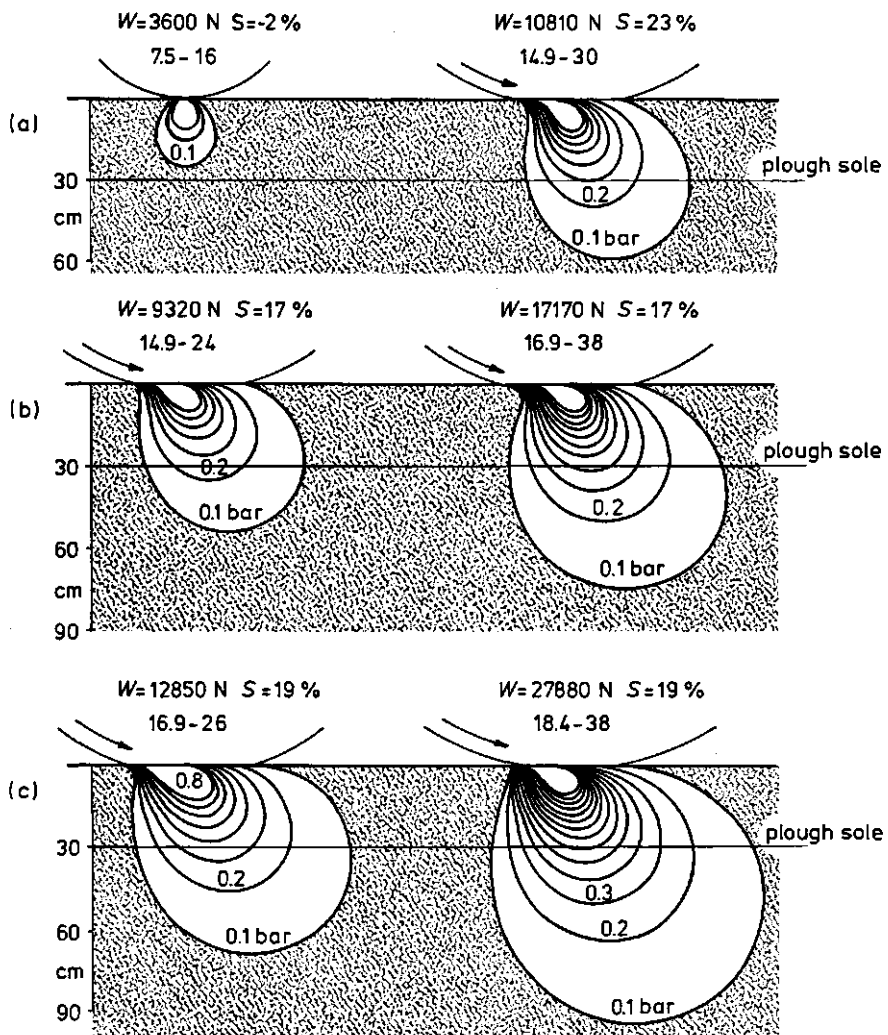


Fig. 4.14.a-c. Pressure bulbs under three tractors.
 (a) 30 kW Two-wheel drive tractor
 (b) 60 kW Four-wheel drive tractor
 (c) 90 kW Four-wheel drive tractor.

CHAPTER 5

SOIL CHARACTERISTICS CONCERNING LOAD-BEARING PROCESSES

5.1. RELATIONSHIPS BETWEEN "TREATMENT" AND "BEHAVIOUR" OF SOIL

The compaction behaviour of a soil depends on prior processes to which the soil has been subjected. If these prior processes are known they can be used as a basis for prediction of subsequent behaviour (Koolen, 1977).

The treatment of the soil may comprise a series of tillage operations, changes in temperature, changes in moisture content, etc.

In a uniaxial compression test the behaviour of Lexkesveer sandy loam was tested for repeated compressions while the soil was subjected to different treatments between the compressions. Cylinders (81 mm in diameter and with a height of 50 mm) were filled with about 300 grammes of soil. The samples were compressed with a hydraulic press at a speed of 2 mm/s up to pressures of 1.5 and 4.0 bar.

The test consisted of 4 series. Each series had a moisture content range between 10 and 21 percent water content by weight. To get the same starting position for all cylinders, they were precompressed at 0.5 bar.

Series 1: repeated compressions were made with negligible intervals between the compressions. Series 1a was loaded 15 times to 1.5 bar; series 1b 15 times to 4.0 bar.

Series 2: the soil samples were compressed to 4.0 bar and there was a rest-period of 3.5 days. Series 2a was loaded 5 times to 4.0 bar with a rest-period of 3.5 days between compressions; series 2b was loaded 15 times to 4.0 bar with a rest-period of 3.5 days after every 3 compressions.

Series 3: the samples were compressed to 4.0 bar followed by a rest-period of 7 days.

Series 3a was loaded 5 times to 4.0 bar with a rest-period of 7 days after every compression; series 3b was loaded 15 times to 4.0 bar with a rest-period of 7 days after every 3 compressions.

Series 4: like 3, but during the rest-period the soil sample was subjected to a drying/wetting cycle. We used the following procedure during a drying/wetting cycle: after compression the samples were dried in an oven at 105 °C during 0.5 hour. The samples were dried afterwards during one day at room temperature. After one

day the samples were rewetted with crushed ice to the original moisture content.

The results of these tests are given in Fig. 5.1. From these results we can see that in the dry area (under 16 % m.c.) soils do not behave differently as a result of the different treatments. In the moisture content range above 16 % soil behaviour depends on the treatment.

From the series 2 and 3 we can see that a rest-period between compressions results in a higher compressibility of the soil. This can be explained by the phenomenon of entrapped air. When a soil is compressed air pressure builds up in this entrapped air before the density of saturation is reached. This phenomenon of "entrapped air" has been mentioned by Faure (1980). When the rest-period between compressions is long enough the air pressure in the sample will return to normal values. During the next compression this soil can be compressed further than when a rest-period between the compressions is lacking. There is no difference in soil behaviour when the rest-period lasts 3.5 or 7 days. Series 4 shows less compaction of the samples (in the range >16 % m.c.) when they are subjected to a drying/wetting cycle in the rest-period. Because of this drying/wetting cycle this soil partly regains its resistance to compaction. A clear explanation of this phenomenon is difficult to give. Swelling and shrinking processes are not likely to be the cause because this soil hardly has a swelling and shrinking capacity.

In the field soil is exposed to natural forces like freezing and thawing, and shrinking and swelling as a consequence of drying and wetting respectively.

The results of studies on the persistence of compaction after freezing and thawing are contradictory. Krumbach and White (1964) reported decreased bulk densities on a freezing surface soil of Celina loam in Michigan. Wittsell and Hobbs (1965) found a decrease of bulk density after 1 year of freezing and thawing in the 2.5 to 10 cm and the 18 to 25 cm layer of a compacted silt loam.

More recent research results tend to disagree with the above results. In Sweden wheel-induced soil compaction persisted under freezing and thawing (Danfors, 1974). Mech et al. (1967) found that on a compacted silt loam in Washington crop yield problems persisted over a four-year period, even though extreme frost heaving took place. Njós (1976) found on loam and clay-loam soils an effect of autumn compaction on the yield of cereals in Norway. Compactions made in spring resulted in significant yield reductions even after two years. Blake et al. (1976) noted no change in bulk density below the plough layer over a nine-year period in Nicollet clay loam in Minnesota. Neither crop nor the soil water content in the frozen period affected the compacted subsoil.

From these studies we can conclude that in the top soil, freezing and thawing can reduce soil compaction because of lateral soil displacements and a small overburden. Compaction in the subsoil (below the plough layer) persists even after freezing.

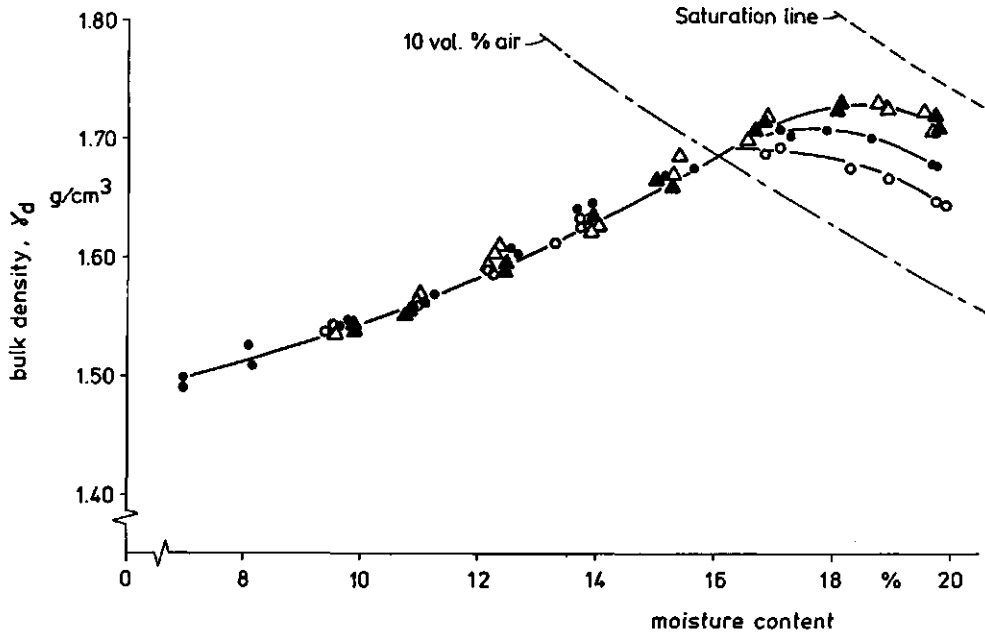


Fig. 5.1. Behaviour of Lexkesveer loam in uniaxial compression tests during different treatments. Series 1 (●), Series 2 (▲), series 3 (△), and series 4 (○) after 15 loadings to 4.0 bar.

Shrinking and swelling, as a result of changes in the moisture content, depend mainly on the type and proportion of clay in the soil. Upon swelling there is an increase in soil porosity. After excessive shrinkage, many cracks are formed in the soil. These cracks facilitate water infiltration and root penetration. Soils with a high sand content have a small capacity for shrinking. Wetting and drying do not seem to alleviate soil compaction. Porosities hardly changed in the compacted zone of a silt loam with a naturally compacted layer (Mech et al, 1967). Van Ouwkerk (1968) observed the effect of time and wetting and drying on soil porosity in a sandy loam. The surface porosity gradually decreased due to natural forces. Where the subsoil had an artificially compacted layer, porosity did not increase with time. Vomocil and Flocher (1965) found on Yolo loam (20 percent clay of which 75 percent montmorillonite) that had been artificially compacted, a persistence of the compaction effect despite many periods of wetting and drying.

5.2. CHARACTERIZING PROPERTIES USED IN SOIL SCIENCE

Soil texture

The compactibility of a soil depends on its particle size distribution (Bodman and Constantin, 1965; van der Watt, 1969; Chancellor, 1976). Static compression tests show that the highest compaction occurs in soils with almost equal amounts of the various particle size classes. An explanation for this has been given by Bodman and Constantin (1965). High soil compaction can only be obtained if coarse sand is present in fair amounts. Porosities and range of pore spaces tend to be higher in clay soils than in sandy soils. Koolen and Kulpers (1983) give credit for this to "the stronger tendency of clay to form aggregates".

Moisture content

The influence of moisture content on soil compaction is shown in Fig. 5.2a. We can see from these uniaxial-compression curves that for dry soils porosity continues to decrease at increasing pressure. Within the limits of 10 to 19 percent moisture content there is a strong increase in compactibility when moisture content increases. When the moisture content exceeds 19 percent the curves have a different shape because the compressed soil comes near to the saturation line. Fig. 5.2b shows the relation between porosity and water content at different pressure levels. The curve AB of the figure shows the water-filled part of the pore space. The soil can be compacted to this limit only by short compression actions. If compression to this limit lasts for some time water will be squeezed out of the soil.

Amir et al. (1976) used these data of Söhne for calculations. In the range of 10 to 20 percent moisture content they calculated a highly significant relationship between porosity, pressure, and soil moisture content:

$$N = A_n - B_n \ln p - C_n \ln \theta$$

where N = porosity (%)
 A_n, B_n and C_n are constants
 p = pressure
 θ = moisture content (% by volume)

Air content

Fig. 5.1 and 5.2 show that the compaction curves do not reach the saturation line; this is caused by entrapped air. During compression of a soil sample air flows out. Not all air can escape freely. Entrapped air can be compressed. After unloading the compressed air may cause a rebound of the soil.

The influence of soil air on rebound will be discussed in section 7.1.2.

When it becomes possible for the air to flow out completely the compaction curve touches the saturation line (Faure, 1980). During compression tests there is a normal amount of entrapped air of about 5 percent.

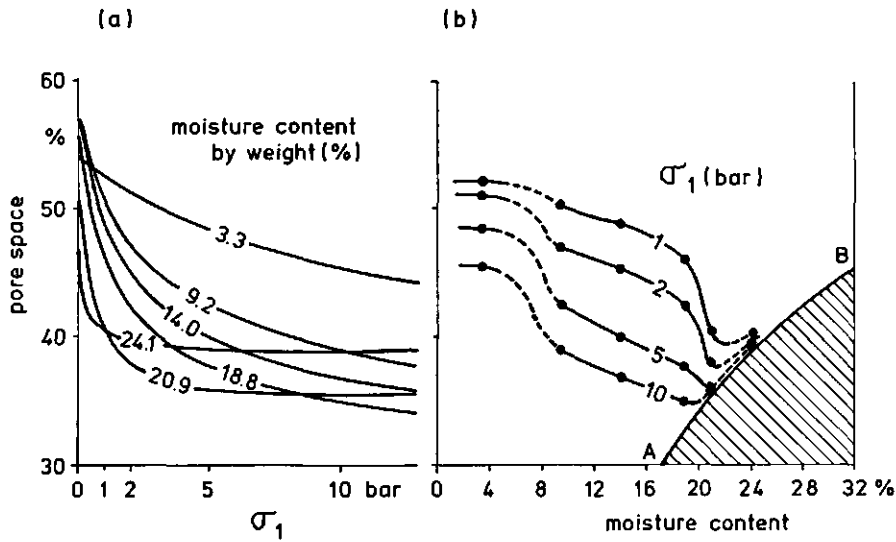


Fig. 5.2. a, b. Soil compactibility as affected by moisture content (Söhne, 1958).

Lime content

Proctor tests carried out by Kezdi (1969) and Sommer (1972) showed a decrease of compactibility if more lime was added. The moisture content at which highest compactions occurred also increased. For a clay loam Sommer found that maximum compaction and the moisture content at which this is obtained changed by liming the soil with about 2 percent by volume and 2 percent by weight respectively. According to Kezdi these phenomena can be explained by the change in soil structure caused by liming: water is needed for hydration and the mobility of coagulated particles decreases.

Organic matter

Organic matter increases soil strength under wet conditions. At a low soil moisture content resistance to compaction is higher in soils containing a normal amount of organic matter than in soils containing a large amount of organic matter. So, during drying, compaction resistance increases most in soils low in organic matter (Kuipers, 1959).

Water suction (pF)

Soil water suction in combination with saturation degree is an important soil strength factor. The pF-curve is sensitive to soil structure. During compression aggregates flatten at the contact points and the size of pores between the aggregates decreases.

Fig. 5.3 shows pF-curves of samples from the plough sole and from the subsoil of Winnigstedt slit loam (Moreno et al, 1974). The curves at $p=0$ bar represent undisturbed soil samples. The $p=14$

curves represent the same samples after static compaction at 14 bar and successive equilibration to the different suctions. These pF-curves show that, below pF2.4, the water content of the undisturbed samples from the plough sole is lower than the water content of those from the subsoil; above pF2.4 the opposite is true.

The curves for $p=14$ bar are almost equal for the plough sole and the subsoil. Below pF2.4 the static compaction results in a decrease of the water content; while an increase has been found between pF 2.4 and 3.7. Above pF3.7 static compaction has no effect on the water content.

Kulpers (1966) also found a decrease of water content (by weight) at pF2.0 after compaction, but after loosening the compressed soil, the water content at pF2.0 increased to higher values than before compaction.

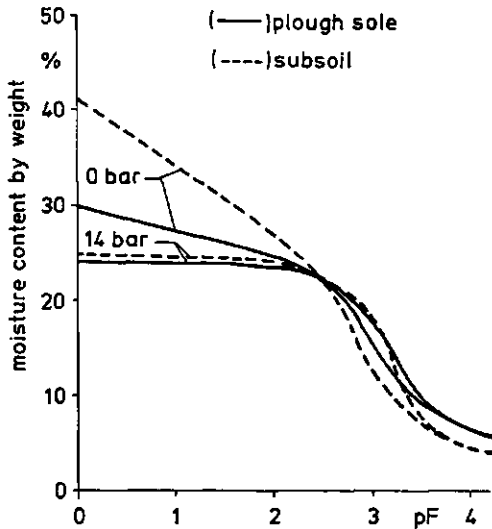


Fig. 5.3. pF-curves (averaged) for soil samples taken from the plough sole and from the subsoil of "Winnigstedt" silt loam.

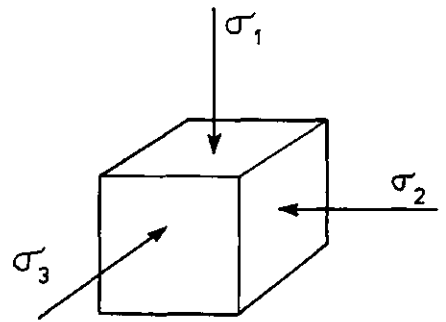


Fig. 5.4. A loaded soil volume element

5.3. MECHANICAL PROPERTIES

The soil mechanical properties comprise the geometrical changes (compaction, deformation, and failure) that a loaded soil volume element (Fig. 5.4) will show for all possible values of σ_1 , σ_2 and σ_3 .

The most important mechanical properties of load-bearing processes are compactibility, deformability, and resistance against shear failure.

5.3.1. COMPACTIBILITY

The loading of soil during soil tillage and agricultural field traffic is a relatively quick type of transient loading. Therefore, we can safely assume that the developed pore-water pressures will not have sufficient time to dissipate and that the role of water in the soil can be limited to its effect on soil strength.

5.3.1.1. MEASURES FOR COMPACTION

Compaction can be expressed in volumetric properties of solid, liquid, and gas phases:

Porosity of a soil volume element is the ratio of volume of pores (water + air) to the total volume of the element. It is expressed as a percentage or as a fraction. Porosity has the advantage of being dimensionless and independent of particle density. Other names for porosity are pore space and total pore space.

Void ratio (e) is the total volume of pores divided by the total volume of solids. According to Karafath and Nowatzki (1978) void ratio is easier to handle than porosity when the volume of the solids remains essentially constant for a given initial total volume of soil solids whereas with porosity both the volume of voids and the total volume change.

Dry bulk density (γ_d) is the weight of solids in a unit of volume. It is usually expressed in g/cm^3 or kg/m^3 . For the interpretation of dry bulk density we need to know the specific density of the solids.

Bulk weight volume (BWV) is $1/\gamma_d$ (cm^3/g).

The relationships between these quantities are given in Fig. 5.6. Besides changes in volumetric quantities compaction is often associated with increased penetration resistance and changes in pore structure properties such as reduction of conductivity, diffusiveness and permeability by water and air.

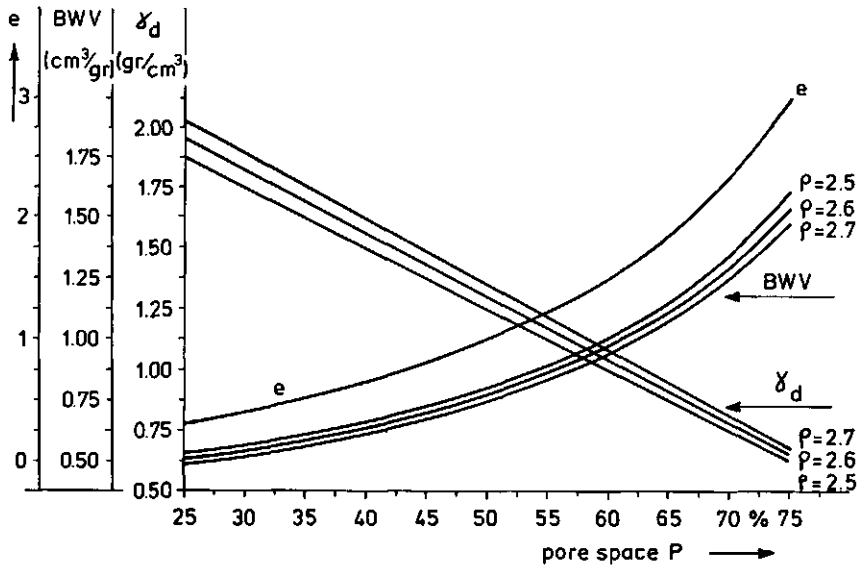


Fig. 5.5. Interrelationships between pore space (P), void ratio (e), bulk weight volume (BWV) and dry bulk density (γ_d).

5.3.1.2. MEASURING COMPACTIBILITY

The process of soil compaction is generally expressed in terms of stress-strain relationships:

$$\text{state of strain} = f(\text{state of stress}).$$

The stresses σ_1 , σ_2 , σ_3 , and their directions change during loading:

$$\text{state of strain} = f(\sigma_1(t), \sigma_2(t), \sigma_3(t)).$$

After some simplifications (Koolen and Kulpers, 1983) this formula may be written as:

$$(BWV)_t = f(\sigma_1(t), \sigma_3(t)).$$

This function can be measured in a triaxial test. In a triaxial apparatus a cylindrical soil sample is enclosed by a cylindrical rubber membrane and rigid top and bottom plates (Fig. 5.6). The enclosed sample is placed in a rigid transparent cylinder and is surrounded by water. The pressure (σ_3) in this water can be measured and regulated. Through a loading ram on the top-plate σ_1 can be changed and measured. By varying σ_1 and σ_3 every desired combination of stresses can be examined. Triaxial tests show that at any moment BWV is only determined by σ_1 and σ_3 . So the formula

can be written as:

$$BWV = f(\sigma_1, \sigma_3).$$

By definition $\sigma_m = 1/3(\sigma_1 + \sigma_2 + \sigma_3)$ and $\tau_{max} = 1/2(\sigma_1 - \sigma_3)$.
Substitution results in another function:

$$BWV = F(\sigma_m, \tau_{max}).$$

For a particular soil at a particular moisture content both f and F can be determined.

In the $(\sigma_m, \tau_{max}, BWV)$ space the compaction surface can be represented as $BWV = F(\sigma_m, \tau_{max})$. F can be determined from a series of triaxial tests with different paths of σ_1 and σ_3 . During such measurements the compressive stresses can be separated from shear stresses. When σ_1 is kept equal to σ_3 then $\tau_{max} = 0$; increase of σ_1 and decrease of σ_3 can be regulated in such a way that σ_m stays constant. At a certain moment it appears that σ_1 does not increase any further with further ram movement, and at the same time sample volume and, therefore, BWV do not change anymore. This situation is called "critical state". In critical state distortion continues at constant σ_m , τ_{max} and BWV. Along the critical state line, τ_{max}/σ_m is constant. This behaviour is described in the "critical state soil mechanics" (CSSM). CSSM has been developed at Cambridge by Roscoe and colleagues and has been described by Schofield and Wroth (1968). There is evidence that CSSM can be applied to unsaturated agricultural soils (Kurtay and Reece (1970); Hettiaratchi and O'Callaghan (1980)). Triaxial measurements of critical states can be found in Bailey and VandenBerg (1968), and Kumar and Weber (1974).

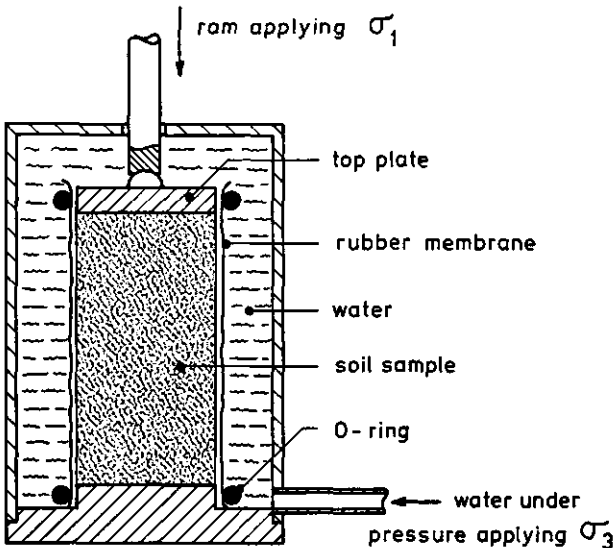


Fig. 5.6. Triaxial apparatus.

In the $(BWV, \sigma_1, \sigma_3)$ space the compaction surface can be represented as $BWV = f(\sigma_1, \sigma_3)$.

Compaction caused by agricultural activities will be along the surface f between the critical state line and the line for compaction at a constant diameter of the sample. For a number of constant values of σ_3/σ_1 , f was calculated from the functions F published by Bailey and Vandenberg, and Dunlap and Weber. From these calculations, made by Koolen and Kuipers (1983), and Koolen and Vaandrager (1984), we can conclude that σ_3 only has little influence on the major principal stress-pore space relationship (see Fig. 5.7).

In agricultural operations σ_3/σ_1 generally is 0.5 (Koolen, 1974). So soil compactibility can be represented by a relation between σ_1 and degree of compaction. For this no triaxial test is needed; uniaxial compression is sufficient.

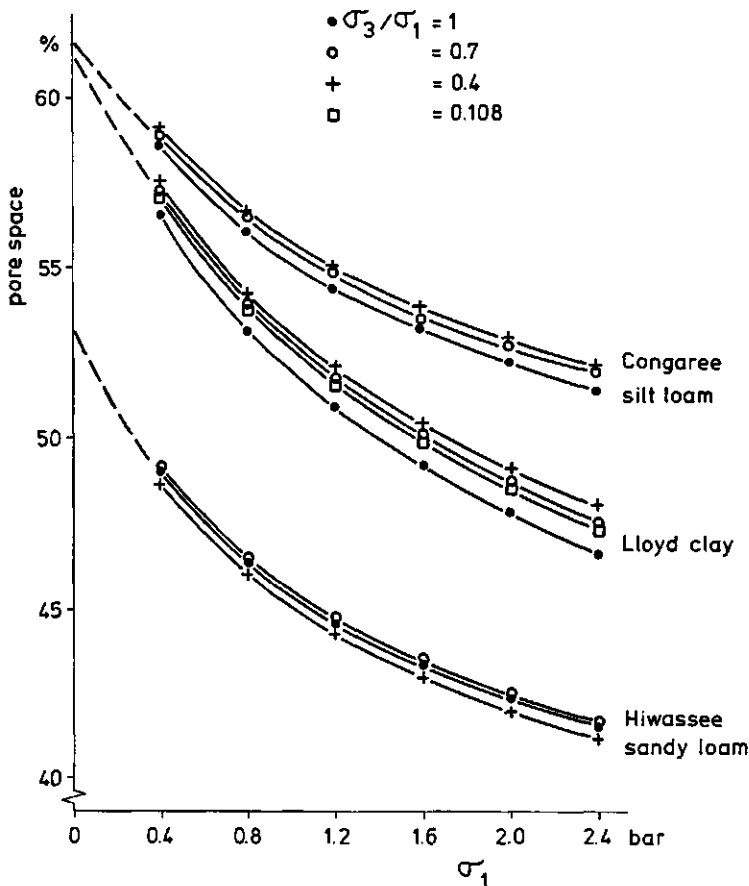


Fig. 5.7. σ_1 -pore space relationships as affected by σ_3/σ_1 ratio.

Uniaxial compression test

During a uniaxial compression test (see Fig. 5.8) a soil sample in a rigid cylinder is compacted under a downward moving piston. The stress on the piston and the sample volume are recorded continuously. Generally the piston moves gradually downward at a constant speed. The ratio of sample height to sample diameter should be rather small to keep the friction between the cylinder wall and the soil negligible. A suitable ratio can be found from the formula (Koolen, 1974):

$$\frac{\sigma_b}{\sigma_t} = \frac{(D/h) - 2K \tan \delta}{(D/h) + 2K \tan \delta}$$

- where: σ_t = mean normal stress on top of the sample
 σ_b = mean normal stress at the bottom of the sample
 D = inner diameter of the cylinder.
 h = actual height of the soil in the cylinder
 $\tan \delta$ = coefficient of friction between the cylinder wall and the soil
 K = σ_3/σ_1 in "ideal" uniaxial compression, without wall friction. In general $K = 0.5$.

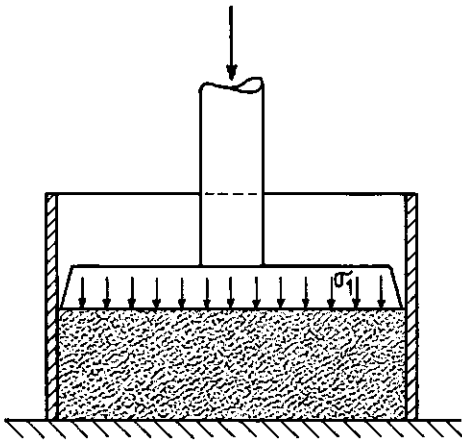


Fig. 5.8. Uniaxial compression test.

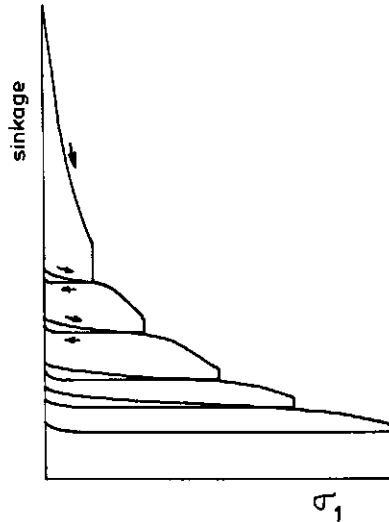


Fig. 5.9. Load-sinkage relationship in an uniaxial compression test with repeated loadings and unloadings (Söhne, 1952).

5.3.1.3. THE INFLUENCE OF REPEATED LOADING, LOADING SPEED, AND VIBRATIONS ON COMPACTIBILITY

Repeated loading

Agricultural field traffic is a process of loading, and several unloadings and reloadings.

In uniaxial compression tests the path of unloading and reloading, in a pressure - sinkage relationship, shows a hysteresis effect (see Fig. 5.9). Such hysteresis effects were found by Söhne (1951,1952,1956), and Yong and Warkentin (1966,1975). This hysteresis effect occurs in many materials; Nadal (1950) shows the same effect in metals.

After reloading the sample behaves in the same way as it would have done if the last (re)loading was continued without unloading.

A uniaxial compression test with several cycles of unloading and reloading shows that compaction continues. Every reloading results in extra compaction. This extra compaction decreases with number of loadings. Söhne (1956) found that further compressibility was still possible after 10 reloadings with no rest-period between the unloading and the next reloading (see Fig. 5.10).

In the field there is generally a rest-period between successive reloadings. During this rest-period the soil can regenerate. If there is entrapped air in the soil during loading, the air pressure can equalize in the rest-period. During the next reloading the soil can be further compressed than when the rest-period is negligible (see Section 5.1).

If there is a drying-wetting cycle during the rest-period the compressibility of the soil is lower (see Section 5.1). During our measurements we found still additional compaction after 15 re-loadings.

Rebound

A loaded soil sample will rebound when the sample is unloaded. A rebound has two components: elastic recovery and creep. Elastic recovery occurs immediately at unloading. Creep increases with time (see Fig. 5.11).

Elastic recovery depends on soil type, soil density, and moisture content. In soil samples where air was entrapped during loading we found an increase in elastic recovery (see Section 7.1.2).

Creep velocity decreases with time. Creep values can well be higher than elastic recovery.

We found that rebound can decrease bulk density up to 0.1 g/cm^3 .

Loading speed

In uniaxial compression tests using Lexkesveer loam, we found no difference in compactibility between loading speeds of 0.25 mm/s and 3.0 mm/s. Söhne (1953a) found a difference in pore space of about 0.5 % between loading speeds of 20 mm/s and 120 mm/s. These speed effects, measured in uniaxial compression tests, are much lower than those found in the field under rollers and tyres; see Baganz (1963/1964), Abaoba (1969), Sitkel and Fekete (1975), Steinkamp (1975), and Karczewski (1978).

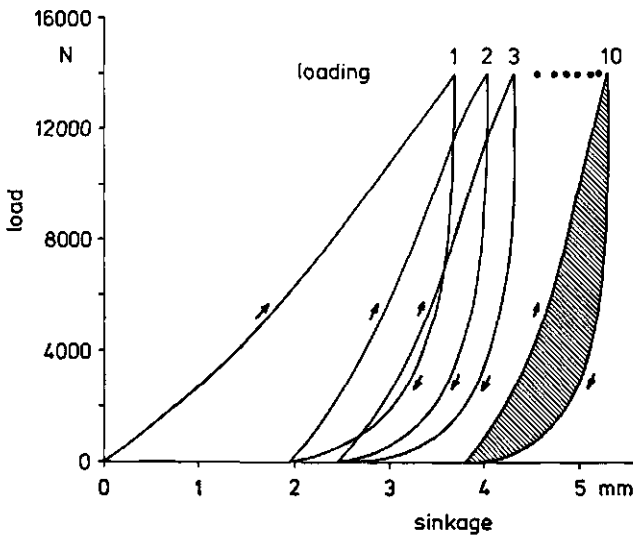


Fig. 5.10. Uniaxial compression with ten repeated loadings.

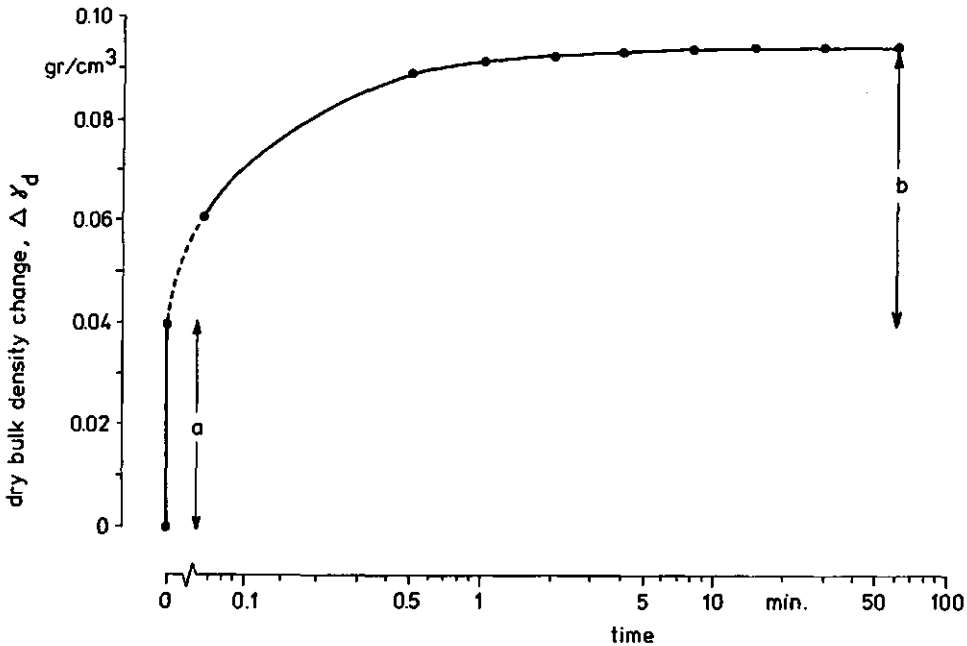


Fig. 5.11. Rebound behaviour of a peaty soil after uniaxial compression to $\sigma_1 = 4.0$ bar.
 a = rebound (elastic recovery)
 b = creep (slow elastic recovery).

Vibrations

Vibrations can cause compaction in two ways: by means of stress changes and acceleration effects (Wu, 1971).

Stress changes due to vibrations, can compact soil in the same way as repeated loadings do. There are hardly measurements known about the compacting effect of stress changes due to vibrations under machinery with pneumatic tyres.

Compaction by acceleration can occur when the upward acceleration of soil particles, caused by vibrations, exceeds the acceleration of gravity; soil particles have the opportunity to fall freely and become very densely packed. This effect will only occur in soils with negligible cohesion. The acceleration effect is used to advantage in highway construction and underwater foundation constructions like the "Oosterschelde-dam" in the Netherlands.

We know that crawler-tractors can highly compact sandy soils. Further research is needed, before we can make statements on vibrating effects of agricultural machinery with pneumatic tyres on compaction.

5.3.2. DEFORMABILITY

The loading of soil by tyres, wheels, and rollers is generally accompanied by soil deformation. The degree of deformation depends on the load, moisture content, soil density, and loading speed.

Soil deformation occurs in a vertical plane A through the tyre center in the direction of travel. The changing position of points at the soil surface in this plane were observed in soil bin investigations. During these tests the vehicle parameters (tyre, load, speed, inflation pressure) were kept constant. The soil conditions were varied in a broad range. Fig. 3.17 shows horizontal displacement of points at the soil surface in plane A versus the accompanying vertical displacement (sinkage). After two runs with a towed tyre we could see that large sinkages were accompanied by large horizontal displacements at the soil surface.

For driven tyres the displacements are backwards because of tyre slip. At normal pull there is 15 - 20 % slip. This means a backward movement of about 0.25 m for the present tractor tyres. These movements decrease with depth.

In another vertical plane B, through the tyre center and its wheel axle, there is also soil deformation. In wet or dense soils deformation will take place at constant volume and soil will bulge beside the tyre. Under drier or looser conditions the deformation will be accompanied by compaction and there will be little or no bulging beside the tyre (Kulpers, 1970).

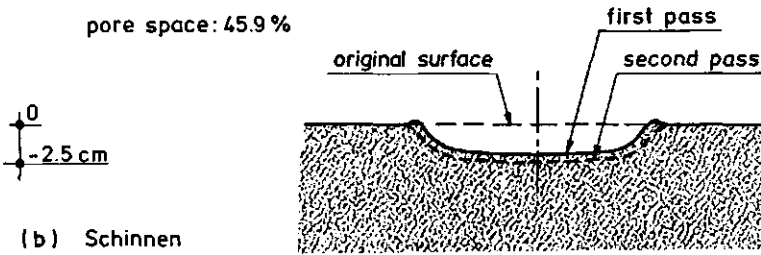
Fig. 5.12 shows two cross sections of our soil bin tests. Fig. 5.12a shows plane B for a dense soil after one and two tyre passes. There is no bulging. Fig. 5.12b shows bulging in a softer soil.

An elementary treatment of deformation has been given by Koolen and Kulpers (1983).

(a) Lexkesveer

moisture content: 17.06 %

pore space: 45.9 %



(b) Schinnen

moisture content: 26.53 %

pore space: 47.1 %

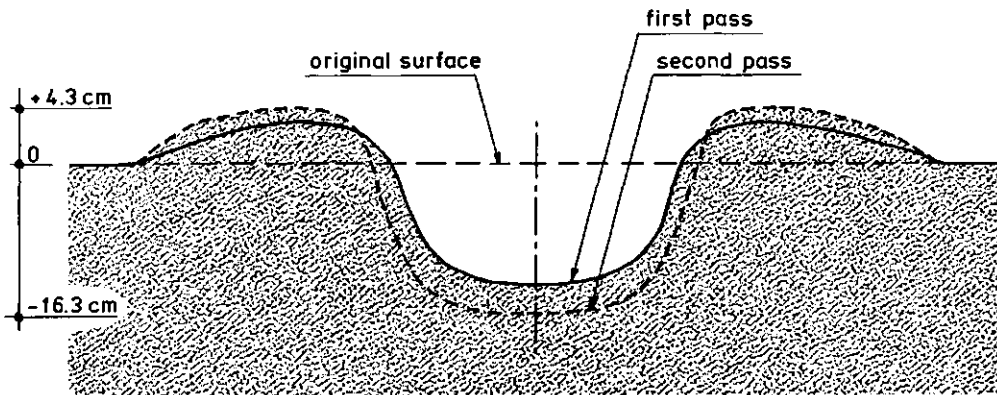


Fig. 5.12. Cross sections of ruts formed by a 7-12 implement tyre with an axle load of 4874 N. The area above the original surface is bulged because of the action of the tyre.

5.3.3. RESISTANCE AGAINST SHEAR

According to the well-known law of Coulomb, shear stress at failure (τ_f) is composed of a cohesion and a friction part:

$$\tau_f = c + \sigma \tan \phi$$

where, τ_f = shear stress at failure

c = cohesion

σ = normal stress on the failure plane

ϕ = angle of internal friction.

For tyre-soil studies not only shear strength τ_f is important, but also the whole shear deformation process.

Shear deformation proceeds as follows: with increasing shear stress elastic and plastic deformation occurs first until maximum

plastic deformation has been achieved and then shear failure planes are formed. At this point shear stress has its maximum value: shear strength τ_f . After this point shear stress decreases and reaches a residual level due to soil-to-soil friction. Fig. 5.13a+c show schematic shear deformation curves for (cohesionless) sand and cohesive natural soil. Fig. 5.13b+d show Coulomb's law for these examples in graphs. The shape of the stress deformation curves depends on soil type, bulk density,

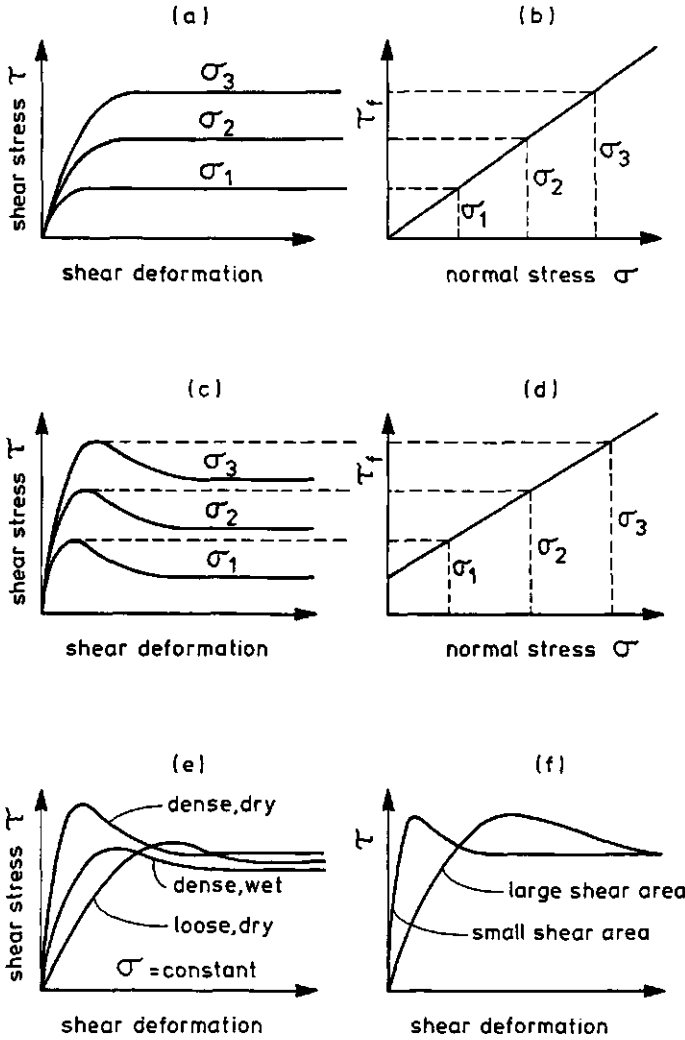


Fig. 5.13. Shear stress - shear deformation relationships for pure sand (a), for cohesive soil (c), for cohesive soil under different conditions (e), and at different shear areas (f). Coulomb's lines for pure sand (b) and for cohesive soil (b). (Söhne and Stubenböck, 1978)

moisture content, and the area of the shear failure plane. Fig. 5.13e shows schematically shear deformation curves for dry, loose and dense, cohesive soil with equal moisture content and for dry and wet cohesive soils of equal density. For dense, cohesive soil with a moderate moisture content shear deformation curves are given at two different areas of shear planes (Fig. 5.13f).

5.4. CHARACTERIZATION PROCESSES

During passing of a wheel the state of stress and strain varies continuously. This makes it very difficult to relate the processes to specific mechanical properties. Research workers therefore often use simpler but comparable processes induced by measuring devices as a method of characterization. A problem with this method of characterization is that there are many different tests in common use. In section 5.4.2 results of comparisons of different methods are shown and discussed. It is clear that if two tests are highly correlated it is enough to use one of them to characterize soil behaviour.

Cone penetration tests

With a cone penetration test resistance to penetration, as a composite soil property, can be measured and described rapidly and in situ.

This test gives no specific soil values such as angle of friction, cohesion, or coefficient of soil-metal friction. Because the results are influenced by the cone type and method used, a standardization of cone type and method is needed for comparing measurements.

A widely accepted cone penetrometer is the one standardized by ASAE (Fig. 5.14). ASAE Standard S313.1 (Hahn et al., 1984) specifies two standard 30 degrees cone sizes (20.27 and 12.83 mm base diameter) with a smooth finish (63 micrometres maximum) and a penetration velocity of 30.5 mm/s.

Cone resistance is usually expressed as the quotient of penetration force and the base area, called cone index (C_I). Cone base size should always be stated.

C_I strongly depends on many factors other than bulk density. The most important of the factors are soil moisture content, type of soil, and pore space. Chancellor (1976) gives examples of relationships between C_I and dry bulk density obtained by several investigators. In these examples the relationships vary from almost linear to strongly curved. Chessners et al. (1972) show that even when the same soil and the same moisture content are used the relationship between C_I and bulk density can be different for soil compacted in the laboratory and soil compacted in the field.

Despite its limitations C_I is frequently used for comparative indications of soil conditions because of the ease and rapidity with which numerous measurements can be made. With the newly developed electronic recording hand-held penetrometer which can be linked to a programmable calculator, C_I can be measured more easily still.

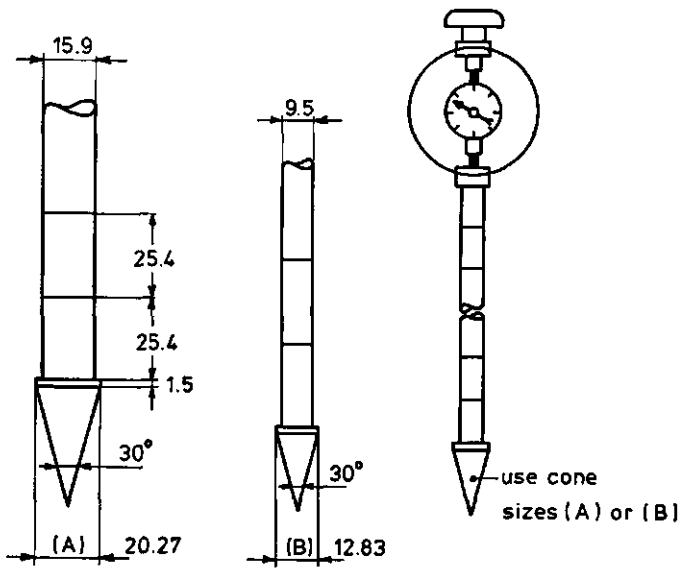


Fig. 5.14. ASAE standard cone penetrometer (Hahn et al., 1984).

Torsional shear tests

These tests may be grouped according to the type of shearing device, namely vane, annulus, cylinder, or plate with grousers (Fig. 5.15).

The vane shear test is a quick test that can be carried out below the soil surface. The height to diameter ratio is normally between 4:1 and 2:1 (Karafiath and Nowatzki, 1978). An annulus with grousers on the bottom (Bekker, 1969) can be pressed into the soil surface, loaded vertically and rotated. A miniature annulus shear test instrument is the "Torvane" made by Soiltest Inc. (NN 1971).

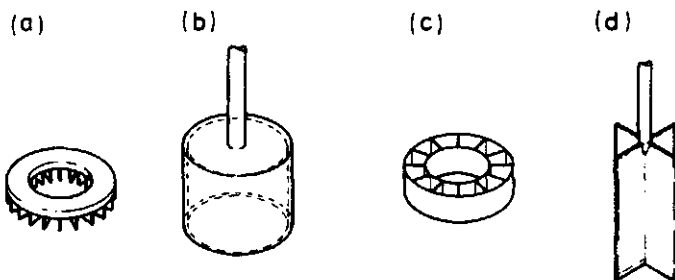


Fig. 5.15.a-d. Torsional shear devices.

A shear annulus of two concentric cylinders with radial grousers has been shown by Söhne (1953b), and Dwyer et al. (1974b). In all torsional shear measuring devices for field use there is uncertainty as to the actual plane of shearing.

Falling weight

To measure the response of soil to vertical impact we used a falling weight. The soil measurement is the depth of a hole formed by a cylindrical iron weight (10 kg, 99,1 mm diameter), which was allowed to fall freely onto the soil surface from a height of 1.0 m. To prevent the weight from tilting as it collided with the soil surface, it was dropped through a perspex pipe having an inside diameter of 99.8 mm, which was placed on the soil surface. The pipe wall was perforated to prevent a build-up of air pressure in front of the falling weight.

5.4.1. COMPARISON OF DIFFERENT CONES

Important aspects of a cone are the base area, the cone surface roughness, and the tip angle.

Two base areas have been standardized: ASAE(A) with a 3.23 sq.cm and ASAE(B) with a 1.39 sq.cm base area. The area of the A-type is a factor 2.5 higher than the one of the B-type. In soil bins we measured penetration resistance with both cones, from 5 to 15 cm depth. Each soil bin was prepared in such a way that a very

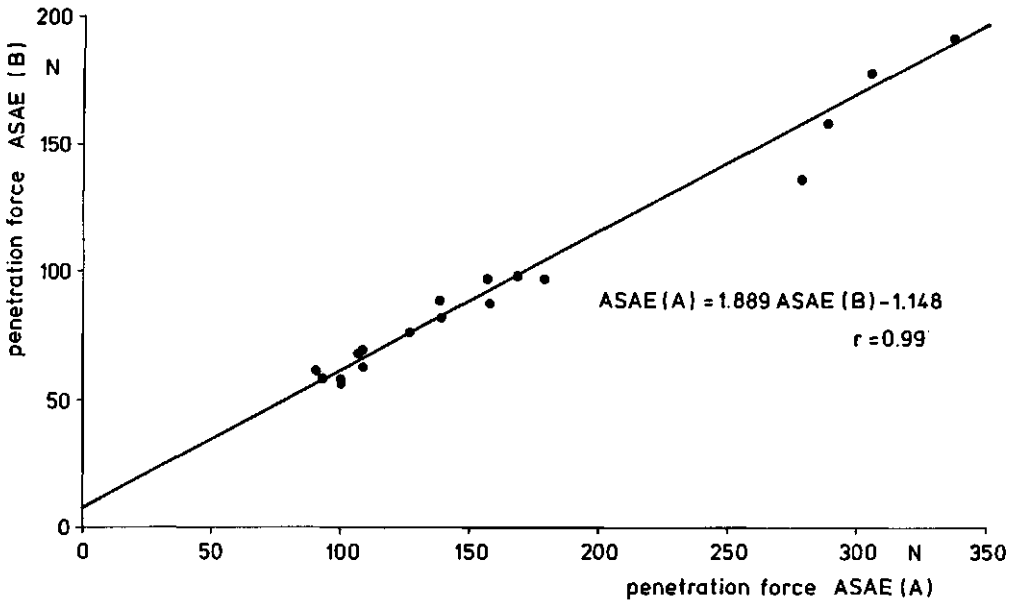


Fig. 5.16. Relationship between penetration force measured with ASAE(A) cone and ASAE(B) cone.

uniform soil condition was achieved over the whole bin. We examined five soil types (see Table 5.1) whose water content and porosity we had varied. The measurements show (Fig. 5.16) that the vertical force of the ASAE(A) cone was a factor 1.9 higher than the one of the ASAE(B)-cone. So C_i decreases with increasing cone base area. Schothorst (1974) found the same effect for cones with a 60° tip angle. To avoid confusion it is desirable to state the size of the cone used.

Gill (1968) shows that teflon coated cones have lower C_i values than steel cones. Therefore, it is advisable to use standard cone-roughness and material: AISI 416 stainless steel, machined to a smooth finish (63 microinches maximum).

The use of a 30° cone tip angle is widely accepted. Occasionally, however, cone measurements with other angles are reported. To give an indication of the influence of the cone tip angle on the results of cone index measurements and to promote the use of a 30° angle in The Netherlands, Tijink and Vaandrager (1983) measured C_i , averaged over the layer between 5 cm and 15 cm depth, with tip angles of 15° , 30° , 60° , 90° , and 180° (all with the same base area), on 87 different agricultural fields. Each cone index value was the mean of five measurements. The measurements showed significant differences in C_i values at different tip angles. The C_i values at a 30° tip angle were significantly the lowest. For each field the mean of all cone index values, irrespective of tip angle, was calculated and called the overall cone index. The results have been presented in a graph giving $C_i/(\text{overall } C_i)$ as a function of the tip angle to which C_i applies (Fig. 5.17). The standard deviation of $C_i/(\text{overall } C_i)$ at a given tip angle was, on the average 15 % of the mean value at that tip angle, and was minimal (9.7%) at 30° . This variability is mainly due to the heterogeneity of each field: standard deviations within each set of five single measurements ranged from 7 % to 20 % of the mean of the five measurements.

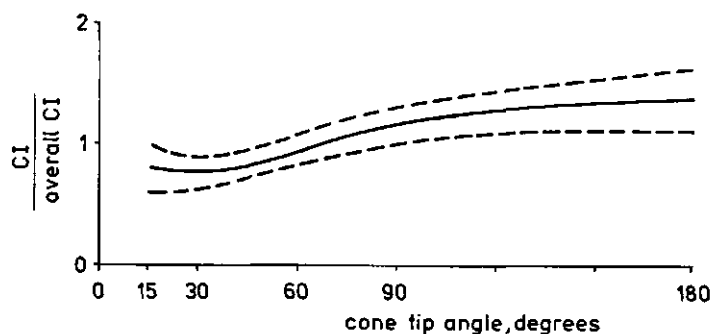


Fig. 5.17. Relationship between cone tip angle and $C_i/\text{overall } C_i$ (Tijink and Vaandrager, 1983).

Koolen and Vaandrager (1984) replaced the $C/(overall\ C/)$ scale by $C/C/$ at 30° . With this curve (Fig. 5.18) it is possible to "translate" cone measurements at unusual tip angles into 30° tip angle measurements.

Despite the possibility of converting cone index measurements at an unusual base area tip angle into standard $C/$ measurements, it is better to use a standard cone.

For interpretation of $C/$ measurements the cone type (the base area and the tip angle) and the units in which $C/$ is expressed should always be mentioned.

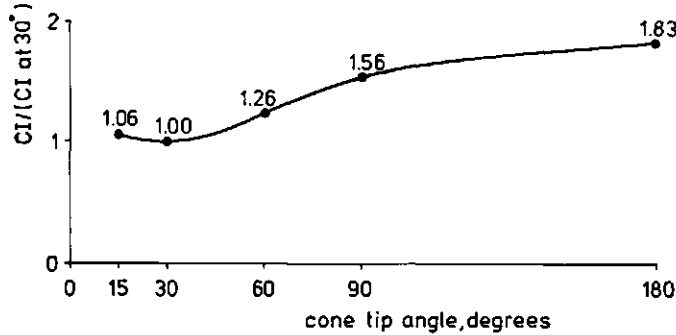


Fig. 5.18. Graph to transform $C/$ at cone angles other than 30° into $C/$ at 30° cone angle (Koolen and Vaandrager, 1984).

5.4.2. COMPARISON OF CONE PENETROMETER, MICRO-PENETROMETER, VANE, AND TORVANE

To investigate the relationships between characterization methods, based on different processes, four different tests were carried out in 15 differently prepared soil bins. In each bin soil bulk density, water content, and pore space were very homogeneous. We used five soil types (see Table 5.1) whose water content and porosity we had varied as indicated in Table 5.2.

Cone penetration resistance was measured with a spring-type hand-operated penetrometer which recorded cone resistance as a function of depth. The cone used was a ASAE standard cone A with a tip angle of 30° and a base area of 3.2 cm^2 . The mean cone index ($C/$) was calculated as the quotient of the mean resistance over the 5 to 15 cm depth layer and the base area of the cone. In each bin ten single cone penetration measurements were made. Each value mentioned in table 5.2. is the mean of ten single $C/$ measurements. Micro-penetrometer tests were carried out with a "Soiltest" pocket penetrometer (N.N. 1971). In each bin tests were carried out ten times. Torsional shear tests were carried out with a "Pilon" direct-reading hand vane tester (Serota and Jangle, 1972) with a 33 mm diameter shear vane and with a "Soil-test Torvane" micro-annulus shear test instrument (N.N. 1971). Both shear tests were carried out ten times in each soil bin.

Table 5.2. shows the data of the measurements.

Table 5.1. Soil description.

Soil	% of minerals			% of soil		pH _{KCl}	Moisture content at pF2 (100 cm suction), %
	<2 μ	2-16 μ	16-50 μ	Humus	CaCO ₃		
Wageningen silty clay loam,	36	27	21	2.3	3.3	7.4	27.3
Lexkesveer loam,	15	12	17	1.6	10.4	7.2	20.2
Schinnen silt loam,	17	14	57	2.1	2.9	7.2	27.2
Ede sand,	3.5	2.5	4.5	3.6	-	4.4	17.4
Almkerk silty clay.	40	24	24	1.2	0.1	6.8	26.9

Table 5.2. Measurements of soil characteristics.

Bin NR.	Soil*	MC %	P vol. %	CI (kPa)	CIM (kPa)	S ₁ (kPa)	S ₂ (kPa)	T (kPa)
1	L	16.96	43.1	782	1.28	3.4	4.8	22.4
2	L	17.16	40.4	933	1.69	4.3	6.1	25.8
3	L	20.18	39.7	497	0.84	2.7	3.7	26.7
4	A	24.79	53.4	539	0.76	3.3	4.6	22.7
5	A	24.47	48.1	761	1.17	5.4	6.9	40.0
6	A	26.66	46.1	532	0.75	3.9	4.8	30.5
7	W	22.85	52.4	700	1.18	4.0	5.7	25.6
8	W	23.12	46.5	870	1.83	6.6	9.5	44.9
9	W	27.58	46.2	436	0.58	3.1	3.8	25.3
10	S	19.76	47.5	779	1.13	3.4	4.6	18.0
11	S	20.05	42.8	1122	2.01	5.0	6.9	26.3
12	S	26.83	42.7	237	0.23	1.1	1.6	12.4
13	E	16.47	46.3	821	1.32	3.0	4.1	12.6
14	E	16.24	44.1	996	1.64	3.6	5.7	13.2
15	E	19.24	45.9	696	0.93	2.2	3.8	12.3

*: soil type (see Table 5.1)

MC = moisture content by weight

P = porosity

CI = cone Index measured with ASAE type A

CIM = cone Index measured with Micro-penetrometer

S₁ = shear strength in the 0 - 4 cm layer

S₂ = shear strength in the 3 - 7 cm layer

T = Torvane shear strength.

By means of linear regression analysis, the correlation coefficients (r) were determined between the soil characteristics: cone Index (CI), micro-penetrometer cone Index (CIM), vane shear strength in the 0 - 4 cm layer (S_1), vane shear strength over the 3 - 7 cm layer (S_2), and Torvane strength (T). See Table 5.3. High correlation between two tests means that it is enough to use one of the two tests to characterize the soil conditions. At a low correlation between two tests the second test gives extra information about the soil condition. We can conclude that for laboratory samples it is enough to measure CI and T , or CIM and T . In the field the best measurements are CI and S_2 . Because of the enormous variations in the 0 to 1 cm top layer CIM , T , and S_1 are less useful.

Table 5.3. Correlation coefficients (r) showing the linear relationship between soil characteristics.

$CI - CIM$	$r = 0.96$	$S_1 - S_2$	$r = 0.98$
$CI - S_1$	$r = 0.63$	$S_1 - T$	$r = 0.83$
$CI - S_2$	$r = 0.71$	$S_2 - T$	$r = 0.75$
$CI - T$	$r = 0.14$		
$CIM - S_1$	$r = 0.73$		
$CIM - S_2$	$r = 0.81$		
$CIM - T$	$r = 0.30$		

5.4.3. RELATIONSHIPS BETWEEN CONE-PENETROMETER, SHEAR VANE, AND FALLING WEIGHT

In our soil bin investigations, aimed at predicting the rolling resistance of a wheel, the depth of the rut, and soil compaction, we used the following soil characterization tests: cone Index (CI), vane shear strength (S_2), depth of hole formed by a falling weight (D), and cone Index measured in the hole (CI_f). See Fig. 5.19. To predict the behaviour of the wheel-soil system at the second wheel pass we also measured CI , D , and S_2 in the first rut.

Between CI , CI_f , D , S_2 we found the linear correlation coefficients shown in Table 5.4.

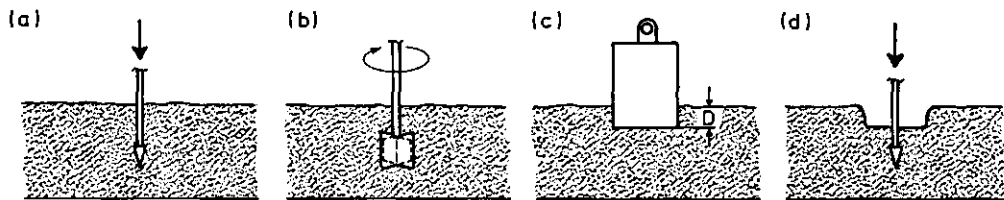


Fig. 5.19. Soil measurements: a) cone resistance; b) shear by vane; c) depth of hole formed by a falling weight; d) cone resistance below the hole formed by a falling weight.

The combination of CI , CI_f , and D proved to be suitable for predicting rolling resistance, soil compaction, and rut depth in the first and second pass of a wheel (see chapter 6.2.2).

Table 5.4. Correlation coefficients (r) showing the relationship between the different soil characteristics used.

$CI - CI_f$	$r = 0.96$
$CI - D$	$r = -0.78$
$CI - S_2$	$r = 0.96$
$CI_f - D$	$r = -0.75$
$CI_f - S_2$	$r = 0.95$
$D - S_2$	$r = -0.73$

CHAPTER 6

RELATIONSHIPS BETWEEN SOIL CHARACTERISTICS AND PROCESS ASPECTS AND THEIR SUITABILITY TO PREDICT PROCESS ASPECTS

It is useful to predict certain aspects of the processes involved in agricultural field traffic. It is particularly useful to predict required pull (rolling resistance), compaction, and rut depth.

To predict a process, we need data on the characteristics of the wheel, the behaviour of the wheel, and the soil. Data on tyre characteristics and the kinematic and dynamic aspects of tyre behaviour are discussed in sections 2 through 4. Soil characteristics concerning load-bearing processes are discussed in section 5.

Two general categories of prediction methods can be distinguished (Koolen, 1977):

- a) methods that are mainly based on observations of relationships between characteristics and process aspects and
- b) methods that are mainly based on knowledge of the mechanism of the process under consideration.

The first category is the most important and may be divided into: comparative methods and methods using empirical formulas or graphs.

A method from the second category is called exact when this method uses a hypothetical mechanism almost equal to the mechanism that is simulated. When this is not the case, the method is called approximate.

6.1. COMPARATIVE METHODS

These methods start with the assumption that a tyre-process aspect y depends on characteristics x_1, \dots, x_n of soil and tyre which can be expressed by the following formula:

$$y = f(x_1, \dots, x_n),$$

Where, f is the way y depends on x_1, \dots, x_n .

Even when f is unknown these methods can be used because a once observed value y at certain values of x_1, \dots, x_n , will be found again when the same values of x_1, \dots, x_n occur again. This means that soils which have equal soil mechanical properties will show equal behaviour in the soil-wheel process.

Rolling resistance as process characteristic depends strongly on the soil mechanical property known as cone index (CI). Table 6.1 shows examples of the same rolling resistance at equal cone index values. These examples are from the investigations reported in 6.2.2.1.

Table 6.1. Equal behaviour at equal soil mechanical properties.

Soil	pore space (%)	moisture content (%)	cone index (MPa)	R ₁ (N)	R ₂ (N)
Schinnen	47.9	17.97	0.95	225	221
Wageningen	42.2	16.98	0.90	223	221

R₁ = Rolling resistance in the first pass

R₂ = Rolling resistance in the second pass

6.2. EMPIRICAL METHODS

These methods use empirical relationships, formulas, or graphs. It is assumed that a process aspect y is dependent on characteristics x_1, \dots, x_n :

$$y = f(x_1, \dots, x_n).$$

Where, f represents the way in which y depends on x_1, \dots, x_n .

The prediction function f is known to such an extent that y can be calculated for any arbitrary values of x_1, \dots, x_n (within certain limits).

Methods that use relationships between soil characteristics and process aspects are not intended to be dimensionally correct. These methods only try to find relationships that can be used for prediction purposes. Section 6.2.2. deals with these methods.

Empirical methods based on dimensional analysis use relationships between soil characteristics and process aspects as well. The main difference, compared to the methods from 6.2.2, is that attempts are made to formulate dimensionally correct prediction functions.

6.2.1. EMPIRICAL GRAPHS

Examples of empirical graphs are presented by Zoz (1972), and Witney and Oskoui (1982).

Zoz (1972) presents a chart that may be used to determine the expected drawbar horse power, travel speed and travel reduction of any two-wheel drive tractor under various soil conditions. This graphical solution is based on average tyre performance for single tyres on four surfaces. Three weight transfer coefficients are used for each soil type. This predictor does not require actual tractor specifications such as tyre sizes, tyre inflation

pressures and front-axle load. Only a reasonable relationship between tractor weight and tyre size is necessary. Therefore, the accuracy of prediction will generally not be very high.

At the Edinburgh School of Agriculture a ploughing performance predictor nomograph has been devised by Witney and Oskoul (1982). This chart, one of the results of a five-year research programme on tractor power selection for ploughing, eliminates laborious calculations to find the most efficient tractor/plough combination for any specific conditions. The predictor uses three plough body types, three compaction levels of the top layer, six soil types, three traction efficiency levels, and several possibilities of depth of cut, width of cut, and drawbar power.

The chart can be used in several ways. It shows the work rate obtainable and the sensitivity of the power requirements to changes in the various characteristics of a particular plough. Specific items such as the best plough type, travel speed and best working depth can be selected by trial and error. In agricultural field practice this chart can be used to examine the existing ploughing procedure. This predictor is most accurate when the soil moisture content is close to field capacity and the compaction level agrees with the one of medium loam soils.

6.2.2. EMPIRICAL METHODS USING RELATIONSHIPS BETWEEN SOIL CHARACTERISTICS AND PROCESS ASPECTS

The main characteristics of a towed tyre-soil system are rolling resistance of the wheel, depth of the rut, and soil compaction caused by the wheel. The numerical value of these characteristics depends not only on tyre parameters, such as size, vertical load exerted by the wheel on the soil, inflation pressure, and forward speed, but also on properties of the soil. A wide range of methods to predict the value of these characteristics from tyre parameters and soil properties are mentioned in literature. Usually, these methods are intended for a range of tyre sizes, vertical loads and inflation pressures. Very often, verification of predictions is limited to one or two typical soil types whose porosity and moisture content were almost always constant. Moreover only a single characteristic to express soil properties (e.g., cone index) or a combination of very few soil characteristics selected a priori are used.

In the investigation presented in this paragraph, tyre parameters were kept constant, and soil types and conditions varied considerably. Different measurements of soil mechanical properties were carried out to predict rolling resistance, rut depth, and compaction under a wide range of soil conditions for the particular tyre parameters tested.

In these tests, the soil was moving instead of the wheel axis. The wheel was suspended in a rigid frame that had been built over a set of fixed rails. Soil bins had been prepared in a separate building and were transported to a carriage which could be pulled along the rails by an electrically-powered cable winch. The linear dimensions of the tyre tested were about half of those of current agricultural trailer tyres. The depth of the soil in the

$$R_1 = 204.CI^{-1.42} \quad \text{with } r=0.98 \text{ (for all bins)} \quad [6.3]$$

$$R_1 = 206.CI^{-1.42} \quad \text{with } r=0.99 \text{ (for all bins except Ede Sands).} \quad [6.4]$$

The two measuring programmes together result in:

$$R_1 = 203.CI^{-1.43} \quad \text{with } r=0.97 \quad [6.5]$$

This analysis shows a high degree of correlation between CI and R_1 in five soils and under a variety of soil conditions. Under all forty-two soil conditions the wheel parameters were kept constant. The slightly different behaviour of Ede Sand is in line with the fact that cone index readings for these bins differed from the readings for the other bins (see Tijink and Koolen, 1985).

Tyre rolling resistance in the second pass (R_2) correlates well with CI , CI_f , and CI_r :

For Almkerk, Lexkesveer, Schinnen, and Wageningen soils:

$$R_2 = 161.CI^{-1.20} \quad \text{with } r=0.92 \quad [6.6]$$

$$R_2 = 181.CI_f^{-1.32} \quad \text{with } r=0.96 \quad [6.7]$$

$$R_2 = 208.CI_r^{-1.23} \quad \text{with } r=0.97 \quad [6.8]$$

For all examined soils:

$$R_2 = 157.CI^{-1.21} \quad \text{with } r=0.92 \quad [6.9]$$

$$R_2 = 175.CI_f^{-1.34} \quad \text{with } r=0.95 \quad [6.10]$$

$$R_2 = 199.CI_r^{-1.23} \quad \text{with } r=0.94 \quad [6.11]$$

Where, R_2 = measured rolling resistance in the second pass (N)
 CI = measured cone index prior to the first pass (MPa)
 CI_f = cone index measured in the hole formed by a falling weight (MPa); see chapter 5.4.
 CI_r = cone index measured in the rut prior to the second pass (MPa).

For all soils the highest correlation was found between R_2 and CI_f (Fig. 6.3). In attempts to find linear relationships between the wheel system and soil characteristics, the following derived values were tried:

$$1/CI^2$$

$$1/CI_f^2$$

$$CI_f \cdot D^2.$$

Moreover, multiple regression was applied.

In the first pass the best linear relationships for rolling resistance were found with $1/CI^2$ (Fig. 6.4):

$$R_1 = 109 + 96.10^{12} (1/CI^2) \quad \text{with } r=0.98 \quad [6.12]$$

In the second pass $1/CI_f^2$ correlated slightly better with R_2 than $1/CI^2$:

$$R_2 = 98 + 82.10^{12} (1/CI_f^2) \quad \text{with } r=0.96 \quad [6.13]$$

$$R_2 = 89 + 65.10^{12} (1/CI^2) \quad \text{with } r=0.93 \quad [6.14]$$

Fig. 6.5 shows the relationship between $1/CI_f^2$ and R_2 .

We can see from this investigation that in a wide range of soils and soil conditions, there is a high correlation between cone index and tyre rolling resistance. We may conclude that rolling resistance can be predicted accurately in uniform soils.

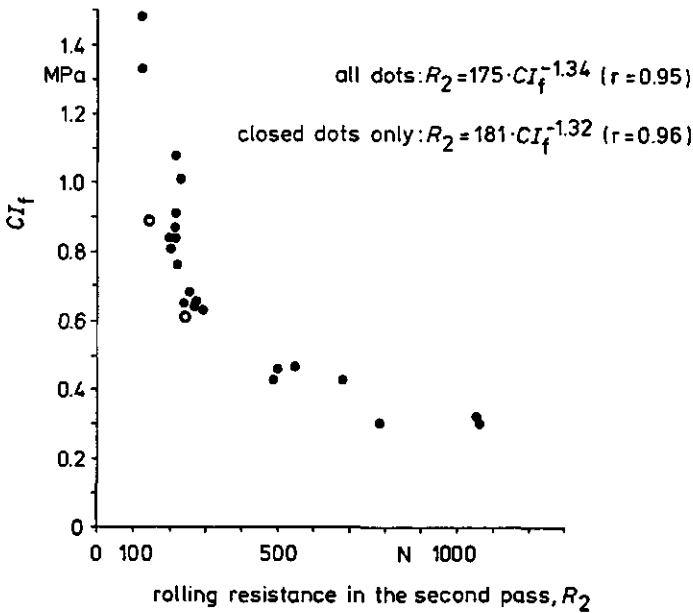


Fig. 6.3. Rolling resistance in the second pass related to CI_f .

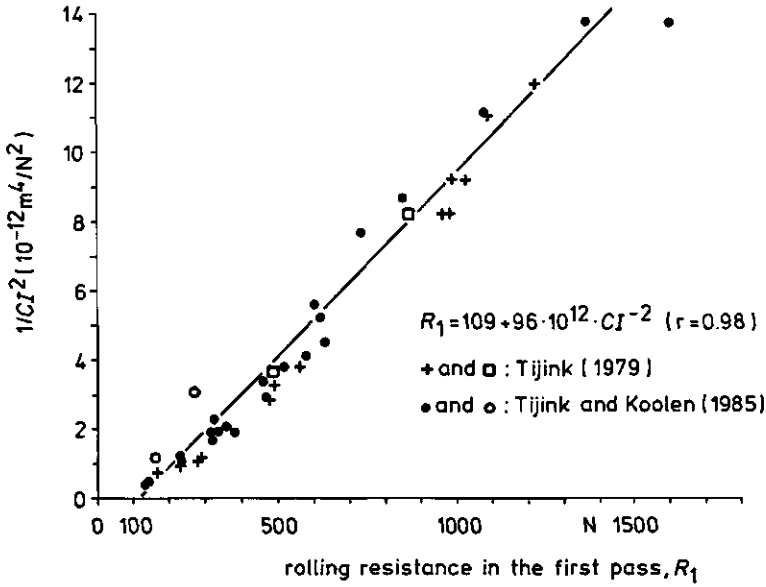


Fig. 6.4. Relationship between measured values of rolling resistance in first passes and $1/CI^2$, where CI is the measured cone index.

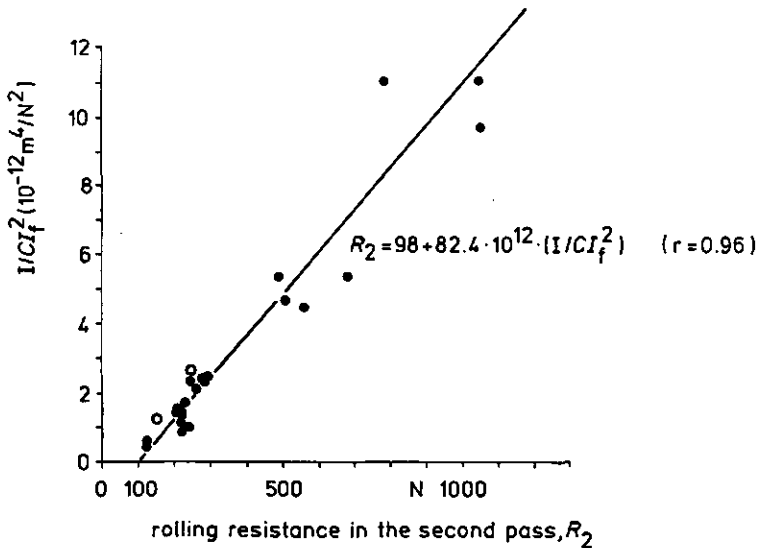


Fig. 6.5. Rolling resistance in the second pass related to $1/CI_f^2$.

6.2.2.2. RELATIONSHIPS BETWEEN SOIL CHARACTERISTICS AND SOIL COMPACTION DUE TO WHEEL ACTION

In the investigations discussed above, soil compaction due to wheel action was also measured. Dimensions of the rut left by the tyre and changes in surface height near the rut were measured with a profile gauge consisting of a row of 51 vertical needles each set 10 mm apart. The row of needles could be placed above the soil perpendicularly to the direction of wheel travel, so that the shape of the surface under the row could be measured by lowering the needles until they touched the soil and by measuring the sinkage of all needles. The measurements were taken at a fixed place in the bin before the first and after each tyre pass, and were presented graphically. We determined the difference between the initial surface area of a vertical cross section of the bin and the surface area of the cross section after each tyre pass from these graphs. The difference is equal to the area lost in compaction due to wheel action (see Fig. 6.6).

Data on soil compaction and soil properties were analysed. High correlations were found between soil compaction and the soil characteristics $C_l.D^2$ and $C_{lf}.D^2$:

$$\Delta A_1 = -6.9 + 0.16C_l.D^2 \quad r=0.94 \quad [6.15]$$

$$\Delta A_1 = -5.3 + 0.13C_{lf}.D^2 \quad r=0.97 \quad [6.16]$$

$$\Delta A_{1+2} = -8.2 + 0.21C_l.D^2 \quad r=0.95 \quad [6.17]$$

$$\Delta A_{1+2} = -4.8 + 0.16C_{lf}.D^2 \quad r=0.95 \quad [6.18]$$

- where,
- ΔA_1 = soil compaction in the first pass expressed as the cross-sectional area lost (cm^2).
 - ΔA_{1+2} = soil compaction in two passes expressed as cross-sectional area lost (cm^2)
 - C_l = measured cone index (MPa)
 - C_{lf} = cone index measured under holes formed by a falling weight (MPa)
 - D = depth of the hole formed by the falling weight prior to the first pass (mm).

With equations 6.15 and 6.17 soil compaction was calculated. Figures 6.7 and 6.8 show the relationships between measured and

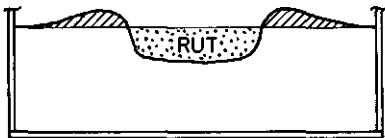


Fig. 6.6. Decrease of soil area in a vertical cross section of the rut, due to compaction of soil by the wheel. This decrease equals the dotted area minus the sum of the hatched areas.

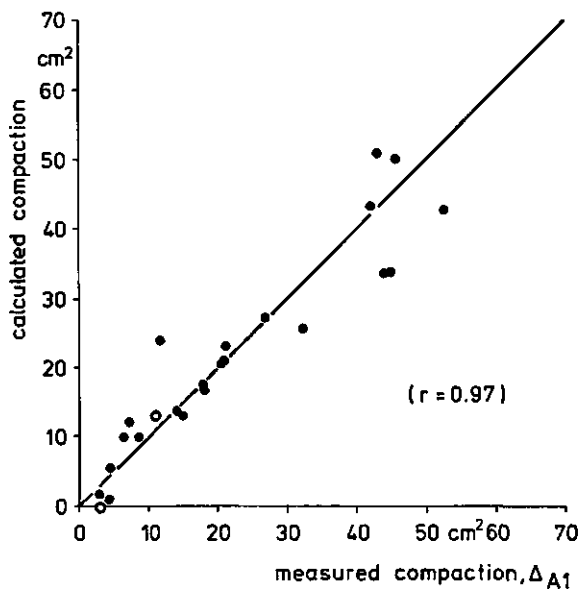


Fig. 6.7. Relationship between measured and predicted compaction in the first pass. Compaction is expressed in cross-sectional area lost due to tyre action.

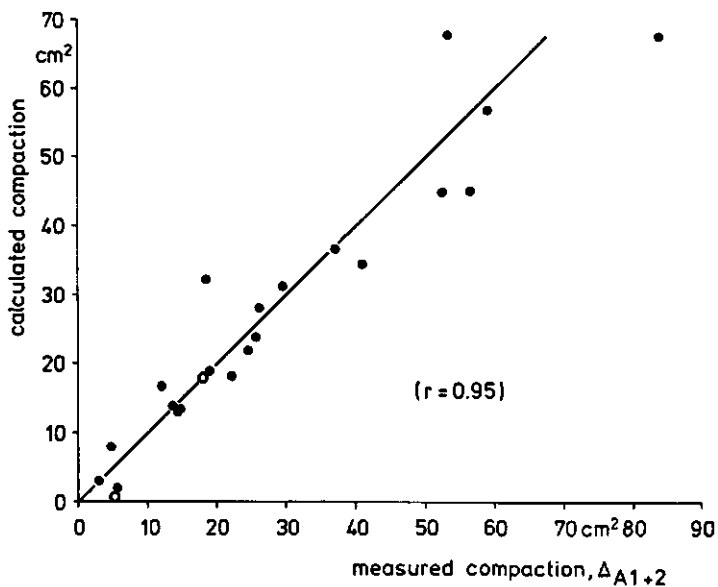


Fig. 6.8. Relationship between measured and predicted compaction due to the first and the second wheel passes.

calculated soil compaction. From this it seems that soil compaction due to wheel action can be predicted satisfactorily from the soil measurements C_1 , C_{1f} , and D . Sometimes it is thought that rut depth is a measure for soil compaction (Boels, 1978). An analysis of data on rut depths and soil compactions showed a poor relationship between these characteristics (see Fig. 6.9). This poor correlation is due to the bulging of soil beside the rut. For the wheel passes with negligible bulging, high correlations ($r=0.99$) between rut depth and soil compaction were found.

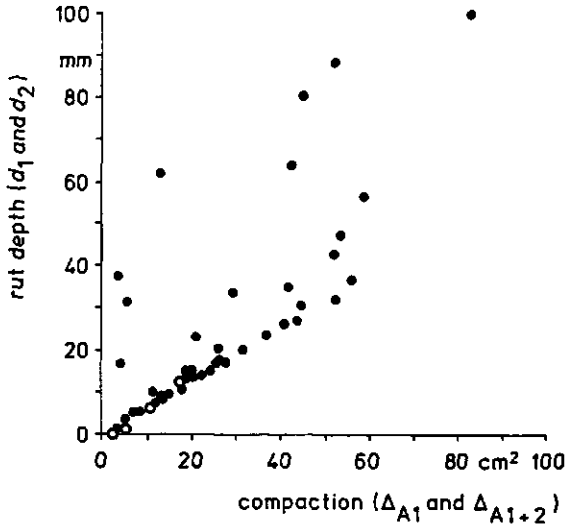


Fig. 6.9. Relationship between soil compaction in cross-sectional area lost due to wheel action in first pass, ΔA_1 , and in first and second passes, ΔA_{1+2} , and rut depth after first pass, d_1 , and after second pass, d_2 .

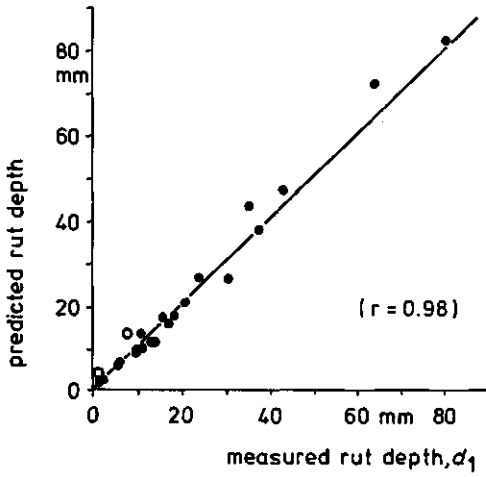


Fig. 6.10. Predicted and measured values of rut depth after the first pass.

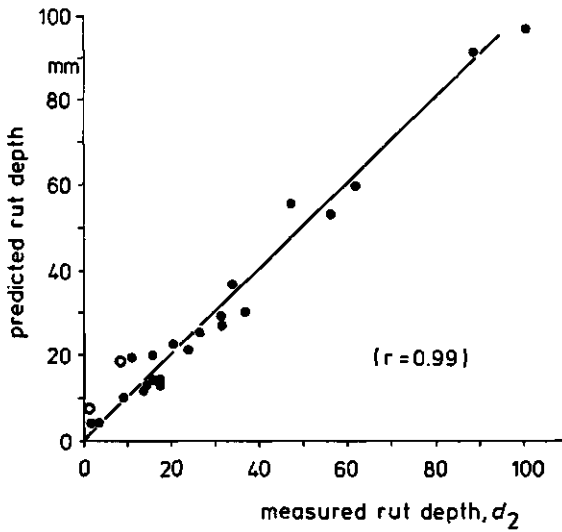


Fig. 6.11. Predicted and measured values of rut depth after the second wheel pass.

6.2.2.3. RELATIONSHIPS BETWEEN SOIL CHARACTERISTICS AND RUT DEPTH

Accurate predictions of rut depth are not known from literature. In our investigations rut depth was measured in the centre of the rut as the difference between the initial soil height and final soil height.

The use of relatively independent soil characteristics C_I and D resulted in good predictions of rut depth:

$$d_1 = -0.85 + 2.85C_I^{-2} + 0.028D^2 \quad r=0.98 \quad [6.19]$$

$$d_2 = -0.01 + 5.01C_I^{-2} + 0.018D^2 \quad r=0.99 \quad [6.20]$$

where, d_1 = rut depth after the first pass (mm)
 d_2 = rut depth after the second pass (mm)
 C_I = cone Index prior to first pass (MPa)
 D = depth of hole formed by the falling weight prior to the first pass (mm).

Fig. 6.10 and 6.11 show the relationships between measured and calculated rut depths after the first and the second pass of the wheel.

6.2.3. EMPIRICAL FORMULAS BASED ON DIMENSIONAL ANALYSES

Empirical formulas for tyre performance predictions often are the result of dimensional analyses. This method evolves from consideration of the variables of the problem and the dimensions of these variables. To apply dimensional analysis it is necessary to determine the variables and their basic dimensions. Application of the Buckingham Π -theorem leads to a set of dimensionless parameters. The number of parameters generally is decreased by reducing the domain of the problem. In tests the relationships between characteristics of the tyre and the soil reactions can be evaluated in terms of dimensionless characteristics. The relationships obtained can be used to predict tyre and soil behaviour.

6.2.3.1. PREDICTING OFF THE ROAD TYRE ROLLING RESISTANCE

Empirical predicting formulas for tyre rolling resistance have been reviewed and examined with data presented in this dissertation and with data published by Perdok (1978) and Lumkes and Perdok (1981).

REVIEW:

Freitag (1965) used the method of dimensional analysis to model the tyre-soil system. Tyre-soil system variables identified by Freitag are presented in Table 6.2. Three basic dimensions are indicated and according to the Buckingham PI-theorem, the number of variables can be reduced by three. The PI-terms which were derived are presented in Table 6.3.

The functional relationship between the PI-terms is:

$$P/W, R/W, T/d.W, z/d = f(\mu, \phi, S, b/d, h/d, \delta/h, c.d^2/W, \gamma d^3/W, g.d/V^2)$$

Terms that include friction angle, cohesion and specific weight can be omitted when the cone index (CI) and the gradient of cone index (G) are used to characterize cohesive soils (clay) and frictional soil (sand) respectively. The influence of driving speed and (h/d) has been considered insignificant. If, in addition, a constant degree of slip is supposed to occur, the functional relation is reduced to:

$$P/W, R/W, T/d.W, z/d = f(CI.d^2/W, b/d, \delta/h) \quad \text{for clay and}$$

$$P/W, R/W, T/d.W, z/d = f'(G.d^2/W, b/d, \delta/h) \quad \text{for sand.}$$

Table 6.2. Tyre-soil system variables used by Freitag.

Variable	Symbol	Dimensions
INDEPENDENT VARIABLES		
Soil		
Internal friction angle	ϕ	-
Cohesion	c	FL-2
Specific weight	γ	FL-3
Penetration resistance	CI	FL-2
Tyre		
Diameter	d	L
Section width	b	L
Section height	h	L
Deflection	δ	L
System		
Load	W	F
Translational speed	V	LT-1
Slip	S	-
Tyre-soil friction	μ	-
Acceleration due to gravity	g	LT-2
DEPENDENT VARIABLES		
Pull	P	F
Rolling resistance	R	F
Torque	T	FL
Sinkage	z	L

Table 6.3. PI terms used by Freitag.

$\pi_1 = P/W$	$\pi_2 = R/W$	$\pi_3 = T/d.W$	$\pi_4 = z/d$	$\pi_5 = \mu$
$\pi_6 = \phi$	$\pi_7 = S$	$\pi_8 = b/d$	$\pi_9 = h/d$	$\pi_{10} = \delta/h$
$\pi_{11} = c.d^2/W$	$\pi_{12} = \gamma d^3/W$	$\pi_{13} = Cl.d^2/W$	$\pi_{14} = g.d/V^2$	

Freitag developed two dimensionless prediction terms (mobility numbers) for treadless, two-ply tyres with circular-shaped cross sections:

$$\text{Clay mobility number } N_C = (Cl.b.d/W).(\delta/h)^{0.5}$$

$$\text{Sand mobility number } N_S = (G(b.d)^{3/2}/W).(\delta/h)$$

Relationships between mobility numbers and tyre performance were presented.

Turnage (1972) extended the clay mobility number (N_C), proposed by Freitag, with an additional factor ($1/(1+b/2d)$) to take the cross-sectional shape (circular or rectangular) into account:

$$M = (Cl.b.d/W).(\delta/h)^{0.5}.(1/(1+b/2d))$$

The shape of the relationships between prediction terms and rolling resistance coefficient are presented in Fig. 6.12.a+b.

Wismer and Luth (1973) used an approach similar to the one used by Freitag and Turnage and developed a dimensionless wheel numeric (C_N) for a tyre moving in cohesive-frictional soil:

$$C_N = Cl.b.d/W$$

This wheel numeric was related to rolling resistance by :

$$R/W = (1.2/C_N) + 0.04 \quad [6.21]$$

The shape of the relationship is given in Fig. 6.12.c. This formula has been adopted by the American Society of Agricultural Engineers: ASAE Data 230.4 (Hahn et al., 1984), and can be applied to cohesive frictional soils of moderate compactibility and to tyres operating at inflation pressures that produce radial tyre deflections of approximately 20 percent of the undeflected tyre section height. Typical tyre dimensions are a section width to diameter ratio (b/d) of 0.3 and a rolling radius to diameter ratio of 0.475.

Values of C_N for typical surfaces are:

- 50 - hard soils
- 30 - firm soils
- 20 - tilled soils
- 15 - soft, sandy soils

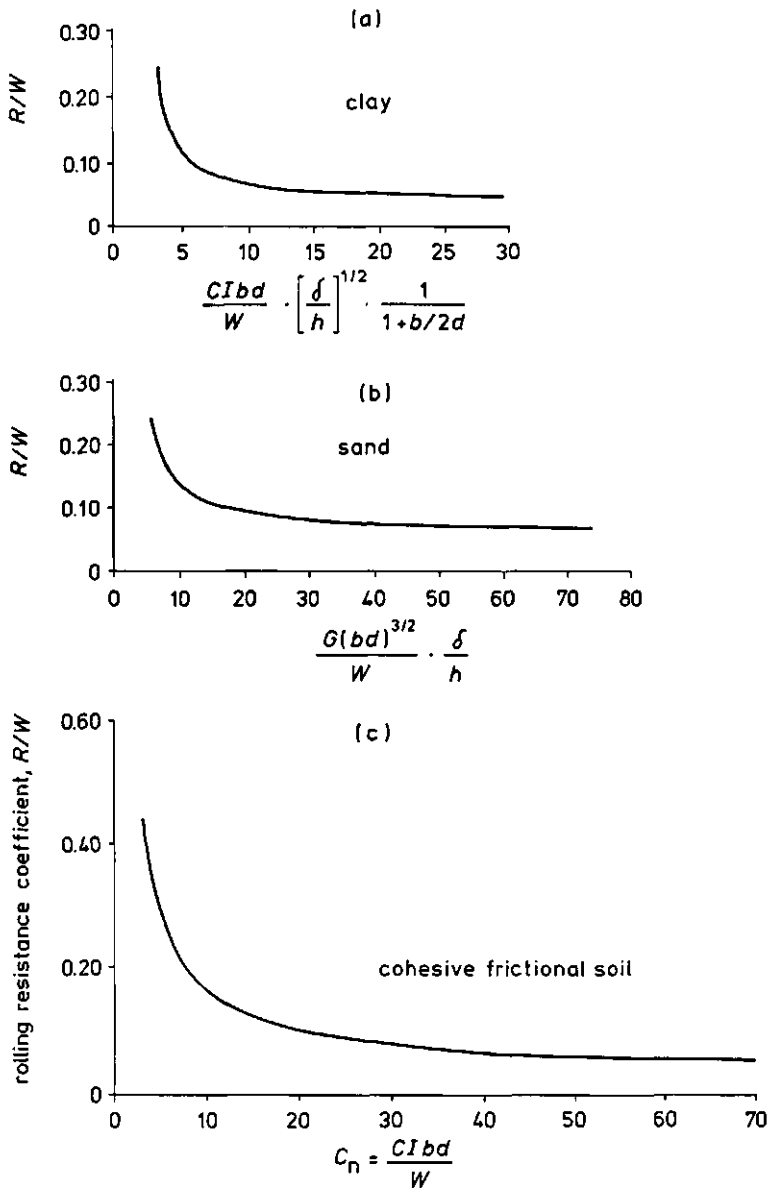


Fig. 6.12. Rolling resistance coefficient of a towed tyre related to clay mobility number (a), sand mobility number (b), and wheel numeric (c).

Dwyer et al. (1975) and Gee-Clough et al. (1978) investigated the field performance of tractor rear tyres ranging in size from 12.4-36 to 18.4-38. The following prediction function for rolling resistance was proposed:

$$R/W = (0.287/M) + 0.049 \quad [6.22]$$

To include the effect of tyre construction, Mc Allister (1983) proposed the following relationships:

$$\text{for cross ply tyres:} \quad R/W = (0.323/M) + 0.054 \quad [6.23]$$

$$\text{and for radial tyres} \quad R/W = (0.321/M) + 0.037 \quad [6.24]$$

ANALYSIS:

In the investigations, described in section 6.2.2, tyre and system parameters were kept constant. So, the parameters b , d , W and δ/h are constants. Mobility numbers change into:

$$N_C = a_1 \cdot C/I$$

$$M = a_2 \cdot C/I$$

where, a_1 and a_2 are constants.

In Fig. 6.1 the relationship between cone index (C/I) and rolling resistance is presented. We may conclude that mobility numbers, used at constant tyre and system parameters, accurately predict tyre rolling resistance.

When tyre deflection measured in a test bin (δ_a) was used almost equal correlations between mobility number M and rolling resistance were found. The use of the actual tyre deflection (δ_a) did not improve the accuracy of prediction.

The drawback of mobility numbers (N_C and M) and wheel numeric (C_n) is that they have no linear relationship with rolling resistance (see Fig. 6.12). Neither do they include the effect of tyre construction (cross ply or radial) and tread pattern. To get linear relationships it can be useful to use C/I^{-2} instead of C/I (see Fig. 6.4).

Equations 6.21, 6.22, and 6.23 were examined using data from our soil bin experiments (see Tijink and Koolen (1985) for soil conditions, soil characteristics and results of wheel-soil system measurements). Using equation 6.21 the accuracy of prediction was poor (Fig. 6.13) although tyre dimensions agreed with the specifications mentioned by Wismer and Luth. In Fig. 6.14 calculated rolling resistance, using equation 6.22, is plotted versus measured rolling resistance. The same poor result was obtained. Mc Allister's prediction formula for cross ply tyres (equation 6.23) also resulted in poor predictions of rolling resistance (see Fig. 6.15).

The differences between these prediction equations and the poor accuracy they achieved in predicting rolling resistance in test bins demonstrate that every equation has a limited field of application and that those equations cannot be extrapolated with confidence. The different equations were developed from investigations with different tyres. Freitag used 4 different tyres with diameters ranging from 0.36 m to 0.72 m. These were all treadless, thin-walled, cross ply tyres with two-ply rating. Equation 6.22 was based on experiments with tractor rear tyres ranging from 1.45 m to 1.75 m diameter. This expression was valid for stubble, ploughed and cultivated fields only ($r=0.73$). Dry grass fields and fields with a loose, wet, top layer showed significantly different results. In Mc Allister's experiments tyre diameter ranged from 0.8 m to 0.95 m. Measured rolling resistance values in Fig. 6.13 to 6.15 have been determined using an implement tyre with a diameter of 0.67 m.

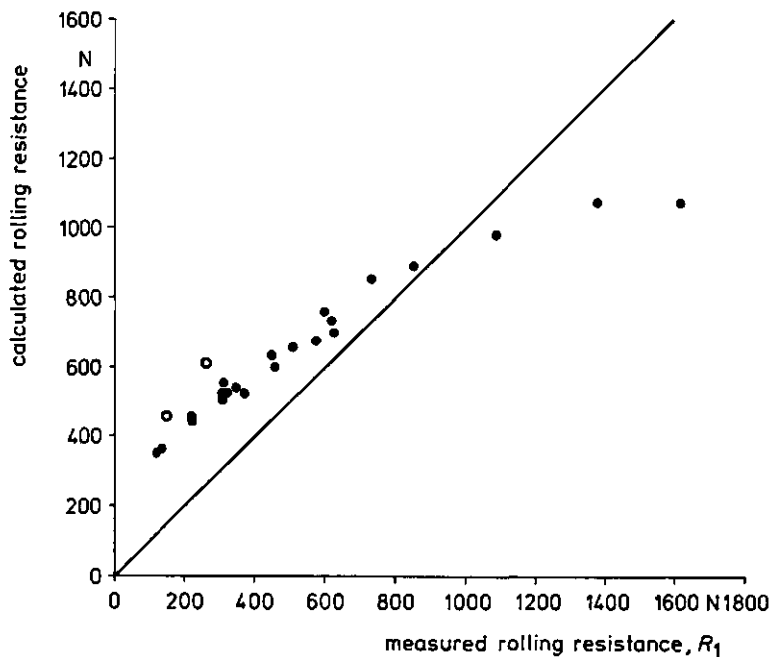


Fig. 6.13. Relation between calculated rolling resistance, calculated using equ. 6.21 proposed by Wismer and Luth, and measured rolling resistance (R_1) of a 7.00-12 implement tyre.

Fig. 6.14. Relation between calculated rolling resistance, calculated using equ. 6.22 proposed by Gee-Clough, and measured rolling resistance (R_1) of a 7.00-12 Implement tyre.

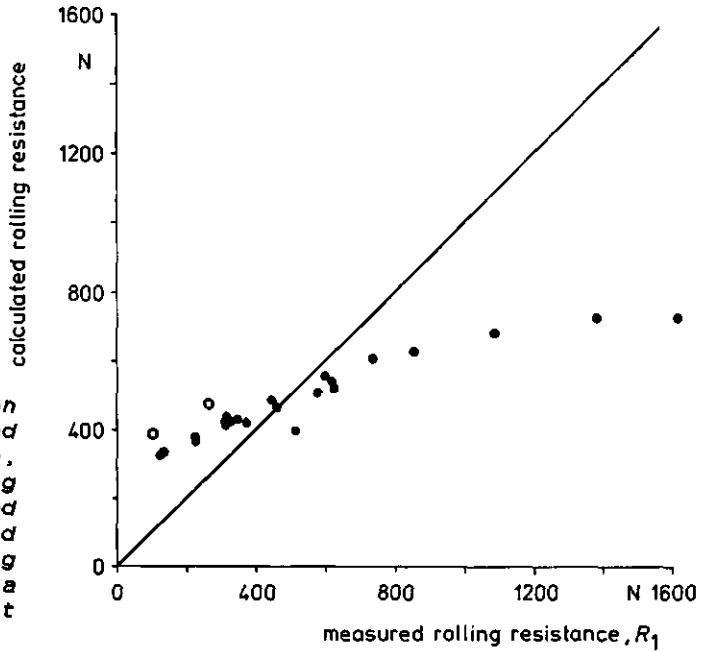
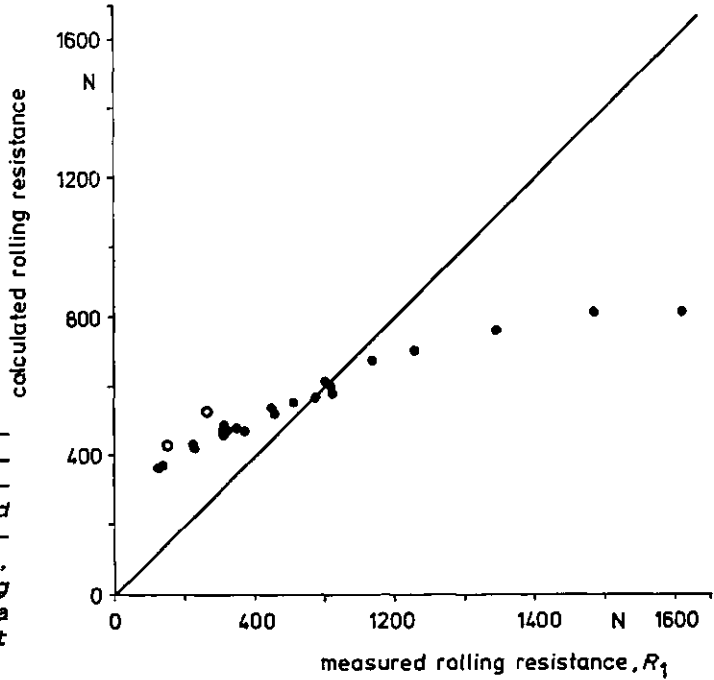


Fig. 6.15. Relation between calculated rolling resistance, calculated using equ. 6.23 proposed by McAllister, and measured rolling resistance (R_1) of a 7.00-12 Implement tyre.



Predicting terms can be improved by using empirical methods in strongly reduced domains. Some examples are given below, using experimental data presented in section 6.2.2 and data published by Perdok (1978).

The domain of the problem can be reduced strongly by the use of the same tyre-system settings in the same field at two different times. On both days rolling resistance was measured at four inflation pressure levels. Only soil conditions differed on these days. Linear relationships between rolling resistance measured on two days are presented in Table 6.4.

Table 6.4. Coefficient of linear correlation between rolling resistance on 2 different days in the same field and with the same tyre-system settings.

tyre		$R_{\text{day 1}}$	-	$R_{\text{day 2}}$
13-16	Implement			$r=0.99$
12-38	Treadless tractor rear			$r=0.95$
16-15.5	Implement			$r=0.99$
16-20	Implement			$r=1.00$
20-22.5	Implement			$r=0.94$

Another example of a very reduced domain is a test carried out under one field condition with only variable levels of tyre inflation pressure. This resulted in high linear correlations between R/W and p_i (Table 6.5).

Table 6.5. Linear correlations between rolling resistance coefficient (R/W) and tyre inflation pressure (p_i).

tyre		day 1	day 2	wheel load
				wheel load allowed at p_i used
13-16	Implement	0.99	0.98	1.09 - 1.57
12-38	Treadless Tractor Rear	0.99	0.89	1.12 - 1.78
16-15.5	Implement	0.98	0.99	0.99 - 1.78
16-20	Implement	0.99	0.98	0.79 - 1.28
20-22.5	Implement	0.99	0.91	0.64 - 1.68

High linear correlations between rolling resistance R and W^2 were also found in our analyses. The variables inflation pressure p_i and wheel load were combined to $p_i.W^2$. Fig. 6.16 shows the relationship between $p_i.W^2$ and R for a 13-16 implement tyre in a particular field. A high degree of correlation ($r=0.99$) between $p_i.W^2$ and R was found. For the other tyres similar correlations were found.

We may conclude that the term $p_i.W^2$ can be applied to make accurate predictions of rolling resistance in a restricted domain. If rolling resistance R is a function of $p_i.W^2$, then the coeffi-

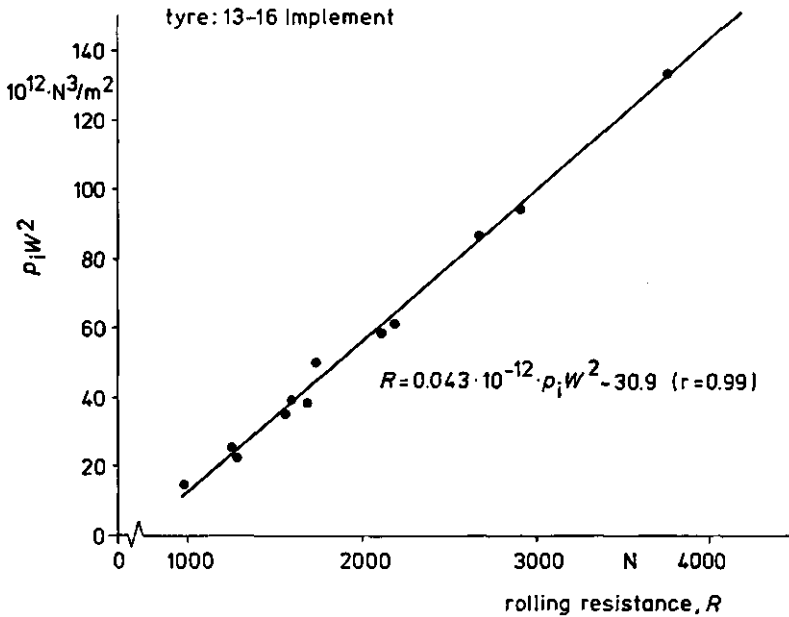


Fig. 6.16. Relation between $p_1 W^2$ and rolling resistance measured in a particular field.

cient of rolling resistance is a function of $p_1 W$.

To achieve dimensionless prediction numbers, we developed terms like:

$$(p_1 \cdot W) / (C l^2 \cdot b \cdot d), \quad (p_1 \cdot W) / (C l^2 \cdot h \cdot d), \quad (p_1 \cdot W) / (C l^2 \cdot h^2),$$

$$(p_1 \cdot W \cdot h) / (C l^2 \cdot b^3), \quad (p_1 \cdot W \cdot b) / (C l^2 \cdot h^2 \cdot d), \quad (p_1 \cdot W \cdot b) / (C l^2 \cdot h \cdot d^2),$$

$$(p_1 \cdot W \cdot b) / (C l^2 \cdot h^3), \quad (p_1 \cdot W \cdot b) / (C l^2 \cdot b^2 \cdot d), \quad \text{etc.}$$

In order to decrease the number of variables, the domain was reduced by choosing only one soil condition. For the tyres tested the dimensionless term $(p_1 \cdot W) / (C l^2 \cdot b \cdot d)$ achieved the highest accuracy in predicting the rolling resistance coefficient (see Fig. 6.17).

Despite the high accuracy achieved in Fig. 6.17 it must be clear that more tyre variables are necessary when an universal prediction term is wanted. It is not enough to characterize a tyre with b, d, h, W and δ/h or with b, d, h, W and p_1 . Additional terms should be used (for tyre construction, tyre flexibility, and tread pattern) or the application of the prediction term is limited to a particular domain.

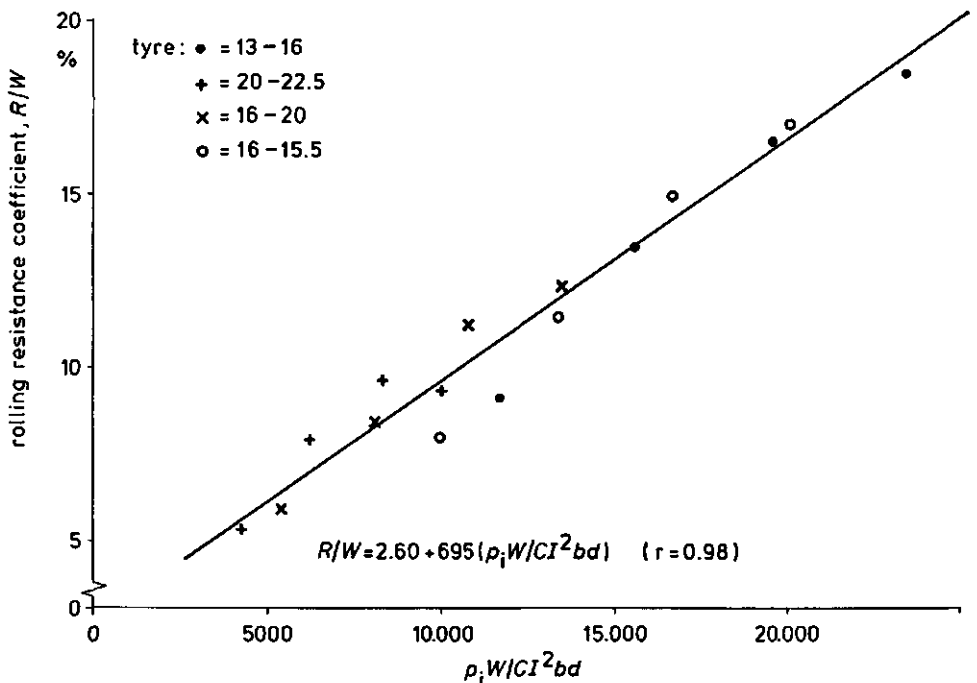


Fig. 6.17. Relation between rolling resistance coefficient and the dimensionless term $(p_1W)/CI^2bd$ for implement tyres in a particular field.

6.2.3.2. PREDICTING TYRE ROLLING RESISTANCE ON A HARD SURFACE

Steiner and Söhne (1979) measured tyre rolling resistance of towed tractor rear tyres on a concrete surface. The test tyres were sized from 11-28 to 16.9-38 and 18.4-26. Both cross ply and radial tyres were examined. It was found that the influence of driving speed can be neglected in the range from 0.8 to 3 m/s. All rolling resistance measurements were made at a driving speed of 0.8 m/s. This proved that tyre rolling resistance on a concrete surface is a function of tyre inflation pressure (p_1), wheel load (W), tyre dimensions, tyre construction, and ply rating.

For equal ply rating and construction: $R/W = f(p_1, W, b, d, h)$

Several dimensionless terms were determined. The dimensionless term bW/h^3p_1 correlated highest with measured values of rolling resistance coefficients. For six-ply agricultural rear tyres the following equations were found:

Cross ply tyres: $R/W = 1.27 + 0.65(bW/h^3p_1)$ (%) with $r=0.85$
 [6.25]
 Radial tyres: $R/W = 1.33 + 0.40(bW/h^3p_1)$ (%) with $r=0.57$
 [6.26]

Perdok (1978) and Lumkes and Perdok (1981) published data on rolling resistance of some cross ply implement tyres. An analysis of these data is presented here.

As expected from section 6.2.3.1, the equations 6.25 and 6.26 could not be extrapolated satisfactorily to implement tyres. However, a good prediction of rolling resistance of the tested implement tyre was possible, using the dimensionless term bW/h^3p_1 (see Fig. 6.18). The prediction function found can be expressed as follows:

$$R/W = 0.46 + 0.83(bW/h^3p_1) \quad (\%) \quad \text{with } r=0.97 \quad [6.27]$$

- where, R = rolling resistance (N)
 W = vertical wheelload (N)
 b = tyre section width (m)
 h = tyre section height (m)
 p_1 = tyre inflation pressure (N/m^2).

We may conclude that for tyres with equal construction and ply rating the dimensionless term bW/h^3p_1 is useful for predicting tyre rolling resistance on a hard surface.

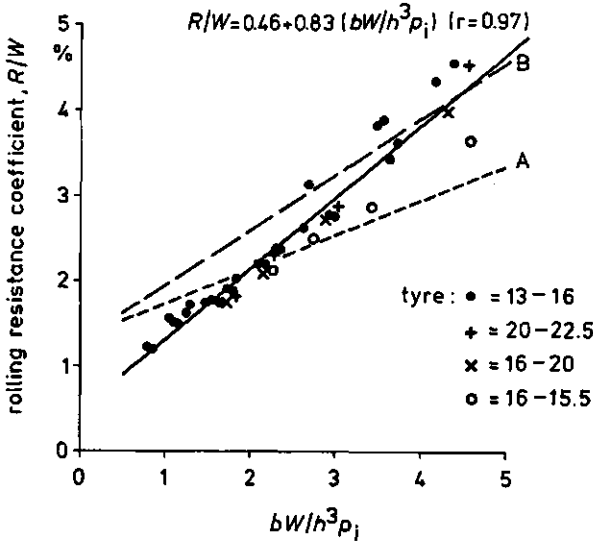


Fig. 6.18. Relation between rolling resistance coefficients and predicting term bW/h^3p_1 using four implement tyres on a concrete surface. Lines A and B are relationships found by Steiner and Söhne (1979) for six-ply tractor rear tyres.

6.3. APPROXIMATE METHODS

Approximate methods to predict off-the-road wheel performance are generally based on pressure-sinkage relationships. Bernstein (1913) stated that rolling resistance of a wheel is due to the vertical work done in rut forming. Predictions have been based on the pressure-sinkage relationships of a rectangular plate:

$$p = k \cdot z^n$$

where, p = pressure on the plate
 k = modulus of soil deformation
 z = sinkage
 n = exponent of deformation.

Bernstein found $n = 0.5$ for agricultural soils. The parameter k proved to be dependent on plate dimensions.

Bekker (1956, 1960, 1969) used the Bernstein theory to predict rolling resistance. To get independent parameters Bekker proposed that the modulus of soil deformation has two components; k_c is the cohesive component and k_ϕ the frictional component:

$$k = k_c/b + k_\phi$$

Bekker's pressure-sinkage relationship of a rectangular plate states that:

$$p = (k_c/b + k_\phi)z^n$$

To obtain values for k_c and k_ϕ , penetration tests with different plate width b are needed.

Assuming that rolling resistance is equal to vertical work done in rut forming and that soil reaction, at a point in the contact area, is always radial to the wheel and equal to the pressure under a vertical plate at the same depth, Bekker formulated the following rolling resistance expression:

$$R = \frac{b(k_c/b + k_\phi)}{n + 1} \left[\frac{3W}{b(k_c/b + k_\phi)d^{0.5}(3 - n)} \right]^{(2n+2/2n+1)}$$

To determine ground pressure (p_g) under a tyre Bekker proposed to use the following expression:

$$p_g = p_l + p_c$$

where, p_l = inflation pressure of the tyre
 p_c = carcass stiffness.

Rolling resistance now becomes:
$$R = \frac{[b(p_l + p_c)]^{(n+1)/n}}{(k_c + bk_\phi)^{1/n}(n + 1)}$$

Uffelmann (1961) also assumed that the soil reaction is radial to the wheel and that the rolling resistance is equal to vertical work done. The pressure beneath a track is expressed as:

$$p = 5.7c$$

where, c = cohesion of the soil.

Uffelmann's rolling resistance equation for towed rigid wheels is:

$$R = W^2/5.7cbd$$

In fact this is a special case of Bekker's theory with $n=0$ and $p=k_c/b + k_\phi$.

Willis et al. (1965) investigated the validity of the Bekker theories. They found that:

- rolling resistance is not only due to vertical work done
- the assumption of a pure radial soil reaction is not correct
- n is a soil parameter
- k_c , k_ϕ and k are dependent on plate dimensions.

In his theory Gee-Clough (1976, 1979) included the effects of slip and deep sinkage on rolling resistance of rigid wheels in sand. He proposed to determine soil sinkage parameters from measurements with a wheel of known dimensions. This principle is the basis of the "Wheel Bevameter". It is less difficult to determine the Bekker soil parameters with the "Wheel Bevameter". The soil reaction under a "Wheel Bevameter" is more similar to the one under a wheel than to the one under a strip footing.

To make the Bekker theory applicable to pneumatic tyres, Perdok (1978) assumed that a flexible tyre of a defined size behaves like a rigid wheel of a larger diameter (see Fig. 6.19). A deformation factor C was introduced:

$$D^* = C.D$$

where, D^* = alternative rigid wheel diameter
 D = tyre diameter.

The deformation factor depends on inflation pressure, wheel load, and soil conditions. Full-sized rigid wheels were used as "Wheel Bevameter".

The "Wheel Bevameter" gives better predictions than the plate sinkage tests. It also makes the pressure-sinkage method more empirical.

Koolen (1976) gives an approximate method for soil compaction under a towed tyre. His theory is based on the hypothesis that the compaction of a volume element of soil under a certain tyre for a certain soil and wheel load can be predicted by uniaxial compression of a sample of that soil (Fig. 6.20). In this uni-

axial compression test the piston pressure is equal to the inflation pressure plus some corrections that should be applied to obtain the same compaction as the volume element of soil under the wheel.

Corrections are to be made for:

- carcass stiffness of the tyre
- unequal pressure distribution in the contact area
- shear stress in the contact area
- decrease of pressure with depth
- area of the contact surface
- bulging of soil beside the tyre
- wall friction in the compression test.

Stienstra (1976) investigated the sum of corrections to be made for a soil sample at 5 cm depth in the longitudinal centre plane of a rut formed by a tyre with an inflation pressure of 3.3 bar and a wheel load of 30 kN. In the uniaxial compression test a pressure of 7.1 bar was needed to achieve the same compaction. So, in this case, the sum of the corrections had a value of 3.8 bar.

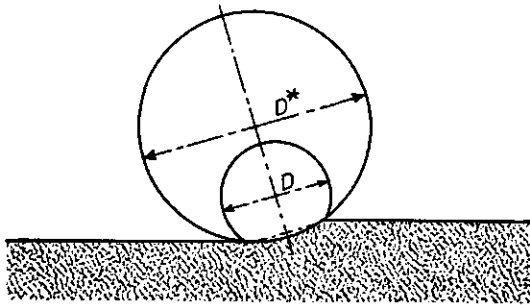


Fig. 6.19. Pneumatic tyre and equivalent rigid wheel.

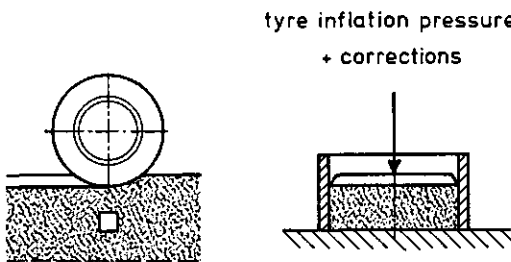


Fig. 6.20. Approximate compaction model.

6.4. EXACT METHODS

Exact methods try to model soil deformation in a mathematical way. Two approaches to predict soil-wheel behaviour have been adopted: the slip-line method and the finite element method.

6.4.1. SLIP-LINE METHODS

In the longitudinal plane of a wheel-soil system two fields of soil failure were found by Wong and Reece (1966,1967). A mathematical model based on limit equilibrium was used to predict the stress distribution under two-dimensional wheels. Good agreement between measured and predicted values was achieved.

The model assumes an incompressible medium and is therefore not adequate for predicting soil compaction due to wheel action.

Karaflath and Nowatzki (1978) showed similar failure zones. Their solutions assumed that a rut was formed. However, this can not be combined with plain strain and an incompressible medium.

6.4.2. FINITE ELEMENT METHODS

Perumpral et al.(1971) adopted the finite element method (FEM) to predict wheel-soil behaviour. The FEM assumes linear stress-strain relationships. Soils do not satisfy this assumption. Therefore, a variable elastic modulus for the soil was assumed. So, each finite element was given such different elastic values that the non-linear stress-strain curve was approximated. Strictly speaking this is incorrect. Yong and Fattah (1976) used a similar method. Wheel performance was predicted in terms of energy components as a function of wheel slip. Investigations with tyres operating on an undeformable surface were made by Yong et al.(1978) to include tyre deformation in the prediction model. Although attempts have been made to apply the FEM to flexible wheels, the FEM-approach is two-dimensional and therefore less useful in predicting wheel and tyre performance in field operations, where bulging occurs beside the wheel.

6.5. CLOSING REMARKS ON PREDICTION METHODS

With empirical methods wheel-soil characteristics can be predicted accurately in uniform soils. The relationships discussed in section 6.2.2 show that easily obtainable soil characteristics can be used for these predictions.

In agricultural field practice soil conditions usually vary with depth. Therefore, further studies should be made to account for soil variations.

Under uniform soil conditions dimensionally correct empirical methods can also achieve a high degree of accuracy in predictions (see section 6.2.3).

Approximate methods can improve the understanding of the mechanism. The complexity of such methods increases enormously the more similar the model is to the practical situation. Accuracy is higher when the model becomes more empirical.

In practice exact methods are difficult to apply because appropriate ways of describing the mechanical properties of soil are not available. Further investigations into the mechanical behaviour of soil are needed before computer-based solutions can be expected to become adequate.

The attraction of exact methods is their ability to predict the state of stress in the entire soil during the passing of a wheel.

Comparative and empirical methods proved to be the easiest and most realistic approaches to predict wheel-soil behaviour under practical conditions. These methods do not improve the understanding of the wheel-soil mechanism.

Further development of approximate and exact methods is needed for a better understanding of the processes. This, in turn, will make it possible to choose better process aspects which can then be used in empirical prediction methods.

CHAPTER 7

SOIL PHYSICAL ASPECTS OF LOAD-BEARING PROCESSES

The physical properties of a soil can change due to load-bearing processes. On the other hand soil physical properties influence the mechanical behaviour of a soil.

For a given soil with specific intrinsic properties (particle size distribution, types of minerals, organic matter content, etc.) important physical factors on the micro level are:

- pore space and the distribution of pore sizes
- the distribution of soil particles within the soil
- soil water content and the distribution of water within the soil
- soil air content and the distribution of air within the soil
- points of contact: number of contacts, bonds, and distributions of these bonds.

These properties, so-called micro-factors, can be changed not only by tillage processes but also by natural forces (freezing, thawing, etc). Tillage processes influence the mechanical properties of the soil as well.

In general farmers are not interested in micro-factors, but in soil qualities such as: pF-curves, water and gas conductivities, thermal properties, penetration resistance, erodibility, tillability, etc. From this point of view soil mechanical properties can be seen as soil qualities as well.

The micro-factors can be seen as the interface between tillage processes and soil qualities.

Koolen (1986) deals with the relationships between micro-factors, soil mechanical properties, mechanical processes, and process effects.

In this chapter we discuss the influence of some physical properties on mechanical properties and the influence of mechanical treatment on physical properties.

7.1. THE INFLUENCE OF PHYSICAL PROPERTIES ON MECHANICAL PROPERTIES

Soil mechanical properties often are divided into compactibility, deformability, and breakability.

Koolen (1986) who uses a more fundamental approach distinguishes between stable and unstable behaviour. The behaviour of a process

is called stable if the process tends to occur throughout the entire soil. An example of stable behaviour is the compaction of loose soil. Unstable behaviour occurs when the process has a tendency to concentrate on a spot. Unstable behaviour occurs on the spots where soil breaking starts.

In practice physical soil degradation generally is not only associated with the effects of increased bulk density but also with those of large soil deformations that occur when the soil volume remains almost constant. Compactibility and deformability are therefore important mechanical properties in relation to soil physical degradation.

A simple test to measure compactibility is the uniaxial compression test. This test and the test facility parameters that influence this test have been discussed in section 5.3.

Soils used in uniaxial compression tests generally have been sieved. Depending on the screens used the soil sample can have a small or a wide aggregate diameter range. For soil samples this may result in different bulk densities during filling and/or a different number of contact points between aggregates. A different number of contact points between aggregates may result in a different compactibility. To investigate a possible effect of aggregate diameter on compactibility, uniaxial compression tests were carried out for different aggregate diameter classes and mixtures of aggregate diameter classes. Section 7.1.1 deals with these tests.

In uniaxial compression tests on a soil with specific intrinsic properties (particle size distribution, type of minerals, organic matter content, etc) the moisture content is probably the major strength-determining factor for compactibility. Koolen (1986) distinguishes between dry compaction and wet compaction. After dry compaction the initial structure is at least locally preserved in the compacted soil. During wet compaction of soil, the bulk density increase is limited by partial water saturation. In this final phase of wet compaction air may be entrapped. In this entrapped air pressure may build up. When the soil is unloaded this air pressure may contribute to rebound. Uniaxial compression tests have been carried out investigate the influence of soil air on rebound. These tests are discussed in 7.1.2.

7.1.1. THE INFLUENCE OF AGGREGATE DIAMETER ON UNIAXIAL COMPRESSIBILITY.

The uniaxial compression behaviour of soil samples with different aggregate diameters has been examined for two soils as follows: Wageningen silty clay loam and Lexkesveer loam were passed through a 10 mm screen. After having been dried at room temperature to a moisture content below the hygroscopic point, each soil was sieved into 3 aggregate diameter classes:

3.0 - 3.4 mm

4.0 - 4.8 mm

6.8 - 8.0 mm.

Aggregate portions of 1 kg were placed on soil water suction bins at a value of pF2.0. One day later suctions were decreased to

pF1.0, pF1.5, pF1.7, and pF2.0. After 5 days the aggregates were taken from the suction bins and measurements of soil moisture content were made. By mixing soils from those different suction bins a range of moisture contents was made. Five days were allowed to equilibrate. Cylinders (50 mm high and 81 mm in diameter) were carefully filled with a spoon. On top of the soil sample a 152.81 gram piston was placed. Uniaxial compressions were carried out at a piston speed of 3 mm/sec until a pressure of 5 bar was reached. Pressure sinkage curves were recorded. After testing the samples were oven dried during five days (at 105°C) to make soil moisture content determinations.

Both soils were tested in the moisture content range from the hygroscopic point to pF2.0. For both soils the following aggregate size classes and mixtures were tested:

Class I: 3.0 - 3.4 mm in diameter

Class II: 4.0 - 4.8 mm in diameter

Class III: 6.8 - 8.0 mm in diameter

Mixture I: 50% (by weight) 3.0-3.4 mm and 50% 4.0-4.8 mm

Mixture II: 50% (by weight) 3.0-3.4 mm and 50% 6.8-8.0 mm

Mixture III: 33.3% (by weight) 3.0-3.4 mm, 33.3% 4.0-4.8 mm, and 33.3% 6.8-8.0 mm.

Aggregates from the three classes have an outside area ratio of 1 : 1.9 : 5.4. Aggregate volume has a ratio of 1 : 2.6 : 12.4.

Before the uniaxial compression tests were carried out determinations were made of pore space of aggregates from the different classes. For both soils and each aggregate diameter class, aggregate pore space was determined (10 fold) on air dry aggregates with the "petroleum method". The petroleum method is described in McIntire and Stirk (1954). Table 7.1. shows the results of these determinations.

Table 7.1. Pore space of air dry aggregates from three diameter classes of Wageningen and Lexkesveer soils.

soil	diameter (mm)	pore space (%)	standard deviation
Wageningen	3.0-3.4	33.91	0.52
Wageningen	4.0-4.8	33.91	0.38
Wageningen	6.8-8.0	33.91	0.34
Lexkesveer	3.0-3.4	34.56	0.39
Lexkesveer	4.0-4.8	34.65	0.49
Lexkesveer	6.8-8.0	34.78	0.67

We may conclude that there is no difference in aggregate pore space between the aggregate size classes tested. So the differences found in the uniaxial compression tests are not due to differences in aggregate pore space.

From the uniaxial compression curves sample heights at σ_1 values of 0, 0.5, 1.0, 2.5, and 5.0 bar were obtained. For these σ_1 values the relationships between void ratio (e) and soil moisture content will be discussed below. Fig. 7.1 and 7.2 show these

relationships for two classes and one mixture.

For both the soils void ratio during filling increases with increasing moisture content. This effect is due to clod forming as the cylinders are filled with a spoon. In the moisture content ranges tested, the void ratio increased from 1.74 to 2.19 and from 1.99 to 3.10 for Lexkesveer and Wageningen soil respectively. The void ratio increase during filling was highest for Wageningen soil because this soil has a stronger tendency to form clods. At the highest moisture content tested aggregate class 1 showed a stronger cloddiness resulting in higher void ratio values. Compared with aggregate classes the mixtures showed lower

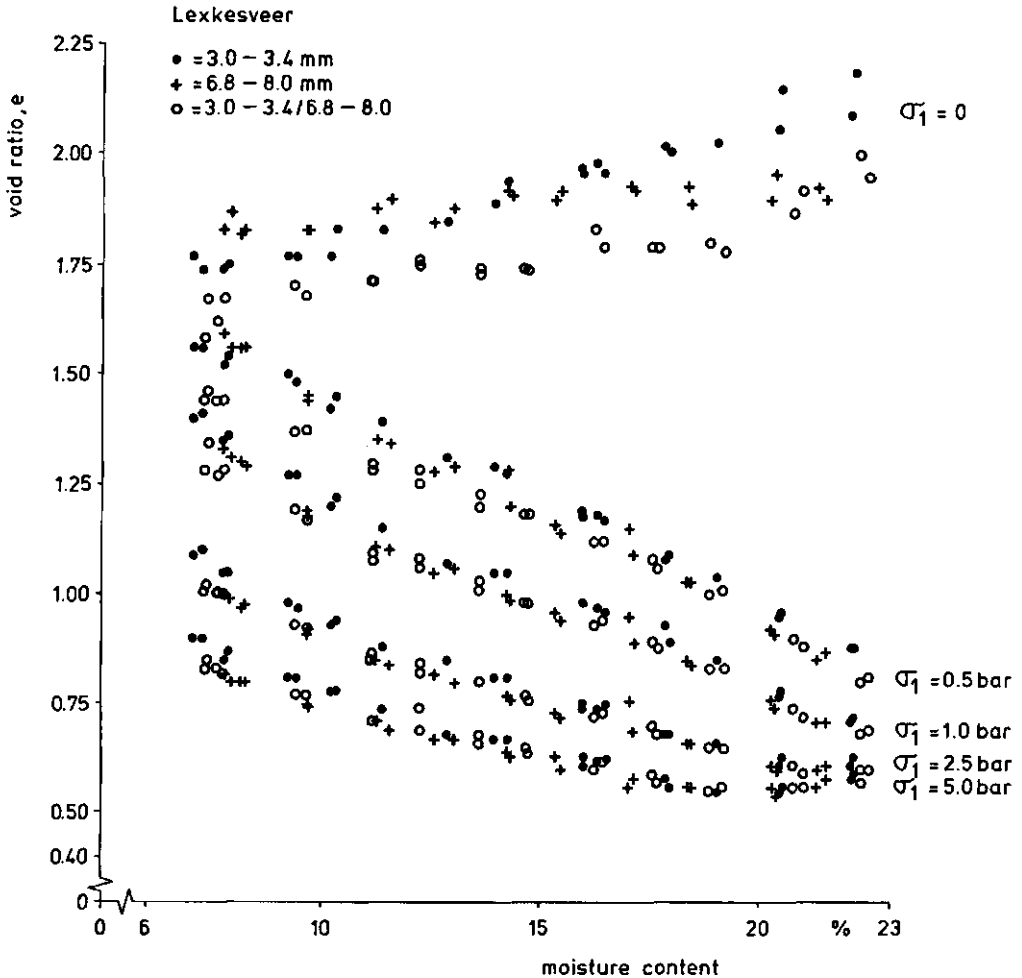


Fig. 7.1. Uniaxial compression behaviour of two aggregate classes and one mixture of Lexkesveer loam.

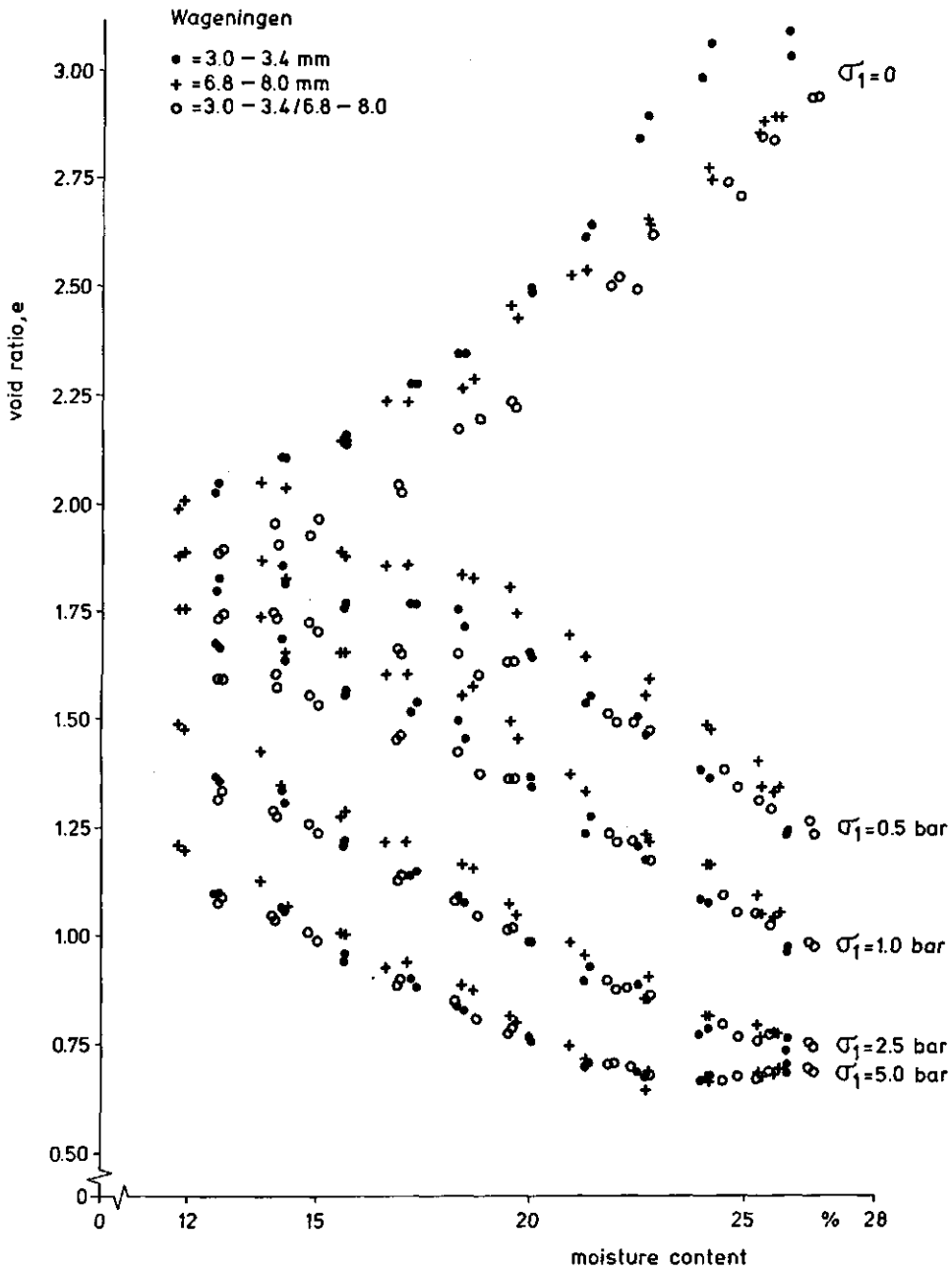


Fig. 7.2. Uniaxial compression behaviour of two aggregate classes and one mixture of Wageningen silty clay loam.

void ratio values during filling. When the moisture content increases the difference disappeared gradually due to clod forming. The lower void ratio of dry mixtures could have been expected because it is known that a denser packing can be achieved with different diameters.

The compaction of a relatively dry sample starts as dry compaction but with increasing pressure compaction it can change into wet compaction. The line that represents 10 volume percent air content was chosen more or less arbitrarily as transition between the dry and wet compaction areas.

In the wet compaction area there is no difference in behaviour between aggregate classes and/or mixtures. In this area aggregates have been damaged to such an extent that they almost disappear.

In the dry compaction area it seems sometimes that a certain aggregate class has more resistance to compaction than another one. For example, in the moisture content range between 7 % and 15 % Lexkesveer class I shows for the pressures applied a somewhat higher pore ratio level compared to class III. The values for class II lie between those of the other classes. These small differences, however, are not due to aggregate size but to differences in packing during filling. Samples with denser packing during filling have somewhat higher void ratio values during compaction. When the moisture content increases these differences disappear both during filling and during compaction. The Wageningen soil class III has in the moisture content range between 12 % and 20 % a somewhat denser packing during filling and therefore somewhat higher void ratio values during compaction than the other classes. Also these small differences disappear when the moisture content increases in this soil. At the lower moisture contents the mixtures have lower void ratio values during compaction, but these differences also disappear when the moisture content increases.

From these tests we may conclude that aggregate size has no influence on uniaxial compactibility. This can be explained by the stable behaviour of the compaction process as described by Koolen (1986). The weakest spot is compacted first and gets stronger. Compaction stops at this spot and starts at the second weakest spot. In this way compaction will occur throughout the entire soil.

For both soils the relationship between critical pressure and moisture content has been calculated from the uniaxial compressions (Fig. 7.3). Critical pressure is the value of the applied pressure at the moment that the critical pore space is reached. Kuipers (1959) defines critical pore space as the pore space at which there is an air content of 10 % at the pF2 moisture content. Critical pore space is reached at void ratio values of 0.71 and 0.92 for Lexkesveer and Wageningen soil respectively. The difference between the two lines in Fig. 7.3 is comparable to the differences in moisture content at pF2. These comparable equal shapes of the curves of these soils agree with the results of uniaxial compression tests carried out by Koolen (1974) for the same soils. At pF2 both soils have a critical pressure of 1.2 bar. For field traffic Fig. 7.3 means that the critical pore

space will be reached at the same tyre settings (inflation pressure, wheel load, speed, etc.) for both soils. Fig. 7.3 shows as well that soil moisture content is the most important soil physical aspect of compactibility.

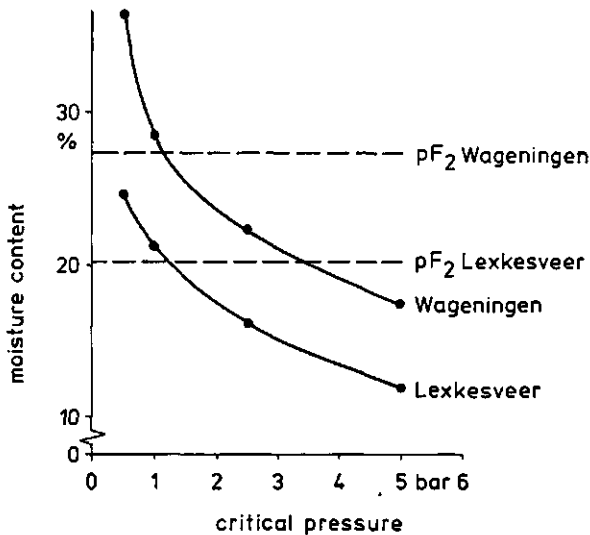


Fig. 7.3. Critical pressure-moisture content relationship for "Lexkesveer" and "Wageningen" in uniaxial compression tests.

7.1.2. THE INFLUENCE OF SOIL AIR ON REBOUND

Söhne (1952, 1956) observed rebound (elastic recovery) in repeated uniaxial compression tests of soil samples. Yong and Warkentin (1966) show a model for soil behaviour during loading and unloading (Fig. 7.4 and 7.5). In this dissertation the elastic recovery during unloading (a in Fig. 7.4) will be called rebound and the relaxation (b in Fig. 7.4) will be called creep.

A hysteresis effect during the unloading and reloading of soil was found not only by Söhne but also by Yong and Warkentin. Similar effects for metals have been presented by Nadai (1950). Stone and Larson (1980) measured rebound on 60 gramme soil samples with a diameter of 5.65 cm. A static load was applied until sample volume and soil water suction were constant. This took about half an hour. The total recovery was measured by reducing the load and holding the new load until the sample height did not change anymore. In these tests the total recovery usually was less than 0.05 gr/cm³ dry bulk density change. No relationship between total recovery and moisture content was found. The tests proved that the clay content was an important factor of total recovery. Because Stone and Larson's experiments used relatively long lasting static loadings, there is no evidence of a possible influence of entrapped air on the recovery.

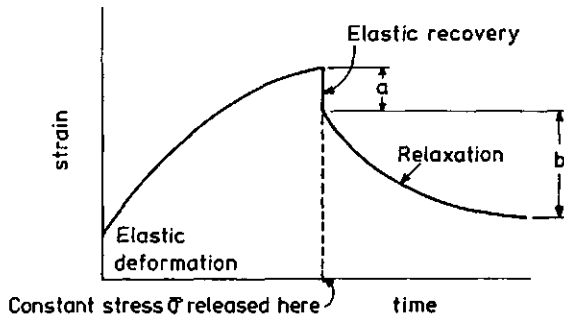


Fig. 7.4. Course of strain in time of a volume element of soil at constant stress and after releasing stress.

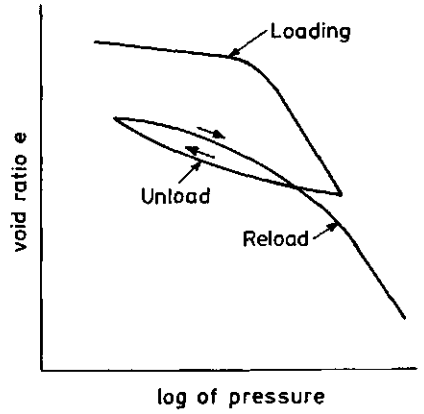


Fig. 7.5. Behaviour of soil at loading, unloading, and reloading.

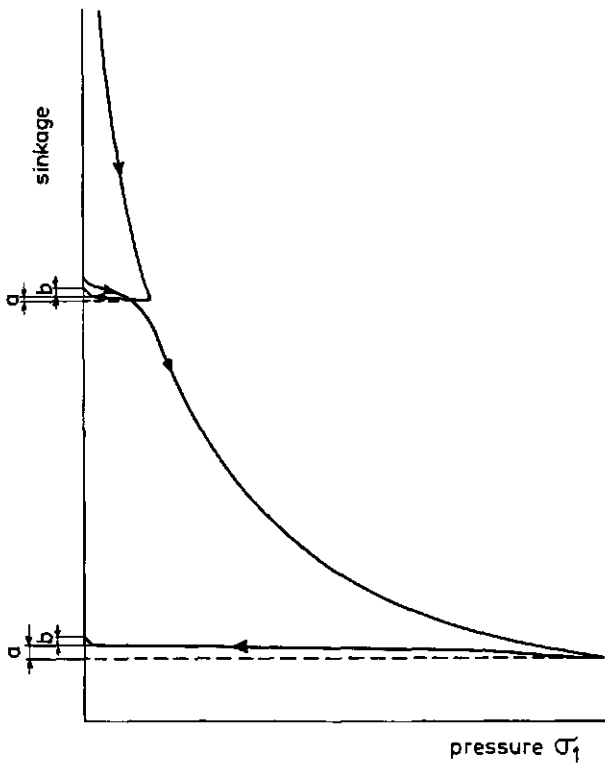


Fig. 7.6. Typical uniaxial pressure-sinkage curve.

Neither Söhne's nor Yong and Warkentin's experiments mention the possible influence of soil air on rebound.

To become better informed about rebound and the influence of soil air on this phenomenon, several series of uniaxial compression tests were carried out with three soil types. Rebound was measured at different loading speeds, soil moisture contents, and in soil samples of varying dimensions.

During uniaxial compression a pressure-sinkage curve was recorded. An example of a pressure-sinkage curve is given in Fig. 7.6. Distance *a* in the pressure-sinkage relationship is rebound. Distance *b* can be seen as creep during relaxation of the weak spring that was placed between piston and pressure transducer. To measure creep the soil sample was placed on a micrometer stand.

Some samples were vacuum saturated and loaded to 0.5 bar with a piston with a diameter that was much smaller than the sample diameter.

The soils tested were Lexkesveer loam, Almkerk silty clay, and Boskoop peat. Lexkesveer and Almkerk were passed through a 3 mm screen; for the Boskoop soil a 5 mm screen was used. A moisture content range was made to correspond to the most common field moisture contents of these soils.

Samples with diameters of 8 cm, 18 cm, 30 cm, and 40 cm were tested at a compression speed of 3 mm/s. All samples had a diameter to height ratio between 1.6 and 1.0. No significant differences in compaction and rebound were found for the different soil sample dimensions. Therefore, in the other tests only sample cylinders with a height of 50 mm and an inside diameter of 81 mm were used.

Precompressing to 0.5 bar and subsequent reloading to 4.0 bar resulted in rebounds almost equal to those occurring when compression was increased to 4.0 bar without precompaction.

Fig. 7.7 shows the rebound for the Lexkesveer and Boskoop soil at two pressure levels and the different air contents of the soils. Soil samples were loaded to 0.5 bar, unloaded, and reloaded to 4.0 bar. The compression speed was 0.25 mm/s. In both soils the rebound increased when the pressure was increased. For Lexkesveer soil the rebound increased when the air content was decreased. At a pressure of 0.5 bar this increase in rebound was less pronounced than at 4.0 bar. When the air content exceeded 20 % the Boskoop soil showed an increase in rebound when the air content decreased. Below an content of 20 % rebound decreased when the air content decreased. The vacuum-saturated samples showed a rebound level that was almost equal to the one of samples with a high air content. Reloading to 4.0 bar was impossible for the two samples from both soils with the lowest air content at 0.5 bar. In these samples water was squeezed out at a pressure below 1 bar. This resulted in such a fast pressure increase in time that loading could not be stopped at exactly 4.0 bar. For one peat sample in Fig. 7.7. a negative air content was calculated. This was due to water that was squeezed out temporarily during compression and that was absorbed again by the soil sample during creep.

No difference in behaviour was found between compression speeds of 0.25 mm/s and 3 mm/s for the Lexkesveer soil. At an air

content above about 5 % by volume the Boskoop soil showed higher rebound values after the faster compression (Fig. 7.8). This is normal behaviour of fibrous materials. At a low air content the soil particles can move easily because of the high water content. Fig. 7.9 shows the rebound-air content relationships for the three soils tested. All samples were precompacted at 0.5 bar and subsequently loaded to 4.0 bar. The compression speed was 3 mm/s. It seems that the Boskoop soil behaves very differently from the Lexkesveer and Almkerk soil.

To understand this behaviour which occurs when the soil air content is low and to find the influence of entrapped air on rebound, rebound was expressed as the difference in soil air content between loading to 4.0 bar and after rebound. For the three soils calculated rebound (expressed in volume percent air)

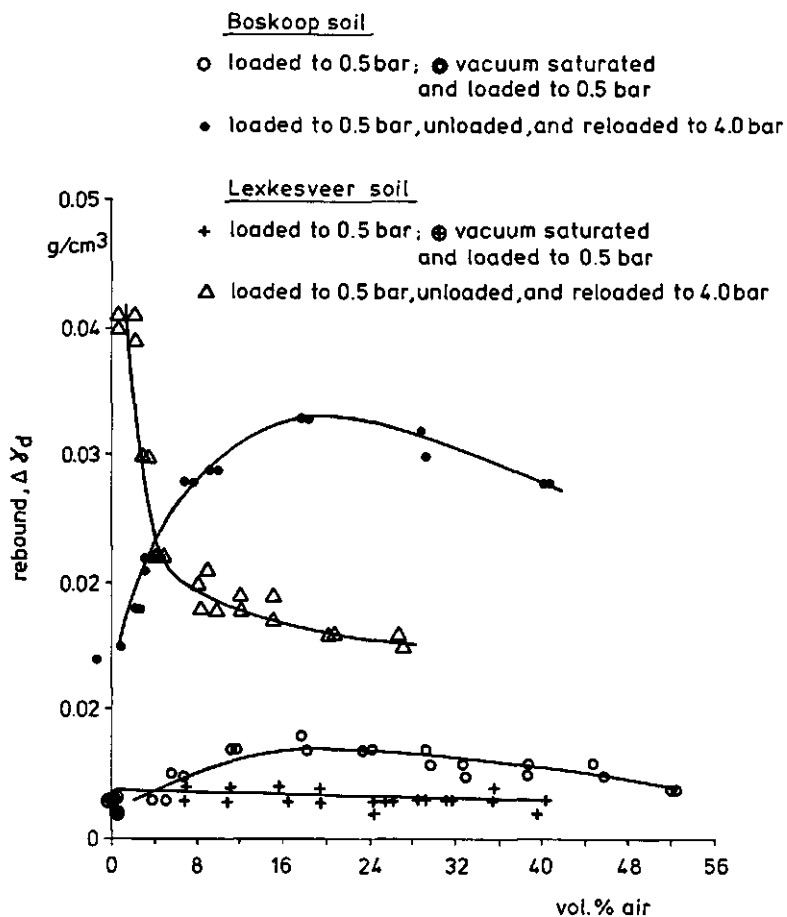


Fig. 7.7. Rebound-air content relationship for "Boskoop" and "Lexkesveer" soils at two stress levels. Compression speed = 0.25 mm/s; cylinder diameter = 81 mm.

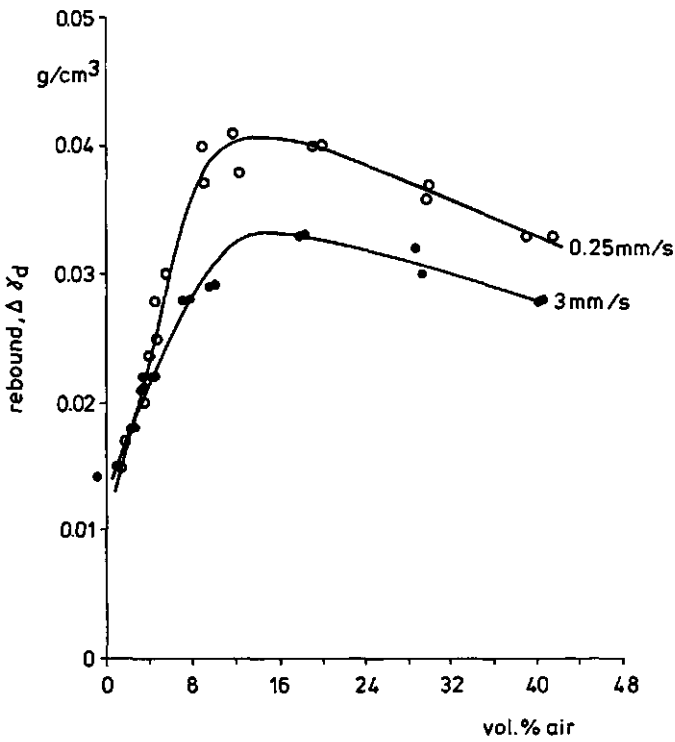


Fig. 7.8. Rebound-air content relationship for "Boskoop" soil at two compression speeds. Precompaction stress = 0.5 bar; compaction stress = 4.0 bar; cylinder diameter = 81 mm.

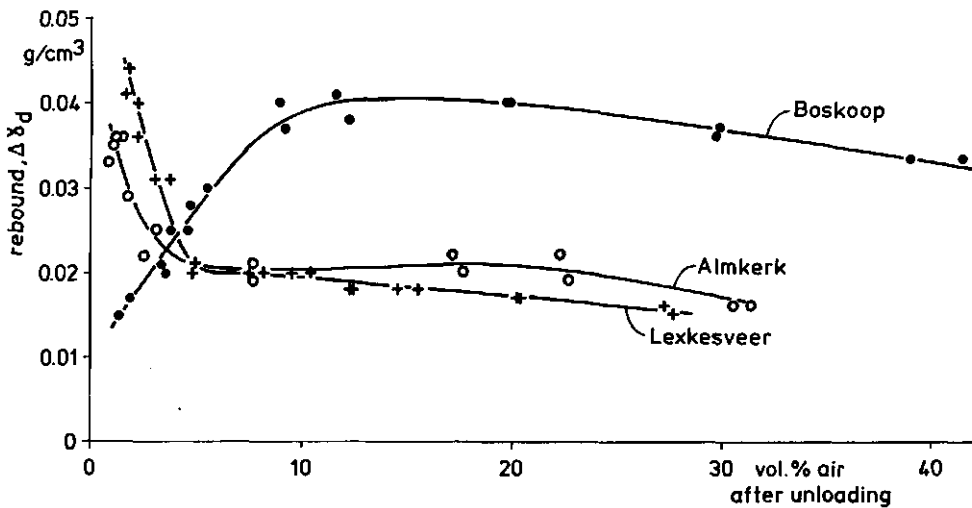


Fig. 7.9. Rebound after loading to 4.0 bar for three soils. Compression speed = 3 mm/s.

was plotted against measured air content after unloading (Fig. 7.10). The straight lines represent volume changes expected at the indicated pressure increases of the entrapped air. An intersection of a rebound curve with the line $p=2$ bar means that the volume of air after unloading had to be compressed to a pressure which is 2 bar higher during compression to account for the volume decrease. We can see that for Almkerk and Lexkesveer soils higher pressures in smaller quantities of entrapped air can account for the increased rebound. The Boskoop soil showed the same effect of an increased rebound and an increasing pressure of the entrapped air when the air content was higher than about 10%. When the air content was lower rebound decreased. This decrease must be explained as follows: when air pressure increases soil water will be squeezed out more easily. For Boskoop soil this means that a further increase in air pressure does not seem to occur when the air pressure exceeds 2 bar because water is squeezed out. Fig. 7.10 seems to suggest that the pressure increase within the entrapped air was higher than 4.0 bar. However, this is not possible because such pressures were not applied. At 4.0 bar loading water was squeezed out of the samples that had been positioned on the left side of the 4 bar air pressure increase line. A part of this water was squeezed out temporarily

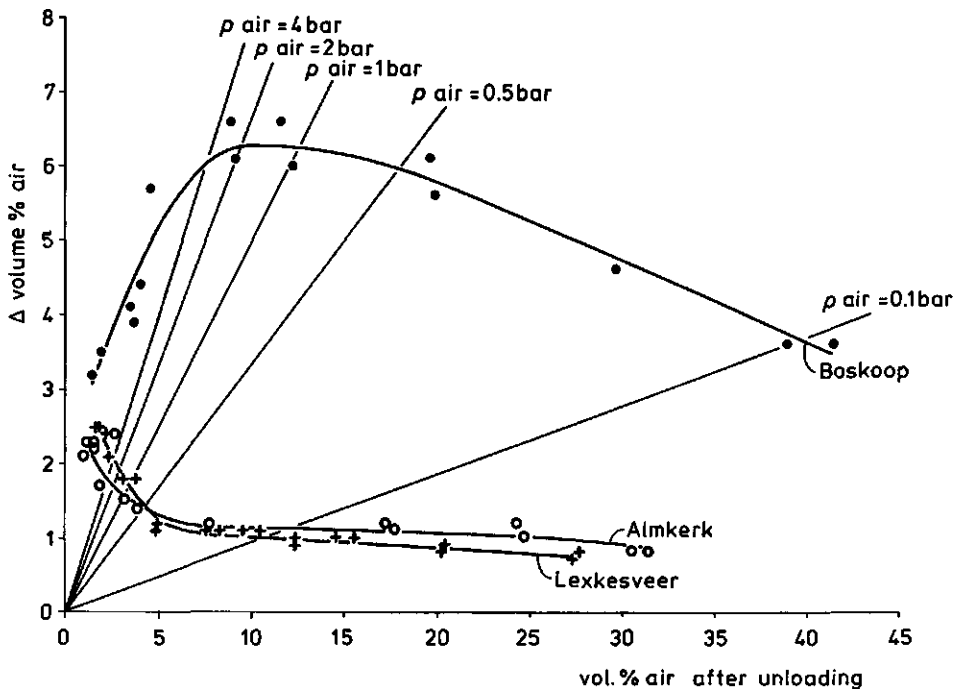


Fig. 7.10. Rebound (expressed as change in air content) after loading to 4.0 bar for three soils. Samples are uniaxially pre-compacted at 0.5 bar and subsequently loaded to 4.0 bar. Compression speed = 3 mm/s.

during compression and absorbed again during rebound and creep. Because of this sponge-like behaviour we can not make exact calculations of maximum pressures built up within the entrapped air.

We can conclude that a build up of air pressure can occur which can influence rebound considerably when air is entrapped during the final part of a compression process.

Total recovery (rebound + creep) is much higher than rebound. Fig. 7.11 shows rebound and total recovery of the Boskoop soil after 1 hour for different soil air contents.

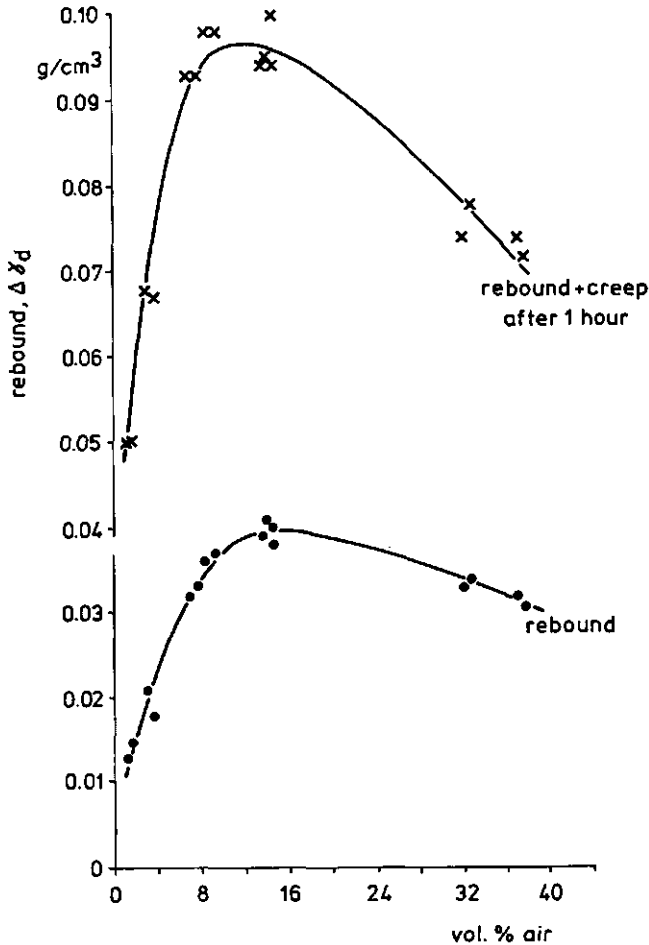


Fig. 7.11. Rebound and total recovery after one hour for "Boskoop" soil. Samples are uniaxially precompacted at 0.5 bar and subsequently loaded to 4.0 bar. Compression speed = 3 mm/s.

7.2. THE INFLUENCE OF MECHANICAL TREATMENT ON PHYSICAL PROPERTIES

Mechanical treatment of the soil by wheels results in compaction and/or deformation. Because of this treatment micro-factors and soil qualities can change. Changes on the micro level influence soil qualities such as pF-curves and conductivities. A review of the influence of mechanical treatment on micro-factors and soil qualities is given in 7.2.1.

In arable farming it is important to know the influence of soil compaction on subsequent tillage operations. The major soil mechanical quality that can change due to compaction is tillability. To investigate the influence of soil compaction on tillability a test is needed that can characterize this influence. Tillability, tillability tests, and attempts to use the unconfined compression test to characterize tillability are discussed in 7.2.2.

7.2.1. THE INFLUENCE OF MECHANICAL TREATMENT ON MICRO-FACTORS AND SOIL QUALITIES

On the macro level compaction reduces pore space. On the micro-level this pore space reduction is at the expense of the largest pores (Sommer et al., 1972; Sommer et al., 1975; Maidl and Fischbeck, 1985). This effect is strongest during wet compaction. Table 7.2 shows the influence of autumn ploughing on pore size distributions under dry and wet soil conditions.

Table 7.2. The influence of ploughing conditions on pore size distributions (after Maidl and Fischbeck, 1985)

Depth	top soil (0 - 35 cm)		plough sole (35 - 40 cm)	
	Adry	Awet	Adry	Awet
Vol. % pores >10 μ	11.2	6.6	7.9	6.0
Vol. % pores 10 - 0.2 μ	14.0	13.0	11.3	11.8
Vol. % pores <0.2 μ	17.5	21.3	22.2	22.2

Adry = autumn ploughed under dry soil conditions

Awet = autumn ploughed under wet soil conditions

Pores >10 μ are important for air conductivity. After wet ploughing the content of these pores was lower than after dry ploughing; in the top soil this amounted to a reduction to 58 % and in the plough pan to 76 % of the values measured after dry ploughing. This reduced air conductivity.

The pores 10 - 0.2 μ determine the amount of water available for plants. Compared to dry conditions the amount of available water decreased in the top soil after ploughing under wet conditions.

Water in pores <0.2 μ is not available for plants. The content of pores < 0.2 μ increased strongly in the top soil after ploughing under wet conditions as well.

A wet compacted soil has a higher content of unavailable water

and a lower content of pores for air conductivity. This means that such a soil is wetter and colder than a dry compacted soil.

Maidl and Fischbeck (1985) also examined the influence of these differences in pore size distributions, due to ploughing under wet and dry conditions, on plant growth. Their investigation proved that the decrease of yield after wet compaction was mainly due to an insufficient supply of nitrogen. The decrease of N supply after wet compaction indicates a lower N mineralization due to lower soil temperature, and higher gaseous N losses (denitrification) due to lower air conductivity.

Inter-particle bonds not arising from water suction can be destroyed at large deformations. The strength of these bonds influences the water suction - moisture content relationship. Dawidowski and Koolen (1987) applied triaxial tests to field samples of Wageningen silty clay loam. The sample volume was almost constant during deformation. Samples were deformed to 50 % of the original sample heights. Many bonds were destroyed by the deforming and smearing action of the test, resulting in a strong increase in water suction. Compared with undeformed samples, the samples tested showed higher values for volumetric shrinkage and dry tensile strength.

Influences of compaction on pF-curves have been reported by Warkentin (1971), Sommer et al. (1972), and Moreno et al. (1974). Koolen (1978) found that the precompaction moisture content greatly influences moisture contents at pF2.0 and pF2.7.

7.2.2. TILLABILITY

Tillability is defined as the degree of ease with which a soil may be manipulated for a specific purpose (ASAE Engineering Practice ASAE EP291.1, Hahn et al. 1984).

In agricultural field practice farmers decide on how to till from experience. However, their experience does not suffice when they need to choose new implements and when they find themselves in unknown situations. Also, field experience is not easy to convey. To obtain an objective approach to tillability, a measurable parameter of tillability, and therefore a tillability test is needed.

7.2.2.1. TILLABILITY TEST

To develop a tillability test it is necessary to take the following factors into account:

- *the initial soil condition.* This condition depends on soil physical properties and the history of the soil.
- *the type of tillage operation.* Primary tillage and field traffic have other demands than secondary tillage operations.

In this dissertation we concentrate tillability on seed-bed preparation in spring.

- *the processes that occur.* In tillage operations we should distinguish between intended processes and accidental pro-

cesses. In seed-bed preparation the major intended process is "crumbling". This process is accompanied by the accidental process of "compaction". Tillability tests should concentrate on the major intended process, but must also take into account the major accidental process.

- *the energy needed for the tillage operation.* Energy needed for tillage is associated with energy needed for tillage processes and for locomotion of the tractor on the field. Gross energy consumption is the amount of energy needed for both tillage processes and tractor locomotion. Net energy consumption only deals with the energy needed for the tillage process (for instance draft).

In the Netherlands soil conditions generally are too wet in the period before seed-bed preparation. Therefore, tillability research has concentrated on the upper tillage limits.

It is advisable to increase the ratio net energy consumption to gross energy consumption. Ultimately tillability depends not only on the results of the tillage operations but also on the energy required. An optimum ratio of tillage results to energy consumption is pursued.

Energy is not yet a limiting factor. Therefore, the interest in tillability nowadays is limited to a tillability test that indicates whether or not the soil can be tilled in order to achieve the intended results. In times of energy scarcity the tillability test should also pay much attention to the energy aspects.

- *the intended tillage results.* The Dutch farmer is generally mostly interested in the results of the tillage operations. Therefore criteria for the results of tillage operations are required in order to determine tillability. Tillage criteria have been published in "Tillage Advice" for cereals (Andringa et al, 1979), sugar beets (Perdok et al, 1974a), and potatoes (van Gilst et al, 1975).
- *the tillage implement to be used.* The tillage implement should also be considered because of the energy consumption and the kind of the work expected. The capacity of the tillage implement can also play an important part in farm management decisions.

7.2.2.2. TILLABILITY TESTS BASED ON PROCESSES OTHER THAN CRUMBLING

Boekel (1977) tried to relate soil tillability to deformability measured with a plasticity meter. The pressure that is needed to force the soil through a small nozzle is measured with this instrument. The required pressure is lower for a wet plastic soil than for a dry crumbly soil. It is proposed that this is a measure for crumbling. This test is not suitable for field samples and does not account for the effect of pore space on tillability.

Havinga and Perdok (1969) developed a tillability test that relates tillability to mechanical properties of soils. The compressibility of loose soil is chosen as major process. The applied pressure is a measure for the energy consumption. In this

test air permeability is measured as a function of soil moisture content and applied pressure. Perdok et al. (1974b) discovered that 20 fields could be tilled for potato seed-bed preparation at a working depth of 8 cm, when their soils still had an air permeability of at least $100 \text{ cm}^2 \times 10^{-10}$ after having been loaded to 4 bar. Aggregates ranging from 2.8 - 4.0 mm were used for these tests. This means that the soil structure was not taken into account. Because this test uses compressibility as a major process it can also be used to predict field trafficability (Perdok, 1976).

Koenigs (1976) determined the upper tillage limit with a micro tillage test. To carry out this test a small saucer is filled with a thin layer of soil aggregates (2-4 mm fraction). With a hammer a sliding action (micro tillage) is applied to the soil in the saucer. After the micro tillage the pull that is needed for moving a spatula through the soil is measured. In a range with increasing moisture contents the draft for the spatula abruptly increased from a certain moisture content on. Koenigs considers this moisture content minus one percent as the upper tillage limit for spring seed-bed preparation.

After some preliminary tests Wageningen silty clay loam was uniaxially compressed to three pore space levels over a wide range of moisture contents. Having been dried these samples were

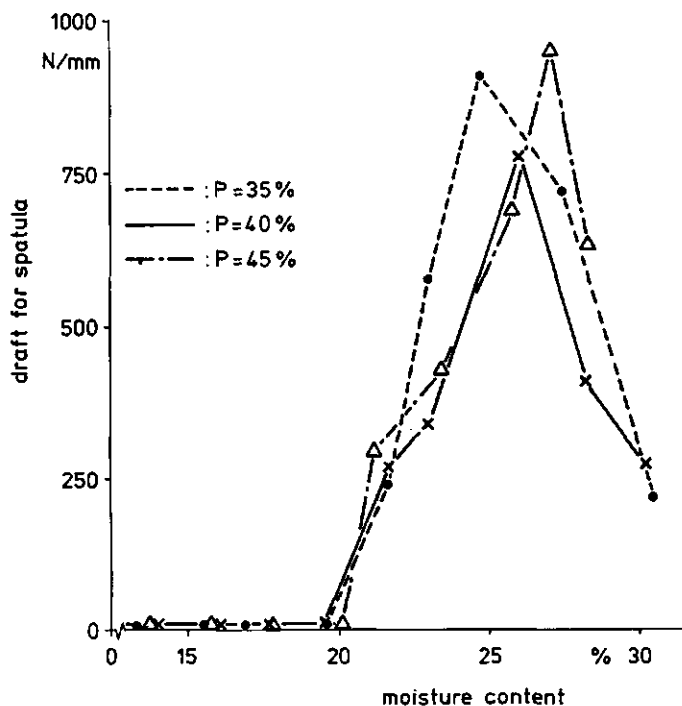


Fig. 7.12. Behaviour of precompacted "Wageningen" silty clay loam at three pore space levels in a micro tillage test.

crushed and sieved. For each sample the 3.4-4.8 mm fraction was rewetted to the moisture content before compression. After one day of equilibration these aggregates were used in a micro tillage test. The relationships between spatula draft and moisture content are shown in Fig. 7.12. For the three pore space levels tested the draft for the spatula suddenly increased. It is remarkable that for each initial pore space level this sudden increase occurs at the same moisture content. This means that this upper tillage limit is independent of pore space at precompression.

Neither does this test use field samples. The micro tillage with the hammer and the draft measurement with the spatula depend on the person who does the test. Some other drawbacks of this test are that soil sometimes sticks to the hammer and that soil may curl up when wet cohesive.

7.2.2.3. TILLABILITY TESTS BASED ON CRUMBLING PROCESSES

These tests try to determine the intensity of crumbling. Furthermore, the energy needed for this crumbling can be measured. In field practice the most interesting aspects of spring seed-bed preparation are indeed crumbling and the energy needed for the tillage operation. Therefore, it is attractive to use these methods to characterize field processes.

Koolen (1977) used a pendulum-type impact machine to measure tillage process aspects on soil blocks in the laboratory. For each test he measured the volume and the mean aggregate size of the loosened soil, and the energy consumption. Although his test showed good results for soil blocks prepared in the laboratory it is difficult to use it for undisturbed field samples.

For our examination the unconfined compression test has been chosen to characterize the crumbling process. In an unconfined compression test a soil sample is made to fail between two plates (Fig. 7.13). At the moment of failure, the sample shortening expressed as a fraction of initial height (ξ_f) and the prevailing failure stress (σ_{max}) are measured. The failure strain ξ_f represents the soil deformation that occurs before failure. This means that ξ_f gives an indication of breakability and therefore of crumbling as well. The unconfined compressive strength (σ_{max}) is a measure of the energy consumption.

Koolen (1973 and 1978) successfully used the unconfined compression test to characterize soil mechanical properties. When laboratory samples are used the influence of bulk density on the crumbling process can be examined by adjusting different levels of pore space. The unconfined compression test can also be applied to field samples.

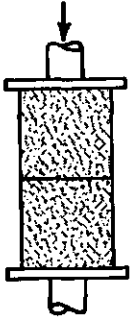


Fig. 7.13. Unconfined compression test.

TESTS OF LABORATORY SAMPLES

At two pore space levels unconfined compression tests were carried out not only to determine the relationship between ϵ_f and moisture content, but also the one between σ_{max} and moisture content. A jaw crusher was used to determine crumbling at these pore spaces and moisture contents. In both experiments Wageningen silty clay loam and Lexkesveer loam were used. The soil moisture content range was chosen between moisture content at pF2 and half of this moisture content. Two pore space levels were made comparable to field pore space levels that can be found in spring.

Soil samples were prepared as follows: the dry soils were passed through a 3 mm screen and subsequently wetted to the desired moisture content ranges. After equilibration the soil was compressed in cylinders with an inside diameter of 50 mm and a height of 100 mm. The inside walls of the cylinder were greased with silicon grease. The compressions were made in layers of 20 mm. The diameter to height ratio of the samples was 0.5 in order to minimize the influence of friction between plates and sample during unconfined compression (Koolen, 1978). Before unconfined compressions were made the samples had two days to equilibrate. From the unconfined compression tests, made at a piston speed of 10 mm/min, ϵ_f and σ_{max} were determined. After the tests the soil moisture content was measured.

The tests with the jaw crusher were made as follows: the two soils and the soil preparation method used were the same as those used for the unconfined compression tests. The cylinders used had an inside diameter and a height of 50 mm. Having been compressed to the desired pore space the samples had two days to equilibrate. The jaw crusher (Fig. 7.14) has a bin with one movable wall (d). A handle is used to oscillate the movable wall. The

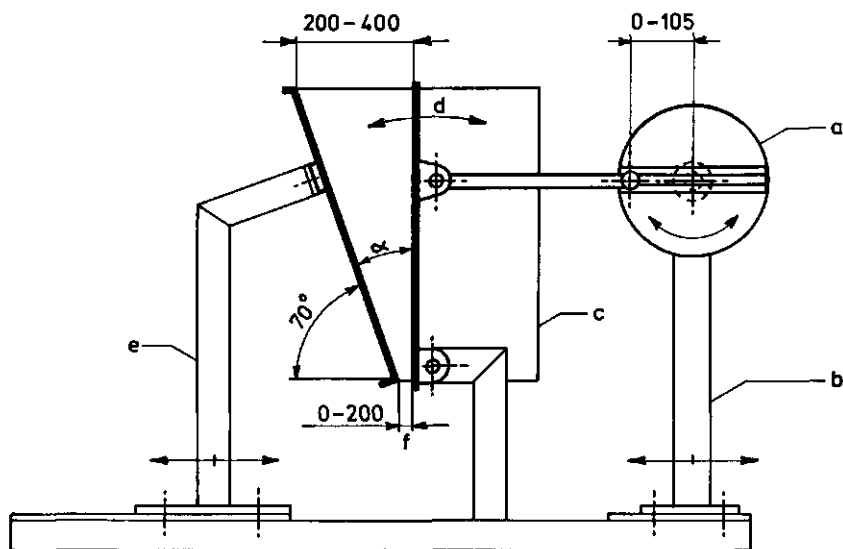


Fig. 7.14. Jaw crusher.

outlet (f) is adjustable between 0 and 200 mm. The oscillating movement of the movable wall can be adjusted by the amplitude of the oscillation and by the angle α between the movable wall and the opposite wall. After three test series the following settings were used:

- a width of the outlet of 11.5 mm
- an angle α ranging from 21 to 59 degrees for the Lexkesveer soil
- during the first five oscillations of the Wageningen soil the angle α was 32 to 41 degrees (to avoid too high pressures on the soil samples); the next oscillations were made at an angle ranging from 21 to 59 degrees.

The aggregates were sieved directly after the tests.

From the unconfined compression tests curved relationships have been found between ϵ_f and moisture content (Fig. 7.15 and 7.16). At increasing moisture content soil deformation before breaking increases. The lowest pore space level shows higher ϵ_f values for both soils. This is due to the lower amount of weak zones in the most compacted soil.

Failure stress σ_{max} shows a linear decrease with increasing moisture content. So under wet conditions these soils need less energy to break than under dry conditions.

In the moisture content ranges tested, the Wageningen soil showed higher levels of ϵ_f and σ_{max} compared to Lexkesveer soil. So the Wageningen soil is harder to break and more energy is needed for this breaking. This agrees with the practical experience that this heavier soil is less easy to till.

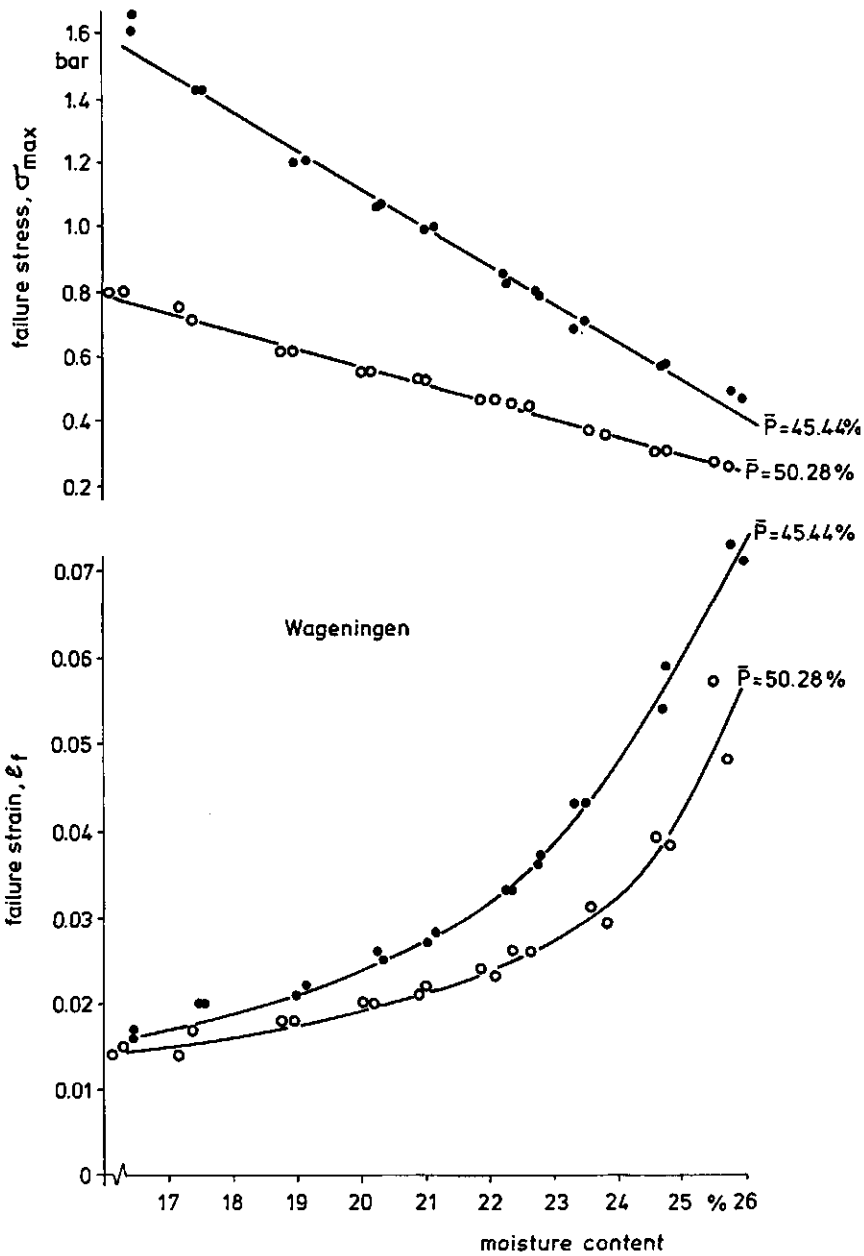


Fig. 7.15. Unconfined compression behaviour of "Wageningen" silty clay loam.

The measurements with the jaw crusher showed a sudden decrease of the amount of soil released from the crusher outlet at increasing moisture content (see Fig. 7.17 and 7.18). At the same moisture content the Mass Median Diameter (MMD) of the soil that passed through the jaw crusher strongly increased. The moisture content at which these sudden changes occurred can be considered the upper tillage limit. For Wageningen silty clay loam the upper tillage limit lies for both pore spaces at a moisture content of about 21 %. This agrees with the tests carried out with the micro tillage test according to Koenigs (Fig. 7.12). The upper tillage limit for Lexkesveer lies between a moisture content of 18 % and 19 %. Because of the low number of measurements made at these moisture contents it was not possible to make a more precise estimation.

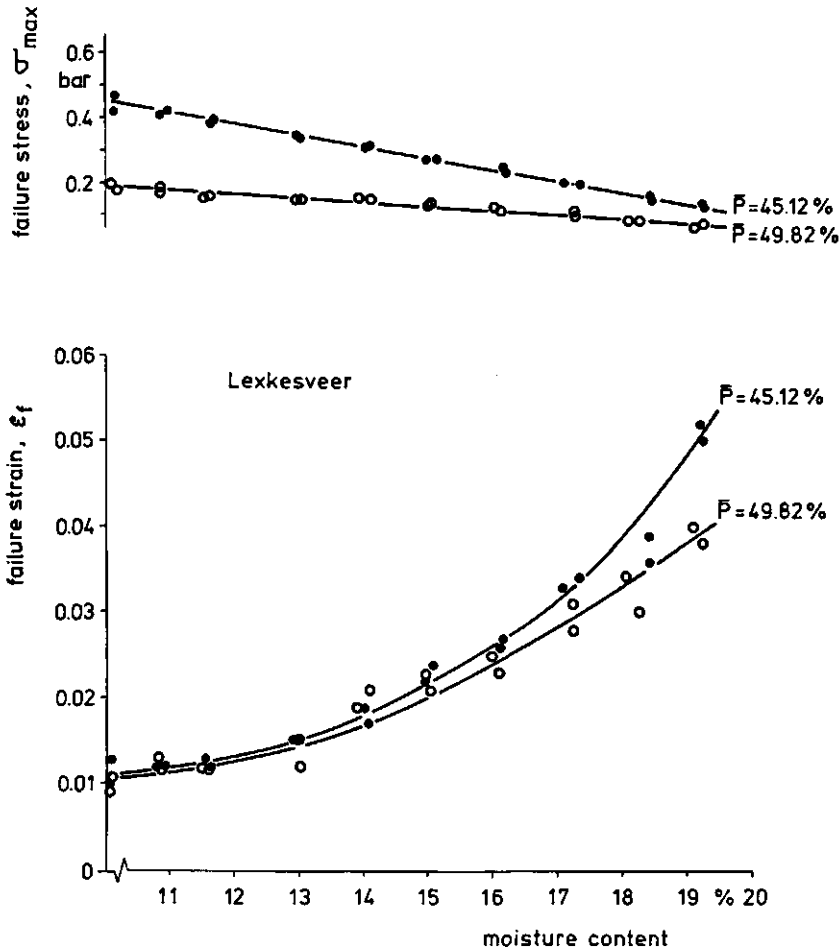


Fig. 7.16. Unconfined compression behaviour of "Lexkesveer" loam.

From the tests applied to laboratory samples of Wageningen silty clay loam and Lexkesveer loam we can conclude that:

- pore space influences crumbling in a soil-breaking process. A loose soil crumbles more strongly than a dense soil.
- an unconfined compression test can be used to investigate the influence of soil compaction on breakability.
- failure strain ϵ_f and failure stress σ_{max} do not give an indication of the upper tillage limit. ϵ_f gives an indication of the breaking sensitivity of a soil and σ_{max} indicates the amount of energy needed for breaking.
- In a soil-breaking process crumbling decreases at increasing moisture content.
- the moisture content at the upper tillage limit is almost equal for the pore spaces tested, although the results of the crumbling tillage operation differ at these pore spaces.

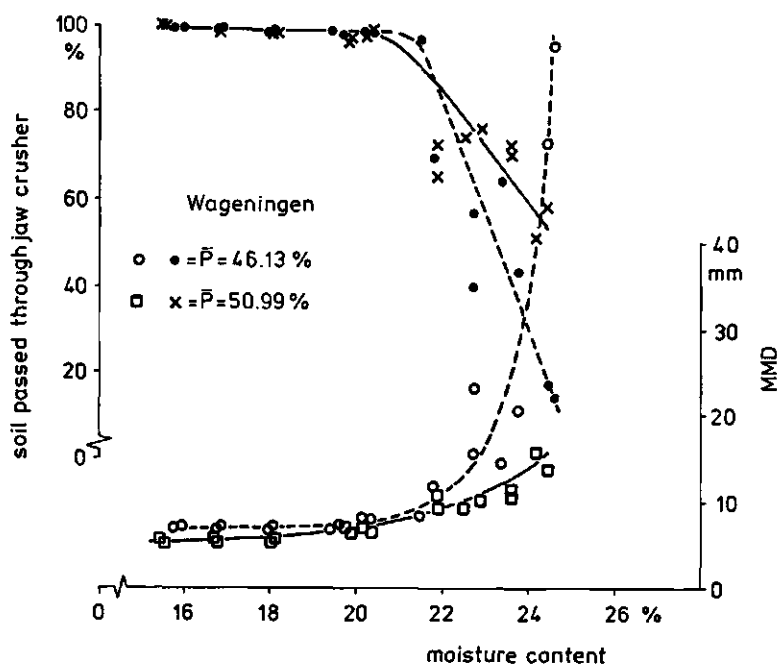


Fig. 7.17. Behaviour of "Wageningen" soil at two pore space levels in a jaw crusher.

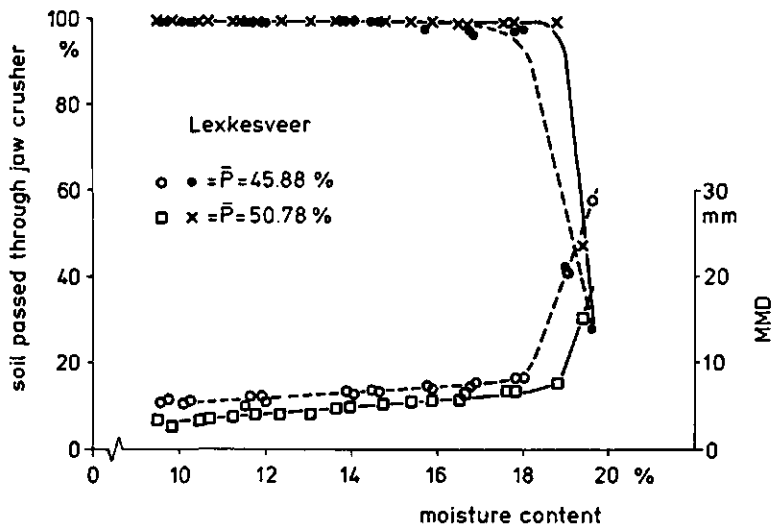


Fig. 7.18. Behaviour of "Lexkesveer" soil at two pore space levels in a jaw crusher.

TESTS OF FIELD SAMPLES

To include soil field structure in tillability tests preliminary investigations were made on the possibilities to use field samples for the unconfined compression test.

The first three series of 80 samples each were used to determine:

- a procedure for taking the field samples
- a procedure for the unconfined compression test with field samples.

The second six series were used to investigate the reaction of the unconfined compression values to changes in weather conditions. The field samples were taken during the months of March and April 1980 on an autumn-ploughed field. The soil can be classified between the Wageningen and the Lexkesveer soil.

The cylinders used have an inside diameter and a height of 50 mm. Before samples were taken the cylinder inside walls were oiled. For each series samples were taken from 8 places in the field from the furrow slice and from the junction area between furrow slices. The soil for seed-bed preparation comes for the greater part from the furrow slices. In the first two series half of the samples were taken from the junction area to get an idea of the differences between furrow slices and the junction area between the furrow slices. All the other samples were taken from the furrow slices.

For sampling the following rules and procedures were used:

- cracks in the soil were avoided.
- cylinders were not allowed to be twisted during sampling, because twisting can create breaking surfaces resulting in

- smaller $\bar{\epsilon}_f$ values. When the cylinder was pushed far enough into the soil it was lifted with a spade, and trimmed with a knife.
- on sampling the soil was compressed. Therefore only samples with a decrease in height of less than 0.5 cm were accepted.
 - the thin dry top layer of about 1 cm in thickness was removed before samples were taken.

The mean moisture content in furrow slices is higher than in the junction area. This difference is just below significance for the first series and significant (95 % probability) for the second series. The mean difference has a value of 1 - 1.5 percent by weight. The average pore space was about 5 percent higher in the junction area. This could have been expected because this soil was loosened from the furrow slices by weathering.

To obtain a height to diameter ratio of 2 in the unconfined compression test two samples were been put on top of each other according to Koolen (1978). Before testing the samples were weighed. The sample pairs were composed of two samples with almost equal weight. This was done to avoid that samples with very different pore space were used as a sample pair in the unconfined compression test.

In the field the moisture content increases with depth. Therefore, soil samples topsides are drier and more crumbly than bottomsides. So there are three ways to combine the sample pairs:

- loose/loose: the upside of the first sample against the upside of the second sample.
- loose/firm: the upside of the first sample against the underside of the second sample.
- firm/firm: the underside of the first sample against the underside of the second sample.

In the sample height values which exist at the beginning of the unconfined compression tests, the decrease in sample height which occurs when the samples are pushed out of the cylinders is accounted for.

In the different combinations no significant differences were found in moisture content and pore space. So the differences found as a result of unconfined compression are due to the method used. For each series the loose/loose method resulted in the lowest values for mean failure strain $\bar{\epsilon}_f$ and mean unconfined compressive strength $\bar{\sigma}_{max}$. The firm/firm method showed the highest values while the loose/firm method resulted in intermediate values. The differences between loose/loose and firm/firm are significant (95 % probability) but no significant differences were found between loose/loose and loose/firm and between loose/firm and firm/firm. Compared with the firm/firm method the standard deviation of $\bar{\epsilon}_f$ is a factor 2.5 lower in the loose/loose method. For $\bar{\sigma}_{max}$ standard deviations are almost equal for loose/loose and firm/firm. It is remarkable that the standard deviation values for $\bar{\epsilon}_f$ are almost constant for all the series within a soil. Standard deviation increases for $\bar{\sigma}_{max}$ when the soil becomes drier. The standard deviation of $\bar{\epsilon}_f$ was almost equal for a series of field samples (loose/loose method) and a series of laboratory samples. For $\bar{\sigma}_{max}$ the laboratory samples had a factor 3 lower standard deviation than the field samples (loose/loose). Fig. 7.19 shows the $\bar{\sigma}_{max}$ - moisture content rela-

tionship for a loose/loose series. This clearly shows the difficulties that arise when field samples are used instead of laboratory samples (Fig. 7.15 and 7.16).

The crack formation differed for the different combinations. In the loose/loose method crack formation always occurred in the middle of the sample pairs. This could have been expected because this part is driest and has more weak zones. Crack formation for the firm/firm method always started on top or at the bottom of the sample pairs. In the loose/firm method crack formation could start everywhere.

The $\bar{\epsilon}_f$ values for furrow slices and the junction area are not significantly different for the three methods. The unconfined compressive strength values are much lower for the junction area. This could be expected because this weathered soil is easy to crumble. Further sampling concentrated on furrow slices because of the reported differences and the knowledge that the soil for the seed-bed comes mostly from the furrow slices.

Six series of forty samples each were taken from the furrow slices on six different dates. The course of the unconfined compression values (loose/loose method) is compared with the climate diagram. The climate diagram (Fig. 7.20) shows that 1980 had a wet spring. There was a dry period between 10 and 18 April. In this period a seed-bed could dry enough in order to be prepared for potatoes. Fig. 7.20 shows the course of $\bar{\epsilon}_f$ and $\bar{\sigma}_{max}$ in time as well. We can see that the unconfined compression values tend to follow the drying of the field top layer. Even when the conditions are known at which this soil reaches the upper tillage limit, we can draw no conclusions about the date in the spring of 1980 on which a seed-bed for potatoes could have been prepared.

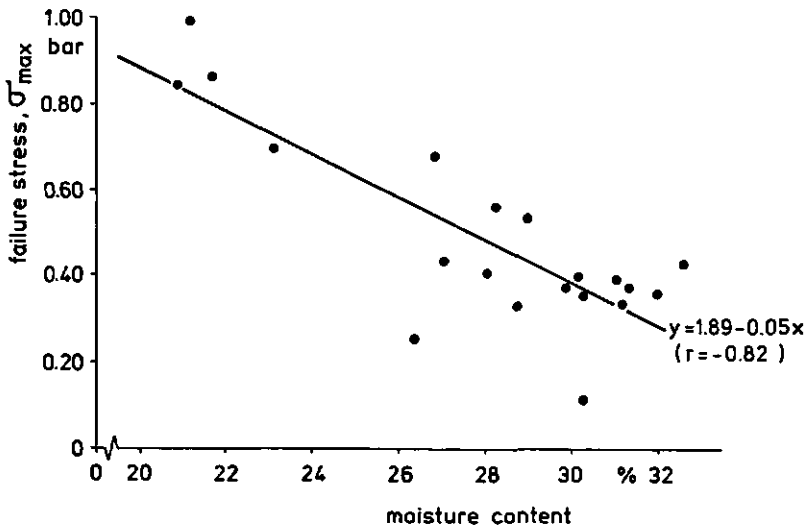


Fig. 7.19. Unconfined compressive strength of field samples.

First, the following questions are to be answered:

- are the sampling depth and the thickness of the top layer that is needed for the seed-bed equal?
- has the dry layer that was removed been taken into account?
- have cracks been avoided?

The thickness of the top layer that is used to prepare a seed-bed has two components: the layer that is used for surface levelling and the thickness of the loose layer that is needed for the seed-bed. The thickness of the levelling layer can be calculated using a reliefmeter (Kulpers, 1957). For a level field a loose top layer of 8 cm is needed for potatoes (Kouwenhoven, 1974). For our test field the necessary sampling depth is estimated at 10.8 cm (2.8 cm of levelling layer and 8 cm for the seed-bed). Our sampling depth was 9 cm: 1.5 cm for the removed top layer, 2 cm for

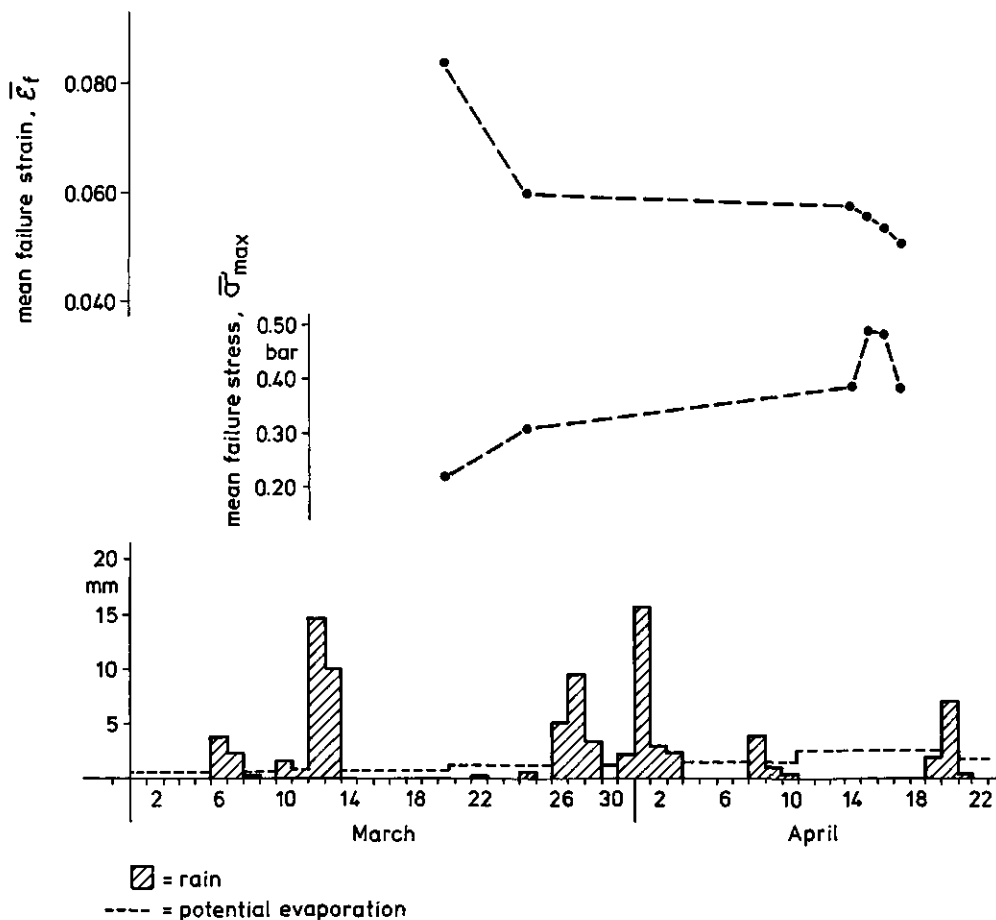


Fig. 7.20. Course of climate and the unconfined compression characteristics of field samples.

trimming, 0.5 cm compression during sampling, and 5 cm cylinder height. This means that the height and diameter of our cylinders were 1.8 cm too small.

From the tests with field samples we can conclude that:

- field samples can be used for unconfined compressions tests.
- for high accuracies a standard sampling method is necessary.
- sampling depth depends on roughness of the field, the needed thickness of the seed-bed, the compressibility of the soil, and the thickness of the removed dry top layer.
- the highest accuracy in unconfined compression tests is achieved when two samples are combined with the upsides against each other (loose/loose method).
- the course of $\bar{\epsilon}_f$ and $\bar{\sigma}_{max}$ tend to follow the drying of a field soil.

CHAPTER 8

SUMMARY

In soil dynamics we distinguish between loosening and load-bearing processes. This dissertation deals with load-bearing processes under agricultural rollers, wheels, and tyres.

Agricultural rollers, wheels, and tyres have been classified. In addition some general aspects of these devices are presented.

This report presents the fundamentals of load-bearing processes, i.e. kinematic, dynamic, and soil physical aspects. Kinematic and dynamic aspects are discussed on three levels: device (roller, wheel, or tyre), contact area, and soil under the device. Physical properties of a soil can change due to load-bearing processes. On the other hand the soil physical properties influence the mechanical behaviour of a soil. In the section on soil physical aspects we have paid special attention to the influence of aggregate diameter and soil air on compression behaviour of soil and to tillability.

Soil characteristics concerning load-bearing processes are presented. Different tests that were used to characterize soil mechanical behaviour are compared. Relationships between soil characteristics and process aspects and their suitability to predict process aspects are discussed. Contributions are made to the prediction of some process aspects of a towed tyre under different soil conditions and in different soil types. Under laboratory conditions the use of characterizing processes (cone, vane, and falling weight) and empirical prediction methods resulted in accurate predictions of rolling resistance, rut depth, and compaction caused by a towed tyre.

CHAPTER 9
SAMENVATTING

In de gronddynamica onderscheidt men losmakende en afsteunende processen. Bij het rijden over grond treden afsteunende processen op onder rollen, wielen en banden. Dit proefschrift behandelt afsteunende processen onder rollen, wielen en banden in de landbouw.

In deze dissertatie worden een indeling en enkele algemene aspecten gepresenteerd van in de landbouw voorkomende rollen, wielen en banden.

De grondslagen van afsteunende processen worden behandeld: kinematische, dynamische en bodemfysische aspecten. De bespreking van kinematische en dynamische aspecten vindt plaats op drie niveau's: werkend deel (rol, wiel of band), contactvlak en de grond onder het werkend deel.

Bodemfysische eigenschappen kunnen veranderen als gevolg van afsteunende processen. Anderzijds hebben bodemfysische eigenschappen invloed op het mechanische gedrag van grond. In het hoofdstuk over bodemfysische aspecten krijgen met name aandacht: bewerkbaarheid van grond en de invloed van aggregaat diameter en bodemlucht op het verdichtingsgedrag van grond.

Bodemkarakteristieken, die verband houden met afsteunende processen worden gepresenteerd. Verschillende voor het karakteriseren van het mechanisch gedrag van grond gebruikte testen worden vergeleken. De betrekkingen tussen bodemkarakteristieken en procesaspecten worden behandeld. Evenals de mogelijkheid om deze betrekkingen te gebruiken in voorspellingsmethoden. Er worden nieuwe bijdragen geleverd aan de voorspelling van enkele procesaspecten van een getrokken band. Nauwkeurige voorspellingen van rolweerstand, insporing en verdichting waren mogelijk met behulp van karakteriserende processen (conus, vane en valgewicht) en empirische voorspellingsmethoden.

REFERENCES

- Aboaba, F.O., 1969. Effects of time on compaction of soils by rollers. *Trans. ASAE* 12(1):302.
- Amir, I., G.S.V. Raghavan, E. Mckyes and R.S. Broughton, 1976. Soil compaction as a function of contact pressure and soil moisture content. *Canadian Agric. Eng.* 18(1):54-57.
- Andringa, J.T. et al., 1979. Grondbewerkingsadvies voor granen. *Bedrijfsontwikkeling* 10(5):495-501.
- Anslow, B.J. and R.J. Warrillow, 1962. Tractor tyres. I. *Mech. E.* Referred in Inns and Kilgour (1978).
- Baganz, K. und L. Kunath, 1963. Einige Spannungs- und Verdichtungsmessungen unter Schlepperlaufwerken. *Agrartechnik* 13:180-182.
- Baganz, K., 1963/1964. Spannungs- und Verdichtungsmessungen im boden bei verschiedenen Fahrgeschwindigkeiten. *Archiv für Landtechnik* 4(1):35-45.
- Bailey, A.C. and G.E. VandenBerg, 1968. Yielding by compaction and shear in unsaturated soil. *Trans. ASAE* 11:307-311,317.
- Bailey, A.C., E.C. Burt and R.L. Schafer, 1974. Digital calculation of rolling radius for wheels and tracks. *Trans. ASAE* 17(5):871-873.
- Bailey, A.C. and E.C. Burt, 1981. Performance of tandem, dual and single tires. *Trans. ASAE* 24(6):1103-1107.
- Bekker, M.G., 1956. *Theory of land locomotion.* University of Michigan Press, Ann Arbor.
- Bekker, M.G., 1960. *Off-the-road locomotion.* University of Michigan Press, Ann Arbor.
- Bekker, M.G., 1969. *Introduction to terrain-vehicle systems.* University of Michigan Press, Ann Arbor.
- VandenBerg, G.E. and W.R. Gill, 1962. Pressure distribution between a smooth tire and the soil. *Trans. ASAE* 5:105-107.
- Bernacki, H., J. Haman and Cz. Kanafojak, 1972. *Agricultural machines, theory and construction.* Vol. 1, Warsaw.
- Bernstein, R., 1913. *Probleme zur experimentellen Motorpflugmechanik.* *Der Motorwagen*, Vol. 16.
- Biller, R.H. and H. Steinkampf, 1978. Einfluss der Profilrichtung von AS-Reifen auf die Zugkraftübertragung des Schleppers. *Landtechnik* 33:57-60.
- Biller, R.H., 1983. Richtige Montage von Frontriebreifen hilft sparen, ohne Zugkraft einzubüssen. *diz* 34(11):1444-1446.
- Blake, G.R., W.W. Nelson and R.R. Allmaras, 1976. Persistence of subsoil compaction in a Mollisol. *Soil Sci. Soc. Am. J.* 40(6):943-948.

- Bock, G., 1952. Feldversuche über die Zugfähigkeit von Ackerschlepperreifen. *Grundl. Landtechnik* 3:88-100.
- Bock, G., 1953. Beobachtungen bei Feldversuchen über die Zugfähigkeit von Ackerschleppern. *Grundl. Landtechnik* 5:42-48.
- Bodman, G.B. and G.K. Constantin, 1965. The influence of particle size distribution in soil compaction. *Hilgardia* 36(15):567-591.
- Boekel, P., 1977. De werkbaarheid van de grond in het voorjaar in verband met de ontwatering en de samenstelling van de grond. Symposium werkbaarheid en bedrijf, Wageningen.
- Boels, D., 1978. Kanttekeningen bij bestekvoorwaarden ter beperking van bandspanning van dumpers en trekkers. *Nota 1081*, ICW-Wageningen.
- Boll, E. und E. Isensee, 1987. Eignung von Geschwindigkeitsgebern. *Landtechnik* 42(2):57-59.
- Bolling, I. und W. Söhne, 1982. Der Bodendruck schwerer Ackerschlepper und Fahrzeuge. *Landtechnik* 37(2):54, 56-57.
- Brixius, W.W. and F.M. Zoz, 1976. Tires and tracks in agriculture. *Am. Soc. Automotive Eng.*, Paper 760653, Milwaukee.
- Buckingham, F., 1976. Fundamentals of machine operations. Tillage. Deere and Company, Moline.
- Cegnar, A. and F. Fausti, 1961. Movements under the contact area of radial and conventional tires. *Trans. ASAE* 4:224-225.
- Chancellor, W.J., 1976. Compaction of soil. *Bull. 1881*, Div. Agric. Sci. University of California, Davis.
- Chessness, J.L., E.E. Ruiz, and C. Cobb, 1972. Quantitative description of soil compaction in peach orchards using a portable penetrometer. *Trans. ASAE* 15(2):217-219.
- Clark, S.K. (Ed.), 1971a. Mechanics of pneumatic tires. National Bureau of Standards Monograph 122. U.S. Government Printing Office, Washington USA.
- Clark, S.K., 1971b. The contact between tire and roadway. Chapter 6 in *Mechanics of pneumatic tires*. National Bureau of Standards Monograph 122. U.S. Government Printing Office, Washington :445-500.
- Corcoran, P.T., 1979. Analysis of tractive performance. ASAE-paper, No. 79-1550, New Orleans, L.A.
- Danfors, B., 1974. Packning i alven. Specialmeddelande S24, Jordbrukstekniska Institutet, Ultuna, Uppsala, Sweden.
- Danfors, B., 1980. Däck för traktorer och redskap. Meddelande 386, Jordbrukstekniska Institutet, Uppsala, Sweden.
- Davies, D.B., D.J. Eagle and J.B. Finney, 1972. Soil management. Farming Press, Ipswich.
- Dawidowski, J.B. and A.J. Koolen, 1987. Changes of soil suction, conductivity, and dry strength during deformation of wet undisturbed samples. *Soil and Tillage Research* 9(2):169-180.
- Domler, K.W. and A.E. Williams, 1978. Tractive efficiency - maximum or optimum? *Trans. ASAE* 21(4):650-653.
- Dwyer, M.J., D.R. Comely and D.W. Evernden, 1974a. Handbook of Agricultural tyre performance. NIAE, Silsoe.
- Dwyer, M.J., D.R. Comely and D.W. Evernden, 1974b. The field performance of some tractor tyres related to soil mechanical properties. *Journ. Agr. Eng. Res.* 19(1):35-50.

- Dwyer, M.J., D.W. Evernden and M. McAllister, 1975. The development of a handbook of agricultural tyre performance. Proc. 5th Int. Conf. ISTVS, Detroit, USA.
- Dwyer, M.J. and G. Pearson, 1976. A field comparison of the tractive performance of two- and four-wheel drive tractors. Journ. Agr. Eng. Res. 21:77-85.
- Dwyer, M.J., M. McAllister and D.W. Evernden, 1977. Comparison of the tractive performance of a tractor driving wheel during its first and second passes in the same track. J. Terramech. 14(1):1-10.
- Dwyer, M.J., 1978. Maximising Agricultural Tractor Performance by Matching Weight, Tyre Size and Speed to the Power Available. Proc. 6th Int. Conf. ISTVS, Vienna, Vol. 1:479-499.
- Eidik Thleme, H.C.A. van, and H.B. Pacejka, 1971. The tire as a vehicle component in Clark (Ed): Mechanics of Pneumatic Tires. National Bureau of Standard Monograph 122, Washington, 545-839.
- Estler, M., H. Knittel und E. Zeitner, 1984. Bodenbearbeitung aktuell. DLG-Verlag Frankfurt (Main).
- Faure, A., 1980/1981. A new conception of the plastic and liquid limits of clay. Soil and Tillage Research 1:97-105.
- Forrest, P.J., I.F. Reed and G.V. Constantakis, 1962. Tractive characteristics of radial-ply tires. Trans. ASAE 5:108,115.
- Freitag, D.R., 1965. A dimensional analysis of the performance of pneumatic tyres on soft soils. Tech. Rep. 3-688. U.S. Army Engineers Waterways Experiment Station, Vicksburg.
- Freitag, D.R., 1979. History of wheels for off-road transport. J. Terramech. 16(2):49-68.
- Fröhlich, O.K., 1934. Druckverteilung im Baugrunde. Springer-Verlag, Wien.
- Gee-Clough, D., 1976. The Bekker theory of rolling resistance amended to take account of skid and deep sinkage. J. Terramech. 13(2):87-105.
- Gee-Clough, D., M. McAllister and D.W. Evernden, 1977a. Tractive performance of tractor drive tyres. I. The effect of lug height. Journ. Agr. Eng. Res. 22(4):373-384.
- Gee-Clough, D., M. McAllister and D.W. Evernden, 1977b. Tractive performance of tractor drive tyres. II. A comparison of radial and cross-ply carcass construction. Journ. Agr. Eng. Res. 22(4):385-395.
- Gee-Clough, D., M. McAllister and D.W. Evernden, 1977c. Tractive performance of tractor drive tyres. III. Running in the furrow bottom. Journ. Agr. Eng. Res. 22.
- Gee-Clough, D. et al., 1978. The empirical prediction of tractor-implement field performance. J. Terramech. 15(2):81-94.
- Gee-Clough, D., 1979. The effect of wheel width on the rolling resistance of rigid wheels in sand. J. Terramech. 15(4):161-194.
- Gee-Clough, D., G. Pearson and M. McAllister, 1982. Ballasting wheeled tractors to achieve maximum power output in frictional-cohesive soils. Journ. Agr. Eng. Res. 27(1):1-19.
- Gill, W.R. and G.E. VandenBerg, 1967. Soil dynamics in tillage and traction. Agricultural handbook 316. U.S. Dep. of Agr., Washington.
- Gill, W.R., 1968. Influence of Compaction Hardening of soil on penetration resistance. Trans. ASAE 11:741-745.

- Gilst, K.B. van, J.K. Kouwenhoven en L.M. Lumkes, 1975.
Grondbewerklingsadvies voor aardappelen.
Bedrijfsontwikkeling 6(10):819-824.
- Gillemeroth, G., 1953. Untersuchungen über Verfestigungs- und Verlagerungsvorgänge im Ackerboden unter Rad- und Raupenfahrzeugen. Zeitschrift für Acker- und Pflanzenbau 96:219-234.
- Grechenko, A., 1967. Vliv nekolika alternativ podvozku koloveho traktoru na napeti v pude.
Zemedelska Technika 13(7):361-378.
- Hahn R.H., M.A. Purschwitz and E.E. Rosentreter (editors), 1984.
ASAE Standards 1984. Standards, Engineering Practices and Data adopted by the American Society of Agricultural Engineers.
American Society of Agricultural Engineers, St. Joseph, Mi.
- Havinga, L. en U.D. Perdok, 1969. Methode ter karakterisering van het mechanisch gedrag van grond. Nota 534, ICW Wageningen.
- Hegedus, E., 1965. Pressure distribution under rigid wheels.
Trans. ASAE 8:305-308,311.
- Hesse, H., 1986. Schlupfregeln - Sprit sparen.
Lohnunternehmen 41(1):39-40.
- Hettiaratchi, D.R.P. and J.R. O'Callaghan, 1980. Mechanical behaviour of agricultural soils.
Journ. Agr. Eng. Res. 25:239-259.
- Hofferberth, W. and R. Reinhold, 1969. Probleme der Reifenentwicklung für die derzeitige Schlepper und Landmaschinen.
Proc. 3th Int. Conf. ISTVS, Essen, Vol. III:44-67.
- Hofman, V.L., 1977. Model tractor demonstration on ballasting 2WD und 4WD tractors for efficient use of horsepower.
ASAE Paper No.77-1519, Chichago.
- Holm, J.C., 1969. Das Verhalten von Reifen beim mehrmaligen Überfahren einer Spur.
Proc. 3th Int. Conf. ISTVS, Essen, Vol. 2:96-123.
- Inns, F.M. and J. Kilgour, 1978. Agricultural tyres.
Dunlop, London.
- Jahns, G. und H. Steinkampf, 1982. Einflussgrößen auf Flächenleistung und Energieaufwand beim Schleppereinsatz.
Grundl. Landtechnik 32(1):20-27.
- Janosi, Z., 1962. Theoretical analysis of the performance of tracks and wheels operating on deformable soils.
Trans. ASAE 5:133,134,146.
- Karafiath, L.L. and E.A. Nowatzki, 1978. Soil mechanics for off-road vehicle engineering.
Trans. Tech. Publ., Clausthal, Germany.
- Karczewski, T., 1978. The influence of passing speed of agricultural machinery wheels on soil compaction. Zeszyty Problemowe Postepow Nauk, Rolniczych.
- Kellermann, F., 1985. 1 Impuls = 1 Zentimeter.
Die Formel für exacte Geschwindigkeitsmessung.
Agrartechnik 64(11):46.
- Kezdi, A., 1969. Handbuch der bodenmechanik.
Band II, V.E.B. Verlag, Berlin.
- Knight, S.J. and A.J. Green, 1962. Deflection of a moving tire on firm to soft surfaces. Trans. ASAE 5:116-120.
- Koenigs, F.F.R., 1976. Determination of the Upper Tillage Limit for spring tillage by lab. test.
Proc. 7th Conf. ISTRO, Sweden 19.1-19.7.

- Koolen, A.J., 1973. Failure patterns in different soils produced by a curved blade with a small angle of approach. NIAE Subject Day on the mechanical behaviour of agricultural soil. Silsoe.
- Koolen, A.J., 1974. A method for soil compactability determination. *Journ. Agr. Eng. Res.* 19:271-278.
- Koolen, A.J., 1976. De invloed van de mechanisatie op de bodemstructuur. 100 jaar onderwijs, voorlichting en onderzoek in de landbouw. Wageningen.
- Koolen, A.J., 1977. Soil loosening processes in tillage. Analysis systematic and predictability. Mededelingen Landbouwhogeschool Wageningen, 77-17.
- Koolen, A.J., 1978. The influence of a soil compaction process on subsequent soil tillage processes. A new research method. *Neth Journ. Agr. Sci.* 26:191-199.
- Koolen, A.J. and H. Kuipers, 1983. *Agricultural soil mechanics.* Springer-Verlag, Berlin etc.
- Koolen, A.J. and P. Vaandrager, 1984. Relationships between soil mechanical properties. *Journ. Agr. Eng. Res.* 29:313-319.
- Koolen, A.J., 1986. Behaviour of elemental soil volumes in compaction and effects on properties of significance in soil use. *Transactions XIII Congress of the Int. Soc. of Soil Science, Hamburg, Vol. IV:1368-1371.*
- Kouwenhoven, J.K., 1974. Ruggenteelt: teeltmaatregel en groeiregulator. *Landbouwmecanisatie* 25:677-682.
- Krick, G., 1969. Druck- und Schubverteilung unter Rädern und Reifen auf nachgiebigem Boden unter Berücksichtigung der Reifendeformation. *Proc. 3th Int. Conf. ISTVS, Essen, Vol. II:50-75.*
- Krumbach, A.W. and D.P. White, 1964. Moisture pore space, and bulk density changes in frozen soil. *Soil Sci. Soc. Am. Proc.* 28:422-425.
- Kuipers, H., 1957. A reliefmeter for soil cultivation studies. *Neth. Journ. Agr. Sci.* 5(4):255-262.
- Kuipers, H., 1959. Confined compression tests on soil aggregate samples. *Meded. Landbouwhogeschool en Opzoekingsstations Staat Gent* 24(1):349-357.
- Kuipers, H., 1966. Die Bearbeitung schwerer Böden in den Niederlanden. *Tagungsberichte* 82, Teil II. Deutsche Akad. der Landw. zu Berlin:233-240.
- Kuipers, H., 1970. Entgegengesetzte Effekte von Reifen und Bodenbearbeitungen. *Ber. Int. Symp. Warna, Sofia* :59-65.
- Kumar, L. and J.A. Weber, 1974. compaction of unsaturated soil by different stress paths. *Trans. ASAE* 17:1064-1069, 1072.
- Kurtay, T. and A.R. Reece, 1970. Plasticity theory and critical state soil mechanics. *J. Terramech.* 7:23-56.
- Liang, T. and C. Yung, 1966. A microscopic study of tractive performance of a lugged tire operating on sand. *Trans. ASAE* 9:513-515.
- Lumkes, L.M. en U.D. Perdok, 1981. Volgteelt van stamslabonen na doperwten. *Publ.* 17, PAGV Lelystad.
- Maidl, F.X. und G. Fischbeck, 1985. Wenn dem Boden die Luft ausgeht. *DLG-Mitteilungen* 100(13):1354-1356.
- McAllister, M., 1983. Reducing the rolling resistance of tyres for trailed agricultural machinery. *Journ. Agr. Eng. Res.* 28:127-137.

- McIntire, D.S. and G.B. Stirk, 1954. A method for determination of apparent density of soil aggregates. *Austr. J. Agric. Research* 5:291-296.
- McKibben, E.G. and J.B. Davidson, 1940. Transport wheels for agricultural machines. *Agr. Eng.* 21(2):57-58.
- Mech, S.J., G.M. Horner, L.M. Cox and E.E. Cary, 1967. Soil profile modification by backhoe mixing and deep plowing. *Trans. ASAE* 10(6):775-779.
- Melborg, R.H. en U.D. Perdok, 1979. Grondbewerking en vermogensbehoefte. Rapport 11, IMAG Wageningen.
- Melzer, K.J. and S.J. Knight, 1973. Dual-wheel performance in sand. *Trans. ASAE* 16:204-207.
- Melzer, K.J., 1976. Power requirements for wheels operating in sand. *J. Terramech.* 13(2):75-85.
- Moreno, F., C. Sommer and W. Czeratzki, 1974. Einige bodenphysikalische Untersuchungen an der Schleppersohle einer degradierten Schwarzerde. *Landbauforschung Völkensrode* 24(2):123-132.
- Nadal, A., 1950. Theory of flow and fracture of solids. Vol. 1. New York.
- Njøs, A., 1976. Long term effects of tractor traffic in two field experiments in Norway. Report 45, Division of Soil Management of the Agr. Coll. of Sweden, Uppsala.
- N.N., 1971. Soiltest Inc. Gen. Catalog, vol 2a. Evanston.
- N.N., 1980. Two-wheel-drive tractor slip down the field. *Farmers weekly* sept. 26th.
- N.N., 1981a. There's danger in use too much tyre ballast. *Farmers weekly* sept. 18th.
- N.N., 1981b. Landbouwbanden. *Vlugschrift voor de landbouw* 335, Wageningen.
- Onafeko, O. and A.R. Reece, 1967. Soil stresses and deformations beneath rigid wheels. *J. Terramech.* 4:59-80.
- Ouwkerk, C. van, 1968. Two model experiments on the durability of subsoil compaction. *Neth. Journ. Agr. Sci.* 16:204-210.
- Painter, D.J., 1981. A simple deflection model for agricultural tyres. *Journ. Agr. Eng. Res.* 26:9-20.
- Perdok, U.D., P. Boekel en J. Jorritsma, 1974a. Het grondbewerkingsadvies voor sulkerbleten. *Bedrijfsontwikkeling* 5(10):861-865.
- Perdok, U.D., J.J. Klooster en M.C. Sprong, 1974b. De bewerkbaarheid van de grond tijdens de voorjaarswerkzaamheden. Rapport 249, ILR Wageningen.
- Perdok, U.D., 1976. Bewerkbaarheid en berijdbaarheid van grond. *Landbouwkundig Tijdschrift* 88(6):173-178.
- Perdok, U.D., 1978. A prediction model for the selection of tyres for towed vehicles on tilled soil. *Journ. Agr. Eng. Res.* 23:369-383.
- Perdok, U.D. en J. Terpstra, 1983. Berijdbaarheid van landbouwgrond. Bandspanning en grondverdichting. *Landbouwmecanisatie* 34(4):363-366.
- Perumpral, J.V., J.B. Liljedahl and W.H. Perloff, 1971. The finite element method for predicting stress distribution and soil deformation under a tractive device. *Trans. ASAE* 14(6):1184-1188.

- Poletayev, A.F., 1964. The compaction of soil under a rolling wheel. *J. Terramech.* 1(3):7-17.
- Reaves, C.A. and A.W. Cooper, 1960. Stress distribution in soils under tractor loads. *Agric. Engineering* 41(1):20-21, 31.
- Reece, A.R., 1970. The shape of the farm tractor. Paper presented at Inst. Mech. Eng. Conf. "Agricultural and Allied Industrial Tractors", London.
- Renius, K.T., 1985. *Traktoren. Technik und Ihre Anwendung.* BLV Verlag, München.
- Renius, K.T., 1986. Zur Entwicklung des Traktors nach 1945. *Landtechnik* 41(10):420-425.
- Riemer, G., P.W. Bakker Arkema en L.H. Hulsman, 1957. *Handboek voor landbouwwerktuigen en trekkers.* Tjeenk Willink, Zwolle.
- Rutherford, I., 1973. Wheeled and tracklaying tractors - utilization, performance and tyre and track costs. *Proc. Int. Conf. "Perspectives of Agricultural Tractor Development"*, Warsawa:115-156.
- Schäfer, W., 1983. Theoretische Untersuchungen zur optimalen Kombination von Allradschleppern und gezogenen Geräten zur Bodenbearbeitung. Dissertation Univ. Hohenheim, Stuttgart.
- Scheltema, W., 1974. Puddling against dry plowing for lowland rice culture in Surinam. Dissertation Agricultural University Wageningen.
- Schilling, E., 1962. *Landmaschinen.* Schilling, Köln.
- Schmitt, H., 1986. Einsatz von Radarmessgeräten in der Landwirtschaft. *Landtechnik* 41(10):434-435.
- Schofield, A. and P. Wroth, 1968. *Critical State Soil Mechanics.* McGraw Hill, London.
- Schothorst, C.J., 1974. De meting van Indringingsweerstand in het terrein. Intern rapport, ICW Wageningen.
- Schüring, D., 1968. Zur Theorie des Geländerads. *Forsch. Ing.-Wes* 34:165-200 und 35:7-12.
- Serota, S. and A. Jangle, 1972. A direct-reading pocket shear vane. *Civil Engineering - ASCE* 42(1):73-74.
- Sitkel, G., 1969. Die Kennzahlen von AS-Reifen und die Probleme der Bereifung. *Proc. 3th Int. Conf. ISTVS, Essen, Vol. III:23-43.*
- Sitkel, G. and A. Fekete, 1975. Design of Off-the-road vehicles for minimum soil compaction. *Proc. 5th Int Conf. ISTVS, Detroit, 534-545.*
- Söhne, W., 1951. Das mechanische Verhalten des Ackerbodens bei Belastungen, unter rollenden Rädern sowie bei der Bodenbearbeitung. *Grundl. Landtechnik* 1:87-94.
- Söhne, W., 1952. Die Kraftübertragung zwischen Schlepperreifen und Ackerboden. *Grundl. Landtechnik* 3:75-87.
- Söhne, W., 1953a. Druckverteilung im Boden und Bodenverformung unter Schlepperreifen. *Grundl. Landtechnik* 5:49-63.
- Söhne, W., 1953b. Reibung und Kohäsion bei Ackerboden. *Grundl. Landtechnik* 5:64-80.
- Söhne, W., 1956. Einige Grundlagen für eine Landtechnische Bodenmechanik. *Grundl. Landtechnik* 7:11-27.
- Söhne, W., 1958. Fundamentals of pressure distribution and soil compaction under tractor tires. *Agr. Eng.* 39:276-281,290.

- Söhne, W., 1963. Beitrag zur Mechanik des Systems Fahrzeug-Boden unter besonderer Berücksichtigung der Ackerschlepper. Grundl. Landtechnik 17:5-16.
- Söhne, W., 1969. St. Christopher Lecture. Agricultural engineering and terramechanics. Third Int. Conf. ISTVS, Essen.
- Söhne, W. und H. Stubenböck, 1978. Theoretische Grundlagen der Mechanik der Bodenbearbeitung. Berichte über Landwirtschaft 56:390-414.
- Söhne, W., 1980. Entwicklungstendenzen und -möglichkeiten bei Allradschleppern. Landtechnik 35(4):156-161.
- Söhne, W. und I. Bolling, 1981. Der Einfluss der Lastverteilung auf die Triebkraft-Schlupf-Kurve von Ackerschleppern. Grundl. Landtechnik 31(3):81-85.
- Sommer, C., 1972. Modellversuche über den Einfluss hoher Kalkgaben auf die Verformung und Verdichtbarkeit eines Bodens. Mitteilungen Deutschen Bodenkundlichen Gesellschaft 15:65-72.
- Sommer, C., K. Stolnev und H.J. Altemüller, 1972. Das Verhalten vier verschiedener Modellböden unter vertikaler Belastung. Landbauforschung Völknerode 22:45-56.
- Sommer, C., H. Steinkampf, M. Zach und W. Czeratzki, 1975. Ein Beitrag zum Problem der Bodenverdichtung beim Einsatz leistungsstarker Schlepper. Landbauforschung Völknerode 25(2):69-74.
- Sonnen, F.J., 1970. Über den Einfluss von Form und Länge der Aufstandsfläche auf die Zugfähigkeit und den Rollwiderstand von AS-Reifen. Landbauforsch. Völknerode, Sonderheft 3.
- Steiner, M., 1978. Messungen für Triebkraft-Schlupf-Kurven verschiedener Ackerschlepperreifen in der Bodenrinne. Grundl. Landtechnik 28(5):169-208.
- Steiner, M., 1979. Analyse, Synthese und Berechnungsmethoden der Triebkraft-Schlupf-Kurve von Luftreifen auf nachgiebigen Boden. Dissertation Technische Universität München.
- Steiner, M. und W. Söhne, 1979. Berechnung der Tragfähigkeit von Ackerschlepperreifen sowie des Kontaktflächen mitteldruckes und des Rollwiderstandes auf starrer Fahrbahn. Grundl. Landtechnik 29(5):145-162.
- Steinkampf, H., 1971. Zur Methodik der Rollradien- und Rad-schlupfmessung. Grundl. Landtechnik 21:40-44.
- Steinkampf, H., 1974. Probleme der effizienten Umwandlung der Motorleistung in Zugleistung bei Leistungsstarken Schleppern. Grundl. Landtechnik 24(1):14-20.
- Steinkampf, H., 1975. Ermittlung von Reifenkennlinien und Gerätezugleistungen für Ackerschlepper. Dissertation Techn. Universität Braunschweig.
- Steinkampf, H., 1977. Problematik der Leistungsumwandlung über die Triebräder bei Leistungsstarken Schleppern. Grundl. Landtechnik 27(5):168-172.
- Steinkampf, H., 1981a. Zur Entwicklung der Schlepperreifen. Landtechnik 4:178-181.
- Steinkampf, H., 1981b. Ergebnisse aus Reifenvergleichsversuchen. Landtechnik 10:479-482.
- Stienstra, J., 1976. De voorspelbaarheid van verdichting onder banden. Unpublished thesis, Tillage Laboratory, Agricultural University, Wageningen.

- Stone, J.A. and W.F. Larson, 1980. Rebound of five one-dimensionally compressed unsaturated granular soils. *Soil Sci. Soc. Am. Journ.* 44:819-822.
- Taylor, P.A. and N.Y. Williams, 1959. Traction characteristics of 11-36 agricultural tractor tyres on hard surfaces. *Journ. Agr. Eng. Res.* 4:3-8.
- Taylor, J.H., 1973. Lug angle effect on traction performance of pneumatic tractor tires. *Trans. ASAE* 16:16-18.
- Taylor, J.H., 1974. Lug spacing effect on traction of pneumatic tractor tires. *Trans. ASAE* 17(2):195-197.
- Taylor, J.H., 1976. Comparative traction performance of R-1, R-3, and R-4 tractor tires. *Trans. ASAE* 19(1):14-16.
- Terpstra, J. en J. van Maanen, 1972. Aspecten van het trekkerbandenonderzoek. Publ. 160, ILR Wageningen.
- Terpstra, J., 1973. Performance characteristics of deep lug tires. *Beiträge der Int. Konferenz "Entwicklungsperspektive landwirtschaftlicher Schlepper"*, Warschau, Vol 1:233-258.
- Terpstra, J., 1978. Wetenswaardigheden over banden. Publ. 108, IMAG Wageningen.
- Thansandote, A. et al., 1977. A new slip monitor for traction equipment. *Trans. ASAE* 20:851-856.
- Tijink, F.G.J., 1979. Mechanische eigenschapsmetingen en bandproeven gericht op het ontwikkelen van voorspellingsmethodes. Unpublished thesis, Tillage Laboratory, Agr. University Wageningen.
- Tijink, F.G.J. en W.P. den Haan, 1981. Wielslip tijdens ploegen. *Landbouwmechanisatie* 32(10):961-964.
- Tijink, F.G.J. en P. Vaandrager, 1983. De conusvorm bij penetrometerwaarnemingen. *Cultuurtechn. Tijdschr.* 22(6):377-383.
- Tijink, F.G.J. and A.J. Koolen, 1985. Prediction of tire rolling resistance and soil compaction, using cone, shear vane, and a falling weight. *Proc. Int. Conf. on Soil Dynamics, Auburn, Alabama USA, Vol. 4:800-813.*
- Tijink, F.G.J., P. Lerink and A.J. Koolen, 1988. Summation of shear deformation in stream tubes in soil under a moving tyre. To be published in *Soil and Tillage Research*.
- Trabacchi, G.W., K.V. Lask and W.F. Buchele, 1959. Measurements of soil-tire interface pressures. *Agr. Eng.* 40:678-681.
- Traulsen, H. und W. Spingler, 1978. Schlepper mussten auf schwerem Boden ihr Können beweisen. *Top Agrar*:68-71.
- Turnage, G.W., 1972. Tire selection and performance prediction for off-road wheeled-vehicle operations. *Proc. 4th Int. Conf. ISTVS, Stockholm, Vol. 1:61-81.*
- Uffelmann, F.L., 1961. The performance of rigid wheels on clay-soils. *Proc. 1st Int. Conf. Soil Vehicle Mechanics, Turin.*
- Vomocil, J.A. and W.J. Flocker, 1965. Degradation of structure of Yolo Loam by compaction. *Soil Sci. Soc. Am. Proc.* 29(1):7-12.
- Wann, R.L. and I.F. Reed, 1962. Studies of tractor tire-tread movement. *Trans. ASAE* 5:130-132.
- Warkentin, B.P., 1971. Effects of compaction on content and transmission of water in soils. Chapter 5 in *Compaction of Agricultural Soils. ASAE St. Joseph, MI.:126-153.*
- Watt, H.v.H. van der, 1969. Influence of particle size distribution on soil compactability. *Agrochemophisica* 1:79-86.

- Werkhoven, C., 1975. Ontwikkeling van een enkelwieltester voor het bandenonderzoek. Publ. 17, IMAG Wageningen.
- Wills, B.M.D., E.M. Barret and G.J. Shaw, 1965. An investigation into rolling resistance theories for towed rigid wheels. *J. Terramech.* 1(1):24-53.
- Wismer, R.D. and H.J. Luth, 1973. Off-road traction prediction for wheeled vehicles. *J. Terramech.* 10(2):49-61.
- Witney, B.D. and K.E. Oskoui, 1982. Ploughing performance predictor. *Power farming* 61(12):46-49.
- Wittsell, L.E. and J.A. Hobbs, 1965. Soil compaction effects on field plant growth. *Agron. J.* 57:534-537.
- Wong, J.Y. and A.R. Reece, 1966. Soil failure beneath rigid wheels. Proc. 2nd Int. Conf. ISTVS, Quebec, Canada.
- Wong, J.Y., 1967. Behaviour of soil beneath rigid wheels. *Journ. Agr. Eng. Res.* 12(4):257-269.
- Wong, J.Y. and A.R. Reece, 1967a. Prediction of rigid wheel performance based on the analysis of soil-wheel stresses. Part I, Performance of driven rigid wheels. *J. Terramech.* 4(1):81-98.
- Wong, J.Y. and A.R. Reece, 1967b. Prediction of rigid wheel performance based on the analysis of soil-wheel stresses. Part II, Performance of towed rigid wheels. *J. Terramech.* 4(2):7-25.
- Wong, J.Y., 1978. *Theory of ground vehicles.* John Wiley & Sons, New York.
- Wu, T.H., 1971. *Soil Dynamics.* Allyn and Bacon, Boston.
- Yong, R.N. and B.P. Warkentin, 1966. *Introduction to soil behaviour.* Mac Millan Co, New York.
- Yong, R.N. and B.P. Warkentin, 1975. *Soil properties and behaviour.* Elsevier, Amsterdam.
- Yong, R.N. and E.A. Fattah, 1976. Prediction of wheel-soil interaction and performance using the finite element method. *J. Terramech.* 13(4):227-240.
- Yong, R.N., E.A. Fattah and P. Boonsinsuk, 1978. Analysis and prediction of tyre-soil interaction and performance using finite elements. *J. Terramech.* 15(1):43-63.
- Zoz, F.M., 1972. Predicting tractor field performance. *Trans. ASAE* 15:249-255.

CURRICULUM VITAE

Franciscus Gerhardus Jozeph Tijink werd geboren op 11 september 1955 te Denekamp.

Na het behalen van het diploma HBS-b in 1973 aan het Twents Carmellyceum te Oldenzaal begon hij zijn studie aan de Landbouwhogeschool te Wageningen. Het doctoraalexamen in de studierichting Landbouwtechniek legde hij af in september 1979. Naast de hoofdvakken Grondbewerking en Landbouwbedrijfsgebouwen omvatte de doctoraalstudie het vak Landbouwwerktuigkunde.

In aansluiting daarop trad hij in dienst als promotie-assistent bij de Landbouwhogeschool, waar hij tot 1 augustus 1982 bij de vakgroep Grondbewerking het onderzoek naar afsteunende processen in wiel-grond systemen heeft uitgevoerd. Vervolgens was hij als docent verbonden aan de Agrarische Hogeschool te Dordrecht. In deze periode heeft hij dit proefschrift voltooid.

Per 1 september 1987 is hij in dienst getreden als hoofd van de afdeling Tractie en Grondbewerking bij het Instituut voor Mechanisatie, Arbeid en Gebouwen (IMAG) te Wageningen.